NOTICE

The quality of this microform is heavily dependent upon the quality of the original thesis submitted for microfilming. Every effort has been made to ensure the highest quality of reproduction possible.

If pages are missing, contact the university which granted the degree.

Some pages may have indistinct print especially if the original pages were typed with a poor typewriter ribbon or if the university sent us an inferior photocopy.

Reproduction in full or in part of this microform is governed by the Canadian Copyright Act, R.S.C. 1970, c. C-30, and subsequent amendments.

AVIS

La qualité de cette microforme dépend grandement de la qualité de la thèse soumise au microfilmage. Nous avons tout fait pour assurer une qualité supérieure de reproduction.

S'il manque des pages, veuillez communiquer avec l'université qui a conféré le grade

La qualité d'impression de certaines pages peut laisser a désirer, surtout si les pages originales ont été dactylographiées à l'aide d'un ruban usé ou si l'université nous a fait parvenir une photocopie de qualité inférieure

La reproduction, même partielle, de cette microforme est soumise à la Loi canadienne sur le droit d'auteur, SRC 1970, c. C-30, et ses amendements subséquents

PRESTRESSED STEEL CONTINUOUS BOX GIRDERS

Naser Rabbani-Farani

A thesis in the

Department of Civil Engineering

Presented in Partial Fulfilment of the Requirements

for the Degree of Doctor of Philosophy at

Concordia University

Montréal, Québec, Canada

May 1991

ISBN 0-315-68776-2

ABSTRACT

Prestressed Steel Continuous Box Girders

Naser Rabbani-Farani, Ph.D.
Concordia University, May, 1991

The trend of structural design, to achieve better economy, proper serviceability, acceptable strength and aesthetically appealing structures, has been progressively improved through the use of new design techniques and better quality structural materials. The prestressing techniques and the use of closed sections may well be fit in this category.

Prestressed / post-tensioned steel box girders are considered structurally efficient, economically valuable, aesthetically attractive and technically advanced. Box girders are built of comparatively thin plates and when prestressed by cables of high strength steel at the tension region, the load bearing capacity of the section can be considerably increased.

The advantages of prestressing/post-tensioning of steel girders have made it attractive in rehabilitation, strengthening and in the design of new structures, mostly bridges.

Steel box girders and prestressing of simply supported girders have already been investigated, although not to the full extent. The analysis, design concepts and experimental study of continuous steel box girders when prestressed/post-tensioned by tendons are the main topics of this thesis.

The degree of indeterminacy of the prestressed girders is increased by one due to the secondary stresses induced by prestressing force increment (PFI). The detailed calculation of PFI and the reduced negative bending moment at middle support of prestressed steel

continuous box girders are presented. Numerical examples are solved and comparison is made between prestressed and non-prestressed girders having similar geometry and applied service loads.

Existing literature on the subject has been reviewed. The methods of prestressing, the general criteria for the selection of a proper tendon configuration and the design concepts of prestressed continuous girders are presented.

To evaluate the analytical study, a scaled down model based on the designed prestressed steel continuous box girder prototype was fabricated. Experimental tests were performed in various loading stages and intensities. The test results in comparison to the developed theoretical calculations are satisfactory.

ACKNOWLEDGEMENTS

The author wishes to express his gratitude to Dr. M.S. Troitsky for his advice, interest and guidance in the course of this investigation.

The recommendations and advices provided by Dr. Z.A. Zielinski during the author's studies are highly appreciated.

The author wishes to extend his gratitude to the members of the examining committee for the comprehensive exam and thesis defence in reviewing the author's report and thesis.

The financial support provided by the National Research Council of Canada is gratefully acknowledged.

Naser Rabbani Farani

Concordia University

Department of Civil Eng.

Montréal, Québec

March 1991

TABLE OF CONTENTS

LIST OF FIGURES:

LIST OF TABLES

LIST OF SYMBOLS

A	Cross-Sectional Area of the member
A_t	Cross-Sectional Area of the tendons
α	The angle of the inclination of the tendons
CFA	Correction Factor for the cross-sectional area
CFS	Correction Factor for the section modulus
D, DL	Dead Load
d	Total depth of the girder
Δf_{sr}	Stress due to steel relaxation
ΔP	Prestressing Force Increment
ΔP_f	Prestressing Loss due to friction
ΔP_{sa}	Prestressing Loss due to anchorage slippage
ΔP_{sr}	Loss of prestressing force
Δ_{s+L}	Deformations due to superimposed dead and Live loads
δ_{mn}	Deformations at section m due to a unit force at n
E	Modulus of Elasticity of the member
E_t	" " " tendons
e	Eccentricity of the tendons from the centroid at the tension region
e_1	" " " " " " compression zone
f_a	Stress due to axial prestressing force
f_{bb}	Bending stress at the extreme bottom fibre
f_{bt}	Bending stress at the extreme top fibre
f_d	Stress due to dead load
f_{d+pre}	Combined stresses due to dead load and prestressing force
f_{ip}	Stress due to the initial prestressing force
f_{pt}	Allowable stress of the tendon
f_{si}	The initial stress

f_{tb}	Combined stresses at the extreme bottom fibre
f_{tt}	Combined stresses at the extreme top fibre
f_{Yt}	Yield stress of the tendon
ϕ	Angle of twist
G	Shear modulus
I_m	Moment of Inertia of the m^{th} section
J	Torsional Constant
k	Scaled down factor
L, l	Length of the girder
l_t	Length of the tendon
l_m	The m^{th} span length
M_{d+s+L}	Bending moment due to Dead, Superimposed Dead and Live load
M_x	Bending moment due to applied service loads
m	Distance of the vertical concentrated load from the left support
m_x	Bending moment due to a unit force at x
N	Axial service loads
N_d	Axial load due to service dead load
N.A.	Neutral axis of the girder
P	Prestressing force
P_e	Effective prestressing force
P_i	Initial prestressing force
P_{ip}	Incoming prestressing force prior to the cable guide
P_{op}	Outgoing prestressing force considering friction loss
q	Unifomly distributed load
r	Radius of gyration of the section
S	Elastic section modulus
SD, sd	Superimposed dead load

T	Applied torque
τ_t	Shear stress due to torsion
V	Vertical concentrated force
w	Uniformly distributed load
y	The distance of the extreme fibres from the neutral axis

LIST OF SUbSCRIPTS / SUPERSCRIPTS

	Representing:
bot.	Extreme bottom fibres of the section
comp	Compression region
d	Dead load
hm	Ideal homologus model
L	Live load
m	Actual fabricated model
p	Prototype girder
s	Superimposed dead load
tens	Tension zone
top	Extreme top fibres of the section

CHAPTER I. ADVANTAGES AND METHODS OF PRESTRESSING

1.1. INTRODUCTION

The design of plate girder bridges has been developed with the advancement of modern technology. Among the progressive methods in the design of the modern bridges are the prestressed steel box girder bridges which are considered economical, advanced in technology and esthetically appealing. The use of high strength steel cables and improvement of welding techniques have considerably improved the efficiency (strength to weight ratio) of prestressed steel box girders.

The study of the design of medium and large span girder bridges reveals that better economy can be achieved by designing the girders having closed cross sectional areas (boxes) in comparison to open sections (I shapes). In general the box girder is most efficient for the spans ranging from 60 m, where plate girder efficiency starts to fall off, to about 250 m, where beyond that span the cable stayed bridge becomes a viable proposition. In the design of girders with similar loading and roadway geometry a weight saving of up to 60% can be reached by using box sections instead of I sections [1]. The efficient utilization of materials in the design of box girder bridges is obtained through the use of thin plates welded or bent to the desired geometry.

The load carrying capacity of steel box girders can be increased by the application of a predetermined prestressing force appropriately placed at the tension region of the girder. In particular the prestressing techniques appear to be very efficient for new structures and mostly favorable in rehabilitation and strengthening of existing bridge structures.

1.2. HISTORY

The use of hollow sections for girder bridges actuated by the design and construction

of the twin girder bridges in 1850, the Britannia bridge with three spans of (70-140-70m) and the Conway railway bridge in Wales England, having box sections made of wrought iron, Figure 1.1 [2 &3]. The bridges were designed by R.Stephenson.

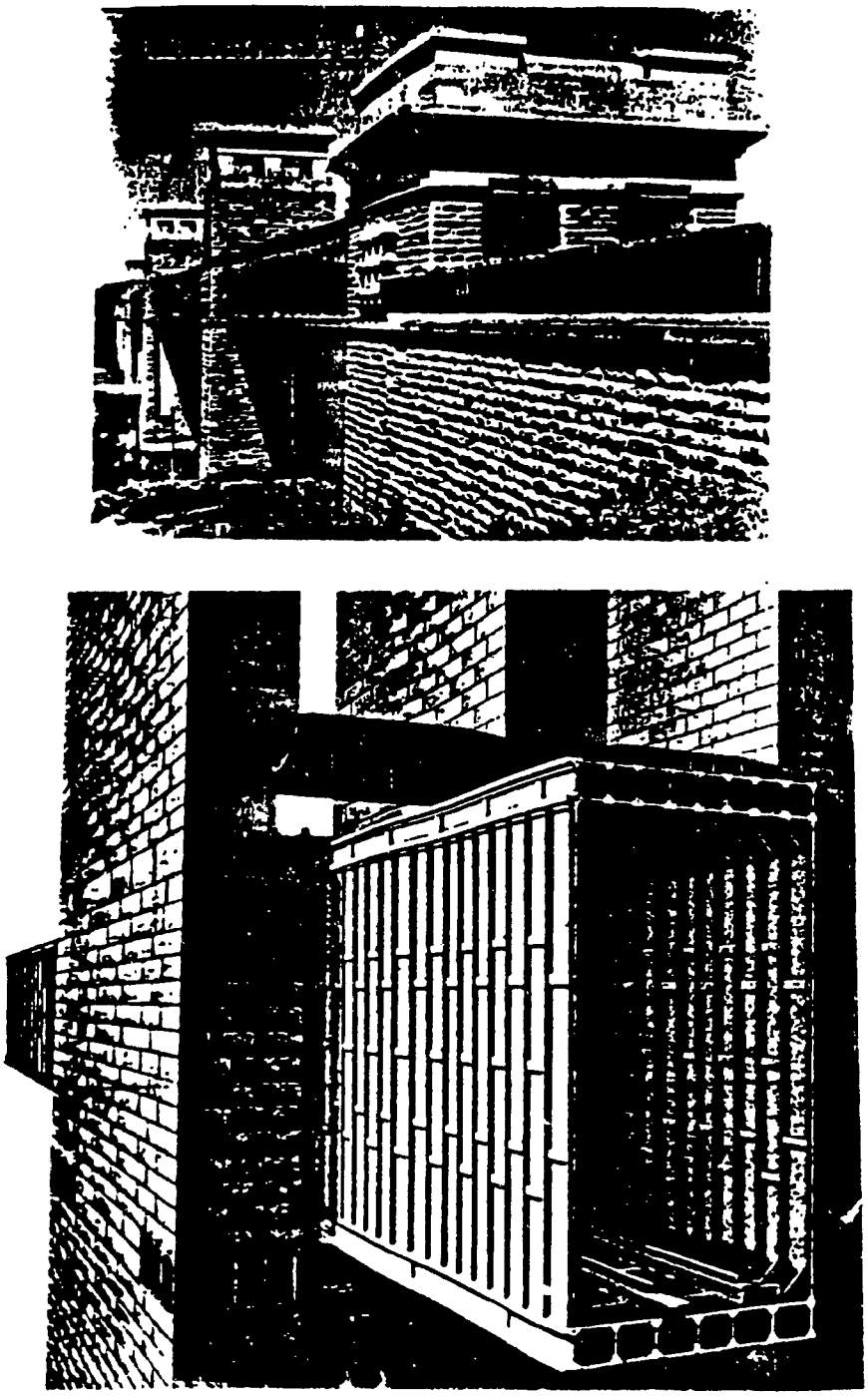

Figure 1.1. Britannia tubular bridge

Other tubular girder bridges such as Victoria Bridge over the St.Lawrence river in Montréal and a bridge over Damietta branch of the Nile river in Africa were also designed by the same engineer. A steel box girder bridge with a span of 15 m on the Baltimore and Ohio railroad junctions was designed in 1846 by James Millholand. Examples of bridges having tubular cross sections include: bridge over the Leeds and Liverpool canal designed by William Fairbairn which was erected in 1846. A bridge over the English Channel was proposed by Boyd in 1858, with 150 m equal spans and the Pennith bridge over the Nepean river, New South Wales, was built in 1865 [4].

The construction of girder bridges having tubular cross sectional areas was not adequately developed until a century later, because of high expenses and hardships in the construction and erection. During that period new steel mills were extensively developed and a major progress started in the advancement of welding technology, construction and structural design practice. The successful utilization of a wide range of steel rolled sections as truss systems, girders and stringers led to the temporary decline in the use of steel box girder bridges. After the second World War the enormous destruction of the bridges in Europe and Asia and at the same time the scarcity of the structural steel encouraged bridge designers to use more economical sections such as steel box sections and orthotropic bridges made of thin plates stiffened longitudinally and transversely. Several bridges were built having a steel box girder continuous or simply supported with reinforced concrete or orthotropic deck.

The design and construction of steel box girder bridges received true consideration in West Germany during the two decades, from 1940 to the end of 1950, where several such bridges were erected [2].

More important steel box girder bridges built are listed in Table 1.1 [2, 4, 5, 6 and 7].

Name of the bridge	Span lengths	Date	Country
Koln-Deutz	132-184-120	1948	W.G.
Bonn-Bevel	99-196-99	1949	W.G.
Porta over the river Weser	64-78-106	1954	W.G.
Düsseldorf-Neuss	103-206-103		W.G.
Speyer over the river Rhine	52-163-107	1956	W.G.
Europa bridge	81-108-198-108-81-81	1964	Austria
Zoo bridge in Cologne	73.5-259-144.5-120.5	1966	W.G.
Concordia Bridge, Montréal	102 - 157.5 - 102	1967	Canada
Papineau Bridge, Montréal	3*44.5-48-51-48-3*44.5	1969	Canada

Table 1.1. Steel box girder bridges built between 1948-1969.

Figure 1.2 shows the trend of the use of box girders in bridge construction in the United States [8].

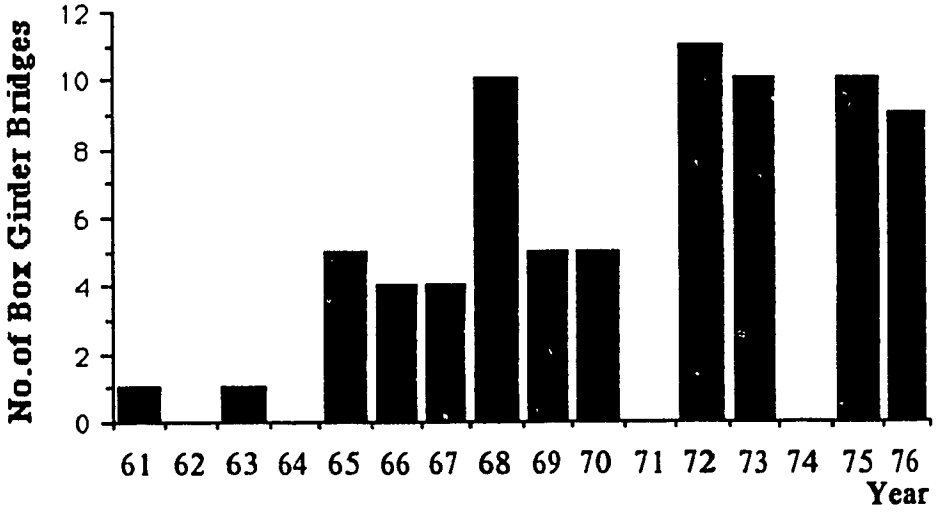

Figure 1.2. Number of box girder bridges built in USA.

The first use of prestressing technique was in 1837 by Squire Whipple to compensate for the effect of brittleness of tension members made of cast iron [9]. To increase the load carrying capacity of the bridges, in the United States many steel floor beams were post tensioned in the late 19th and early 20th century. Since 1930's and later Magnel, Belynia, Samuely, Jenkins, Dischinger and other European engineers greatly contributed to the establishment of a design criteria and to the construction of prestressed steel structures [10].

Examples of prestressed steel box girder bridges are listed in Table 1.2.

Name	Span Lengths	Date	Reference
Canas River bridge, Cuba	50-249-50	1952	[11]
Brits bridge, Transvaal, South Africa	25-25-25-25	1964	[12]
Whatcom County Bridge, Washington D.C.	63	1966	[13]

Table 1.2. Example of prestressed steel box girder bridges.

A large three spans continuous girder bridge of 72 m each, was prestressed by high strength steel cover plates in 1961 [14]. A steel truss railway bridge in Birmingham, England was strengthened by prestressing cables, in 1956 [15]. Bonners Ferry Bridge in USA, having ten equal spans of 46.5 m each, was designed by T.Y.Lin in 1983 [16].

Other examples include: roof of GUM department store in Moscow was prestressed by guy rods in early 20th century [17]. In Poland the long span steel girder of Supersam shopping center was prestressed in order to increase the load carrying capacity of the roof girders [18]. A cable stayed bridge across Vistula River having a concrete deck was prestressed. In Mexico, five railroad bridges with composite concrete deck were also prestressed [19].

1.3. ADVANTAGES

The practicability and feasibility of prestressed steel box girders have been established by numerous bridges already built. Two fundamental concepts for the economy optimization in bridge design are a) reducing the weight of the steel and b) minimizing the fabrication and erection expenses. These characteristics are provided by steel box girders. The efficiency and the economy can be significantly improved by prestressing the steel box girders. The efficient use of thin plates in the fabrication of box girders on one side and the box section being prestressed at the tension zone on the other, reduce the self weight of the girder, which in turn have effect not only on the economy but also decrease the dead load of the girder, the piers and the foundations. A weight comparison for three bridges in Europe which were rebuilt using steel box girders reveals a dead weight saving of 52-60% [1]. Fabrication of box girders has been improved greatly due to the advancement in welding technology, availability of high strength steel cables and plates. Erection of steel box girders is faster and less complicated than slab and beam bridges. Other advantages of prestressed steel box girders include.

-Closed sections have a higher torsional resistance than the open sections.

-The span depth ratio can be increased due to the efficient distribution of steel plates and the counterbalance effect of prestressing and reduced deflection.

-A better performance under the lateral loading

-The decrease in the dead weight of the girder favorably effects other supporting members of the bridge (piers, foundations, etc.), as well as transportation of the prefabricated segments and the erection of the girders.

-Prefabrication under controlled conditions leads to a better welding and/ or press formed quality of the plates.

-Hollow sections allow the passing through of mechanical and electrical service facilities (pipes, cables, etc.) and simplify the maintenance.

-Top flange of steel box either steel or reinforced concrete serves a double function a) it

serves as the deck supporting and transferring the service loads to the webs and b) it is contributing to the strength of the section as integral part of the box section.

-Shallow box girders are esthetically more appealing due to the its slenderness and flat exterior surface.

Steel box sections are considered suitable sections for the medium and large span bridges.

Prestressing is a technique efficient for strengthening, rehabilitation and the design of new structures. The principal advantages of prestressing of steel members include:

-The elastic range of the girder is increased due to the application of the internal stresses induced by the tendons and acting in the opposite direction to stresses induced by the applied service loads.

-The ultimate capacity of the girder is increased by adding tendons to the steel member.

-The weight of the structural steel is reduced due to the use of high strength steel cables which substitutes for the lower strength structural steel.

- Fatigue and fracture strength of the girder is improved by prestressing. The prestressed tendons induce compression to the tension zone reducing the tensile stress range cycle, delaying or preventing the effect of fatigue initiation and development. Furthermore, it is preferable to use tendons having much higher fatigue strength than welding cover plates [20].

-In most cases of strengthening of the existing structures the prestressing process can be executed without interruption of the regular functions of the structure. The top deck need not be touched while prestressing cables are placed under the girder. The installation of prestressing cables is rather simple and does not require lots of initial preparations.

-The prestressing cables are maintenance free when properly placed and fixed by the end anchorages. Any future control and change of the cables are readily possible since the

cables are easily reachable.

The prestressing techniques used in bridge structures (examples are given in section 1.2), have been proved in the design of other structures such as domes [17 & 21], steel roof girders [22], prestressed diagonals in latticed beam columns [23], rehabilitation of indoor parking structures [24], etc.

The age and deterioration of bridges in the United States and Canada which are considered structurally deficient or functionally obsolete [25], create the need for the rehabilitation search for convenient repair method(s). The report in the Journal of Structural Engineers of the American Society for Civil Engineers reveals that about 42% of the total 580 000 bridges in the United States fall in this category.

The post tensioning by tendons is an efficient method for the strengthening of girders which are either not sufficient to carry the passing traffic of today or they are deteriorated and need to be resurfaced [9].

1.4. PRESTRESSING TECHNIQUES

The inducing and storing up of forces by one mean or another to a structural member opposite in character with the stresses caused by the service loadings (dead, superimposed dead and live loads) are termed prestressing techniques. The idea involves the reducing of the applied stresses due to the service loadings and increasing the load bearing capacity of the structural elements by the counterbalance stresses inserted by the prestressing elements.

By definition, prestressing (pre-tensioning) is introduced when the girder is carrying only its own weight or in some cases when it is supported on several temporary supports (shored girders). The effect of prestressing can be efficiently increased due the fact that the

cross sectional area of the girder and of the cables can be properly designed. The term post-tensioning refers to the case when stressing of the member is introduced when the girder is already in service and under partial or total service loads. Therefore the maximum magnitude of post tensioning will be limited to compensate for the stresses due to the total live load (if the member function is interrupted until the prestressing is achieved) or partial live loads only, which is mostly used to increase the load bearing capacity of the existing girders.

The early prestressing techniques involved the placement of the rods at the tensile region of the girder tightened by turnbuckles (truss beams), Figure 1.3 [26]. The amount of stress that could be induced by prestressing was limited because the rods were made of wrought iron or mild steel.

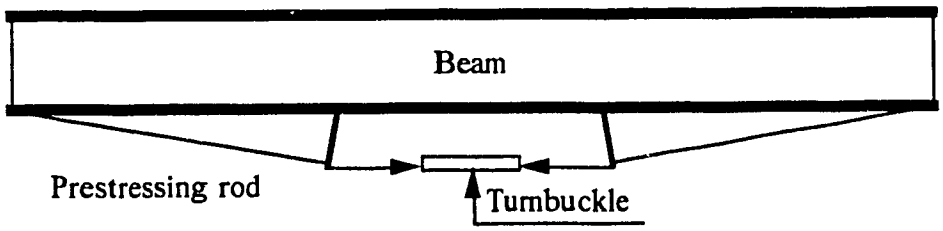

Figure 1.3. Prestressing by rods

The contemporary methods of prestressing include:

1) Prestressing by tendons (strands or cables) of high strength steel which are installed as far as possible from the neutral axis along the tension zone of the member and prestressed by prestressing jack up to a predetermined force, Figure 1.4. The prestressing force is induced to the girder through the end anchorages [14, 17 and 26]. Resulted stress distributions are shown in Figure 1.5.

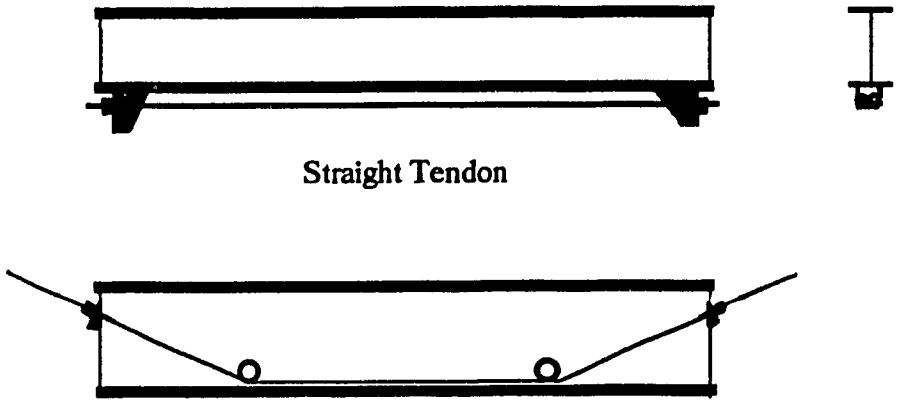

Figure 1.4. Prestressing by tendons.

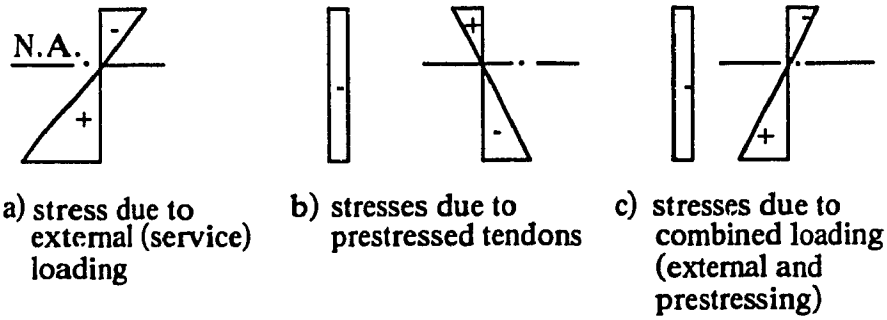

Figure 1.5. Stress distribution in cross section of girders prestressed by tendons

2) Pre-tensioned high strength steel plates, are welded to the tensile components of a T or I section. The stressing means are released when the welding is accomplished [14 & 26].

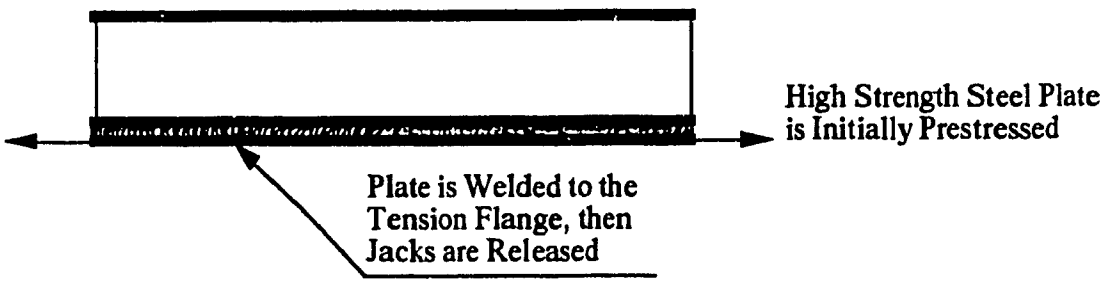

Figure 1.6. Prestressing by welding of pre-tensioned steel plates to the girder

3) Redistribution of bending moments in continuous span girders (Regulation method), by forced displacement of middle supports (lowering down the supports to create positive moments), to obtain forces of the sign opposite to that of the applied forces by the service loads, [21, 26 and 27].

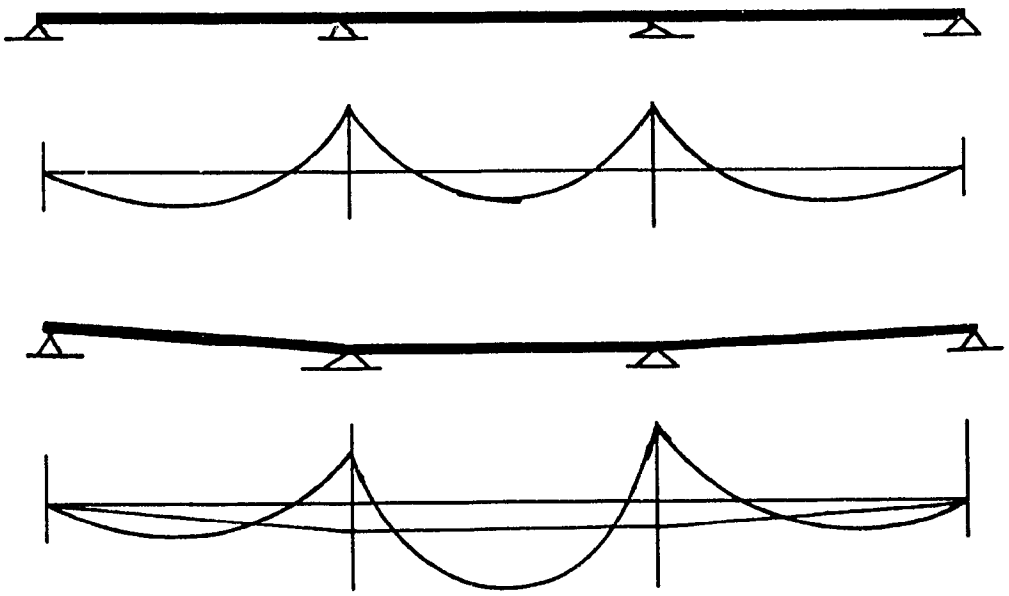

Figure 1.7. Prestressing by redistribution of moments in continuous span girders

4) The high strength steel plate is welded to a predetermined deflected beam. The beam is cambered contrary to the deflections due to the service loads by means of jacking. After the desired deflection is induced to the beam, the high strength steel plate is welded to the flange, Figure 1.8 [14, 21 and 26]. In Figure 1.9 the stress distribution for various stages of loading and prestressing process has been shown.

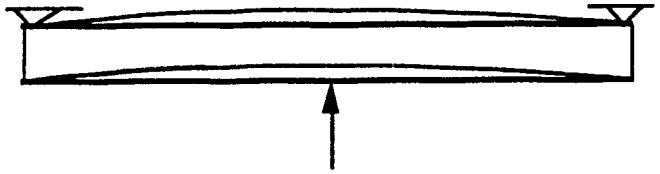

a) Application of load to the girder in opposite direction to the service loads

b) Welding cover plates to the bent girder

Figure 1.8. Prestressing by welding plates to deflected beams

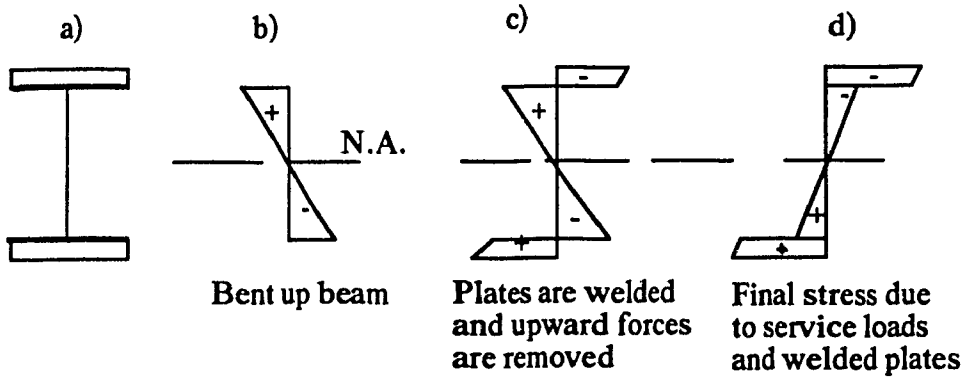

Figure 1.9. Stress distribution for prestressed girders by welding cover plates

(+ means tension)

5) Predeflected technique (Preflex) was developed by Lipski [24 & 28]. The proposed method is considered efficient where shallow construction depths are desired. In the fabrication process the predetermined cambered beam is deflected in the direction of the

loadings producing stresses at least equal to the maximum design stresses. The tensile flange is encased in high strength reinforced concrete while the beam is maintained in the deflected shape. The predeflection is released when the concrete gains the required strength, Figure 1.10.

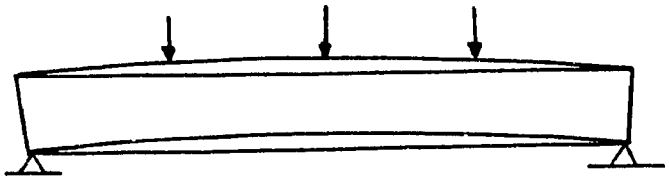

a) The beam is bent in the direction of the loadings

b) The tension flange is encased in concrete

Figure 1.10. Prestressing by Predeflected technique

6) Inserting a tensioned high strength wire in rolled sections and when the wire is released the latter being prestressed [29].

7) Two rolled steel sections (symmetrical or asymmetrical) are cambered contrary to the flexure due to the service loads. The two sections are welded together while the deflected shapes of the beams are held, but released after the welding is accomplished, Figure 1.11 [21 & 26]. The stress distributions are illustrated in Figure 1.12.

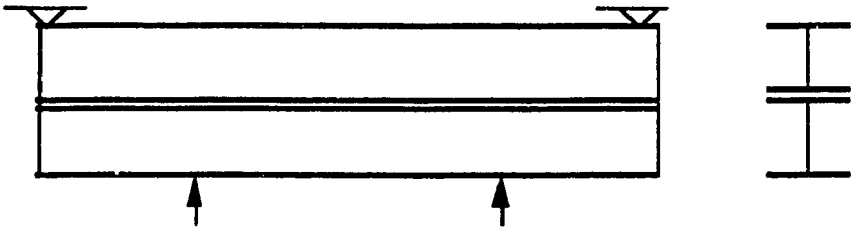

a) Sections are cambered in opposite direction to the service loads

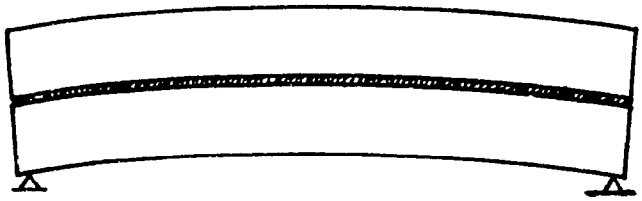

b) Sections are welded and upward forces are released

Figure 1.11. Prestressing by means of welding pre-cambered rolled sections

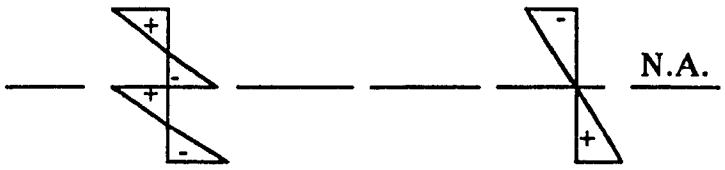

Precambered beams under upward loads

The upward forces are removed when the welding is completed

Figure 1.12. Cross sectional stresses corresponding to various loading stages.

The method of prestressing by tendons of high strength steel has obtained its priority in comparison to the other methods due to the following considerations:

-A variety of high strength steel tendons available on the market providing a wide range of prestressing cables having variable cable strengths and cross sectional areas.

-In the fabrication process of prestressed structure the placement of tendons done more rapidly and in less complicated and less expensive manner compared to the other methods of prestressing. The tendons are placed along the girder to the desired configurations, guided by saddles and end anchorages.

-The amount of stress induced by pre-tensioning cables can be ideally controlled by flexible tendon placements and variable cross sectional areas.

-The replacing of the damaged tendons, as well as the losses of prestressed tendons in the long period can be compensated by rejacking the tendons.

In this research the design of steel box girders prestressed by tendons is studied. The detailed analysis and the design procedure of continuous span steel box girders are the main objective of this dissertation. However general information about the prestressing steel structures is presented along with the existing literature on the subject. In particular the analytical and experimental study on the following topics will be elaborated in more detail:

-Main concept of prestressing techniques and steel box girders

-A proposed analysis and design method for prestressed steel box girders

-Influence lines for the incremental prestressing force and the bending moments of the intermediate supports

-Stress distribution along the girder due to prestressing effects and applied loadings

-A comparison of stresses computed theoretically and measured experimentally for a two spans continuous steel box section having variable cross sections along the girder.

CHAPTER II. SECTION GEOMETRY

2.1. INTRODUCTION

To achieve a better economy and the required serviceability careful considerations should be given in selection of suitable box section and favorable tendon configurations. The great flexibilities in terms of the geometry of the box girder and the prestressing tendons represent the structural efficiency of prestressed steel box girders. The box sections are made of relatively thin steel plates welded along the edges connecting webs to the top and bottom flanges. The trough section may be press formed instead of welding in which the residual stresses due to welding will be substantially reduced. The tendons are fixed along the girder, at the tension zone, within the box section by end anchorages and saddles (guides) are provided to achieve the desired tendon configurations.

The prestressed steel box section ideally fulfills the major functional characterstics required for bridge girders, economy considerations and engineering efficiency in bridge design. These characterstics include:

-Efficient utilization of the material which considerably reduces the dead weight of the structure, 25 - 55 % in steel weight, 52 - 60 % in total weight [1]. The lighter section also favourably effects transportation and the erection of the girder resulting in reduced construction costs.

-The fabrication operations are mostly performed in workshops, where a better quality products and manufacturing controlled conditions can be obtained. This leads to faster erections and as a result extended detours is avoided [30].

-The prestressed high strength steel tendons significantly increase the load bearing capacity of the section along the tension zone and where ideally placed will also induce counterbalance effects to the compressive stresses due to the applied service loads.

-To increase the load carrying capacity of the steel girder it is possible to stiffen and

strengthen the section by welding steel plates or additional prestressing tendons. Similarly for future widening of the bridges additional box girders can be easily welded to the existing ones.

-The advanced welding techniques and availability of high strength steel plates and tendons which are widely used provide better opportunities to use prestressed steel box sections for the long and medium span girder bridges.

2.2. THE GEOMETRY OF THE STEEL BOX SECTIONS

In general a steel box girder bridge consists of a single, multicell or multiple box sections depending on the number of traffic lanes (bridge width), span length and height of the bridge. The steel box sections are composed of relatively thin plates (slender elements) welded or bent to the required shape. The top flange is an stiffened orthotropic steel deck or concrete deck to transfer the service loadings to the webs and bottom flange of the box section. The deck (top flange) is supported by and acting compositely with one or more box girders. In either case of steel or concrete the deck is regarded as a structural element in complete interaction with the webs and bottom flanges.

The steel box girders are characterized by three dimensions of different orders of magnitude. The length is large compared to the cross sectional width and likewise the latter is large in comparison to the plate thicknesses. Also the width thickness ratio of the composed elements (flanges and webs) are large and slenderness ratios are up to 200, [31].

The box sections may have vertical or inclined webs. The trapezoidal sections are suitable in reducing the effect of lateral loads on the box girder, Figure 2.1.

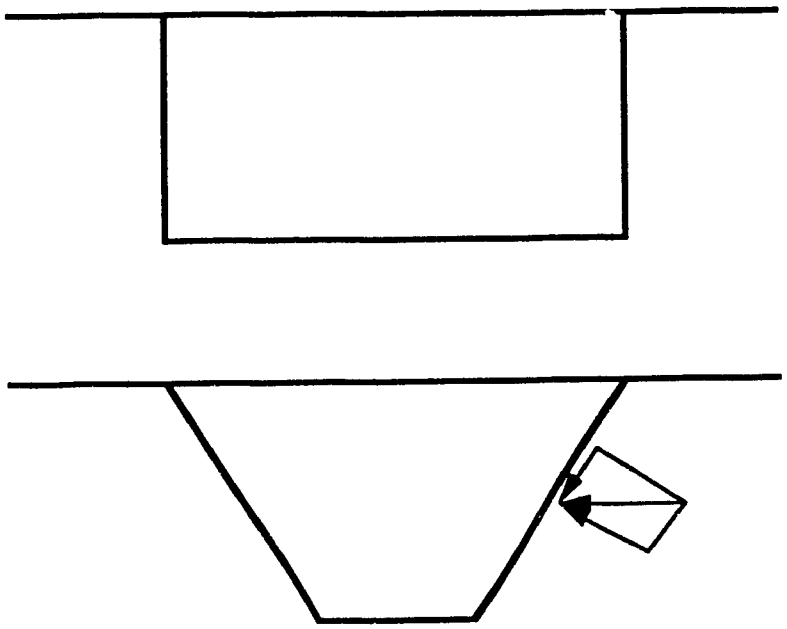

Figure 2.1. Box sections with vertical and inclined webs

To achieve the full reduction in dead weight of the steel box girder it can be built having variable cross sectional areas, in which both the bottom flange width and the height of the girder alter in accordance to the design requirements.

Figure 2.2 illustrates the common shapes of box sections utilized in girder bridges. To ensure the structural efficiency of the section, in which the top flange (reinforced concrete or orthotropic steel deck) are compositely acting with the webs and the bottom flange, sufficient shear connectors or orthotropic deck stiffeners should be provided. The webs and bottom flanges are stiffened longitudinally and transversely, where necessary. The box girder is stiffened with end and intermediate diaphragms on the supports and along the girder.

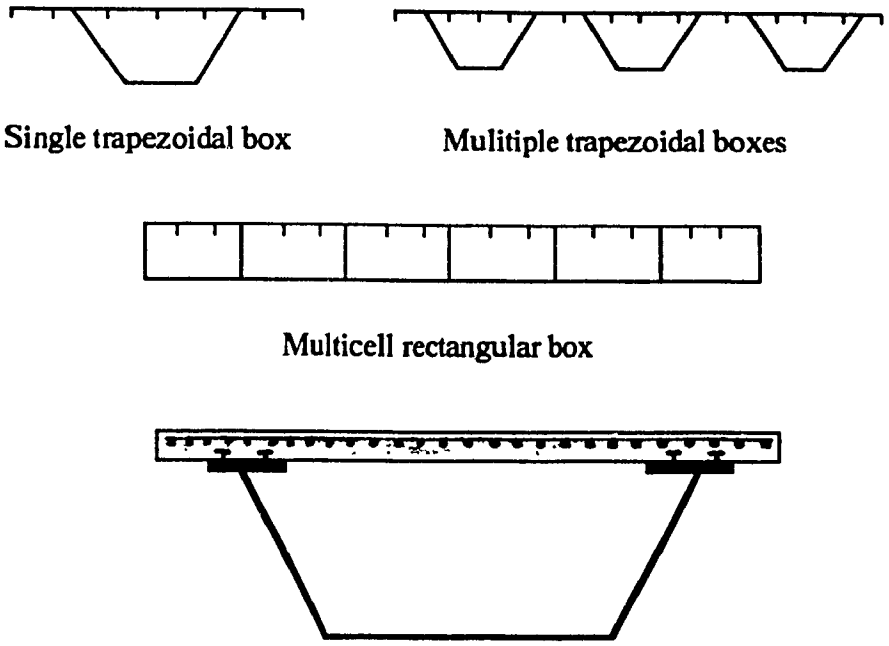

Figure 2.2. Common shapes of box sections

To select a suitable steel box section for a specific bridge several factors should be carefully considered from case to case. In fact there is no unique standard choice for various bridges. The following general ideas can be proposed for the design of the box sections:

-The use of a variable cross sectional area in accordance with the change of the bending moments along the girder.

-The use of asymmetric sections to provide better compensation by the effect of the prestressed tendons, having smaller flange area at the tension region and at the same time increasing the tendon's eccentricity.

-The use of inclined webs to reduce the effect of lateral loadings (mainly wind).

-The use of shallower sections to satisfy the desired height limits and the esthetics of the bridge.

The main parameters defining the structural properties of the steel box girders are:

-Moment of inertia and the cross sectional area.

-The ratio of width to the plate thickness (slenderness ratio of the webs and the flanges).

-The position of the neutral axis.

2.3. PRESTRESSING CABLES

The tendons used for prestressing steel members are high strength steel cables having a wide range of characterstics including: ultimate strength of 900 to1700 MPa (150 to 250, KSI) and more, variety in shape, cross sectional areas, manufacturing, etc.

The prestressing tendons are basically divided into three categories: bars, strands and ropes [19 & 32]. Tendons may be composed of one or more structural ropes, strands, locked coil strands or parallel wire strands or bars.

High tensile strength wires have minimum ultimate strength of 240 Ksi [33]. The maximum effective prestressing force is 0.6 the ultimate tensile strength (rupture), which ranges from two wires at 14.1 Kips to 186 wires at 1315 Kips. The wires shall conform to ASTM A421, specifications for uncoated stress relieved wire for prestressing concrete.

Strands are composed normally of 7 wires and have overall size of 10 mm to 15 mm (0.375 to 0.6 in) in diameters, helically formed around a center wire. The maximum effective strength ranges from a single 0.375 diameter wire at 3.8 Kips to fifty five 0.5 in diameter strands at 1364 Kips. The allowable stresses for strands are limited to 0.4 to 0.6 of breaking (rupture).

Bars with ultimate strength of 145 KSI to 160 KSI and ranging from 0.625 to 1.375 in. diameters. The maximum effective prestressing force of 17 Kips to 143 Kips can be

achieved.The bar lengths are up to 84 feet and beyond that it must be connected by couples.

In Canada CSA Standard G279, steel for prestressed concrete tendons supply information for the prestressed steel members [34]. High tensile strength wire 200 000 MPa. Seven wire strands , having 13 mm nominal diameter and less 185 000 MPa, for more than 13 mm diameter 180 000 MPa and for high strength steel bars 193 000 MPa.

The ropes are the assembly of strands grouped together or helically arranged around a core, manufactured according to ASTMA - 603 Standard Specification [35]. The strands in comparison to the ropes of similar size have better structural characterstics including: greater breaking strength, higher modulus of elasticity and better corrosion resistance. But ropes are better for curved tendons. The strands composed of parallel wires have greater modulus of elasticity, about 28 000 to 29 000 KSI (138 000 to 166 000 MPa) comparing to 20 000 to 24 000 KSI for the Z locked coil strand [36]. The normal sizes of spiral formed strands in USA is 0.5 to 4.0 in. Strands of twisted wires, cables composed of wrapped parallel wires. Figure 2.3 shows the various tendons generally used in prestressing steel structures [37]. The modulus of elasticity of the cables are the catenary shape and given as equation (2.1) [35].

$$(2.1) \qquad E_{equ} = \frac{E_c}{1 + \dfrac{G^2 \cos^5\alpha \; E_c \; A_c}{12 \; P^3}}$$

where G, A_C, E_C and are the weight, the area and the modulus of elastic'ty.

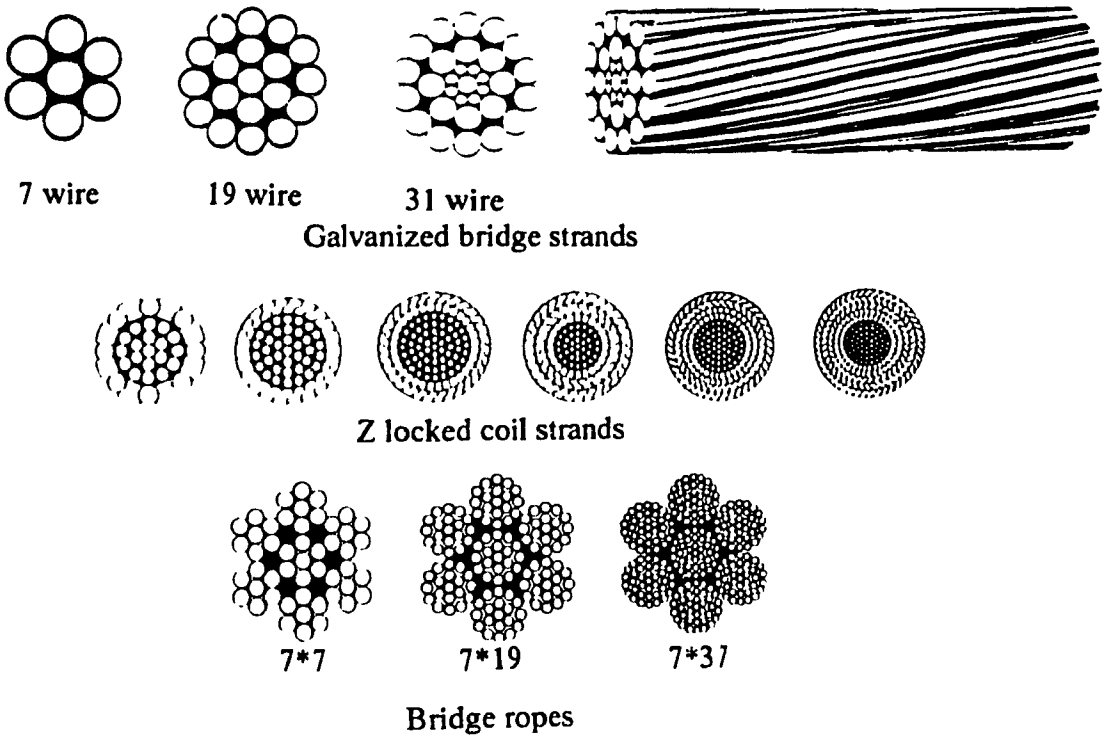

Figure 2.3. Common shape of the tendons.

The cables are protected from corrosion and the environmental effects by thin coatings of zinc to the wires and grouting the cables by epoxy resins, etc. The cables within the box sections are protected from environmental damages and can be maintained efficiently since the cables are easily reachable.

Allowable strength of the cables are calculated based on a factor of safety of 2.5 [35]. The prestressing design strength of seven wire strands are 0.7 f_{pu} to 0.8 f_{pu} , where f_{pu} is the ultimate strength of the cable (the breaking strength), [38]. Troitsky has provided the calculated st ength of the cables in equation (2.2) [35].

(2.2) $$R = R_{all}\ K\ m_1\ m_2$$

where, m_1 and m_2, the material performance coefficients, are equal to 0.8 and 0.74 and K is the effective safety factor against fracture or yielding equal to 1.5 to 2.5.

2.4. SADDLES

Saddles or cable guides are used to keep the cables properly in the desired configurations. Saddles are also working as vibration dampers for the cables[Szilard]. Cable guides along the straight portion of the cables are just supportive elements and no significant structural importance. In particular, saddles placed at the points where the slope of the cable is changing, are subjected to special design considerations which will be discussed in section 2.7 (Prestressing Losses). The contact area and the transverse profile of the saddles to be designed for suitable bearing pressure and should be formed to fit the desired cable placements along the girder. The friction between the cable and the saddle results in loss of initial prestressing force and induce a concentrated force (the resultant force) through the saddle, which should be accordingly supported, Figure 2.4. Therefore the saddles must be as much as possible frictionless to reduce the effect of friction on prestressed member. The use of guides mounted on ball bearings or rollers significantly reduces the effect of friction between the saddles and the cables. Similarly pulleys and other types of smooth surfaces may be used. In either case the losses due to friction and the induced friction force to the prestressed member should be included in the design process.

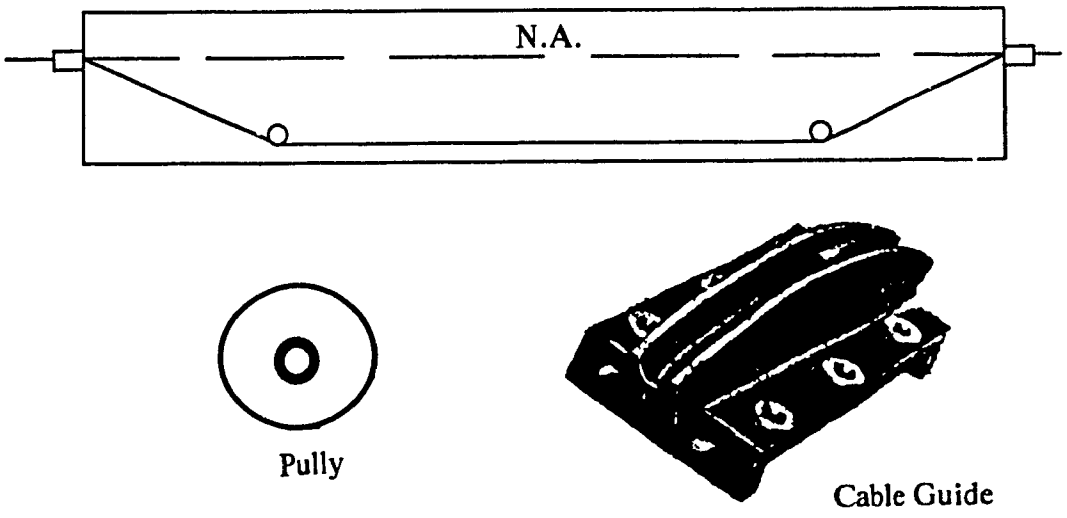

Figure 2.4. Saddles or cable guides.

2.5. END FITTINGS

The prestressed cables are fixed at the two ends by end anchorages. The manufacturing of the end anchorages has been significantly developed and variety of anchorages are available in the market, Figure 2.5 [39 & 40]. The end anchorages are active where the cables are prestressed by jacks and dead end or passive where the cables are only fixed at that end. The end anchorages are also subject to prestressing losses which occurs when the jacks are released (see section 2.7., Losses of Prestressing). The connections of the end anchorages to the member to transfer the cables' prestressing force must be designed in each individual case. Zielinski has performed a study on end blocks of prestressed concrete girders [40].

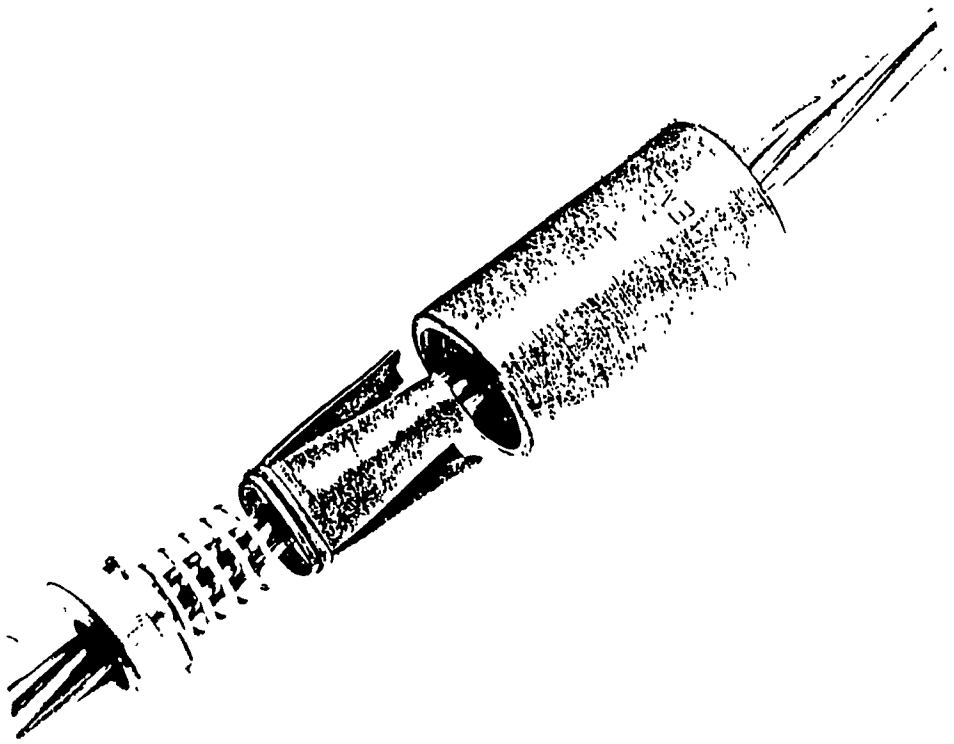

Figure 2.5. End anchorage for simple strand.

2.6. TENDON CONFIGURATIONS

In selection of a suitable longitudinal placement of the cables in prestressed steel girders a wide range of variables should be taken into account including: girder's structural function (whether simply supported or continuous), cross sectional geometry of the girder (symetrical, asymetrical, closed or open sections), cable characterstics (length, strength, cross sectional area), prestressing fixtures (saddles and end anchorages).

In general, to produce the maximum prestressing effect, the tendons should be placed as far as possible to the neutral axis in the tension zone of the girder in accordance with the bending moment diagram. However, at the two ends of the tendon it is appropriate to place the tendon at the neutral axix, otherwise a negative moment will be induced by the eccentric tendon which will have a reverse effect on the load bearing capacity of the continuous girder. In most cases it is not practical, if at all possible, to provide cable configuration exactly in accordance with the bending moment diagram which requires the use of many tendon guides which, in turn, will greatly increase the friction losses and manufacturing costs. Therefore, based on fundamental prestressing characters, several tendon configurations and cable cross sectional areas should be carefully examined before a final decision can be made. The general tendon placements are shown in Figure2.6.

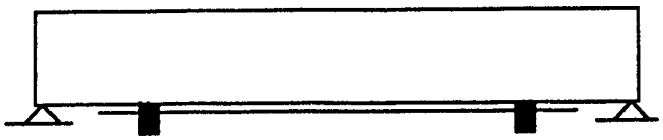

Short Tendon

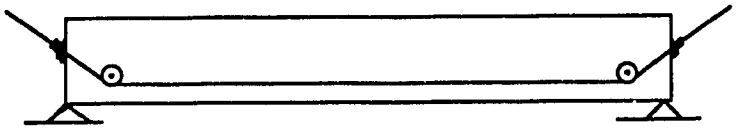

Draped or sloped tendon

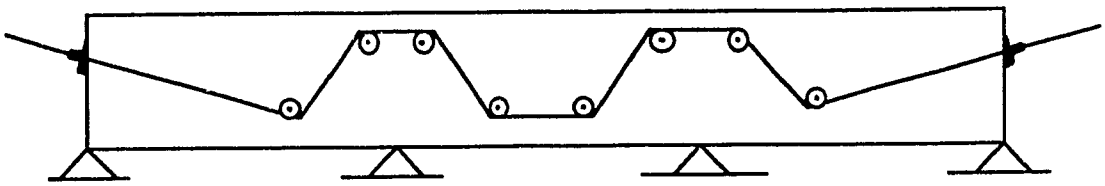

Draped continuous tendon

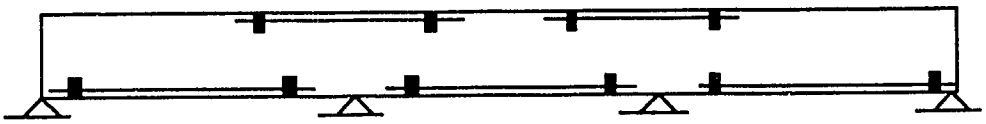

Partially Prestressed Continuous Girder with Short Tendons

Figure 2.6. General tendon configurations.

Basically, increasing the eccentricity of the cables from the neutral axis will proportionally increase the induced counterbalance prestressing force through the cables to the girder, Figure 2.8 shows the large eccentricity of the prestressed cables of a bridge in Germany. Use of large number of cables contributes to the uniform distribution of the cable forces to the girder elements avoiding the application of large values of concentrated forces at the end anchorages and saddles. On the other hand requires large number of saddles which increases the prestressing losses due to friction and significantly elevates the labor and material costs. Choice of fewer number of cables will have less installation problem but

at the points of slope changes where guides are installed large cable forces are induced, which in turn requires stronger connections. Figures 2.7 through 2.12 show practical examples of number of tendon configurations for prestressed steel girders [24, 41, 42, 43 and 44].

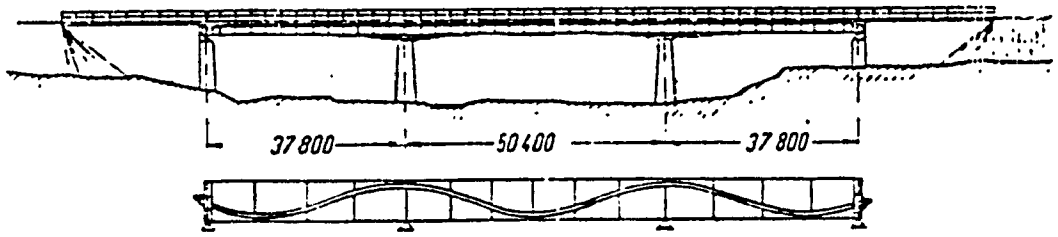

Figure 2.7. Elevation and tendon configuration of the bridge at Montabaur, W.G.

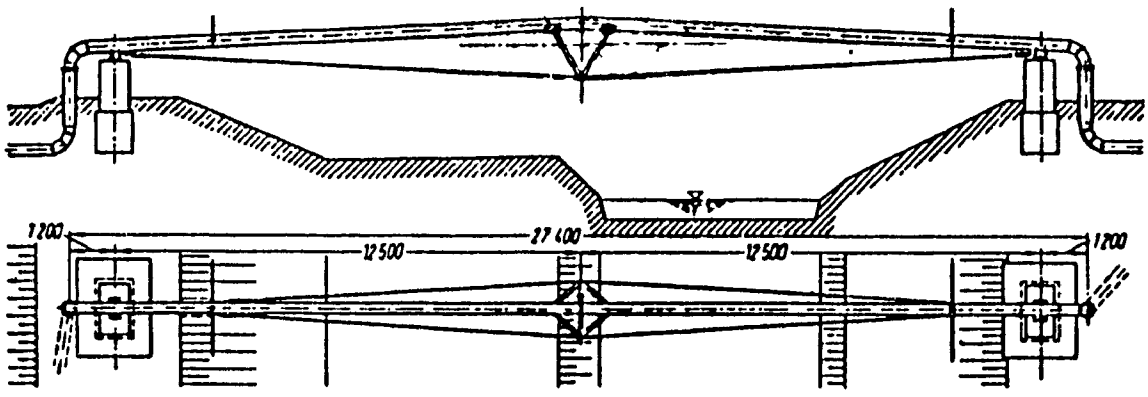

Figure 2.8. Pipe Gas Line over the Nitrica River, USSR.

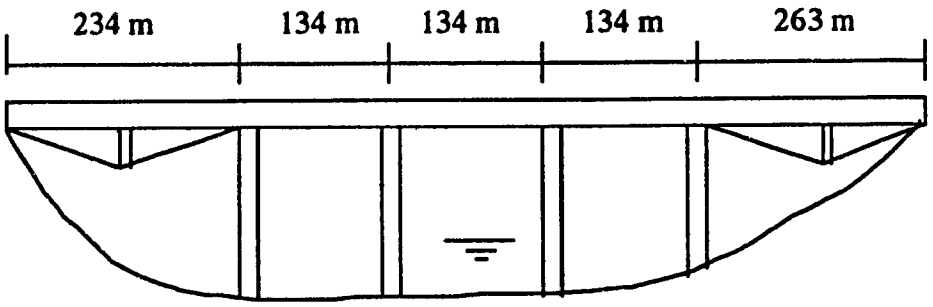

a) Span lengths and the tendon placement

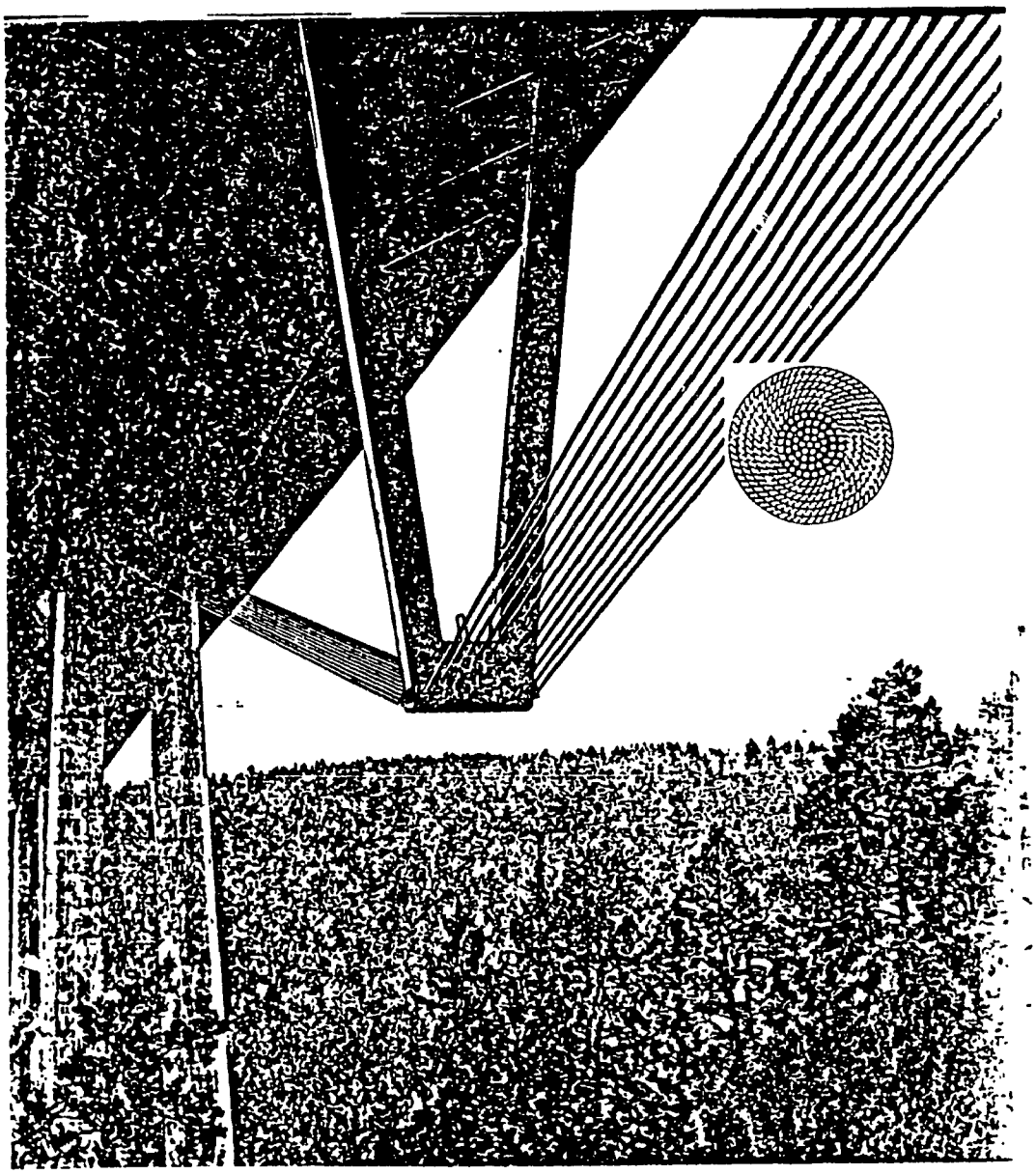

Figure 2.9. Neckar Valley Bridge, W.G., 1978.

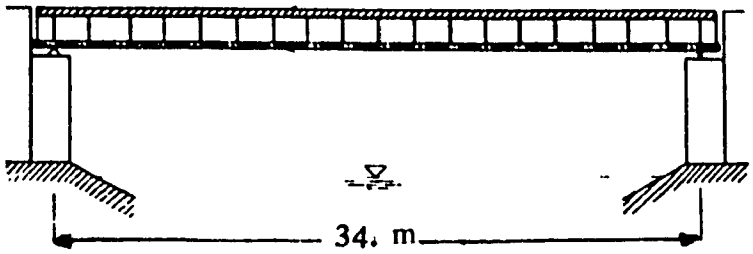

Figure 2.10. Tendon configuration of the prestressed bridge at Lauffen, W.G.

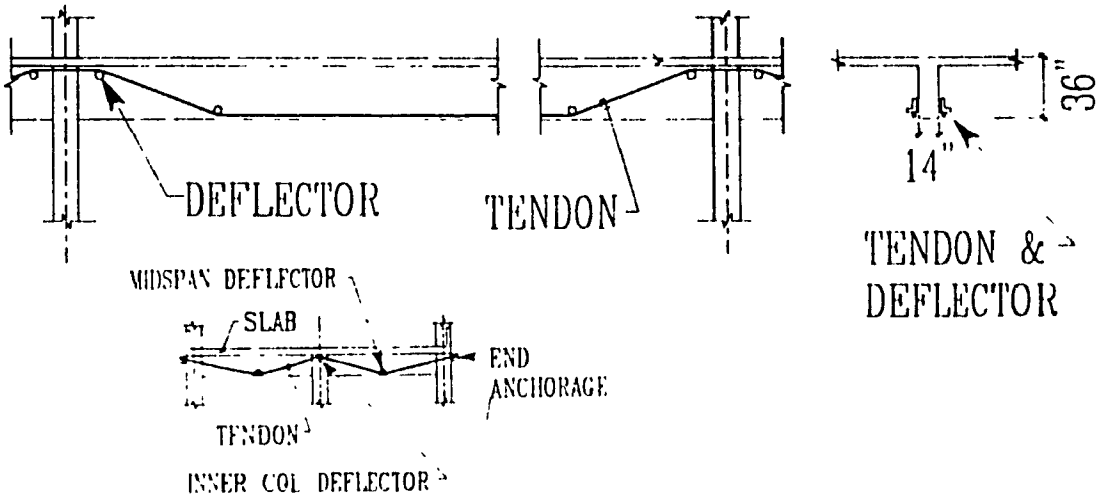

Figure 2.11. Rehabilitation of Pier 39 Parking Garage in San Francisco.

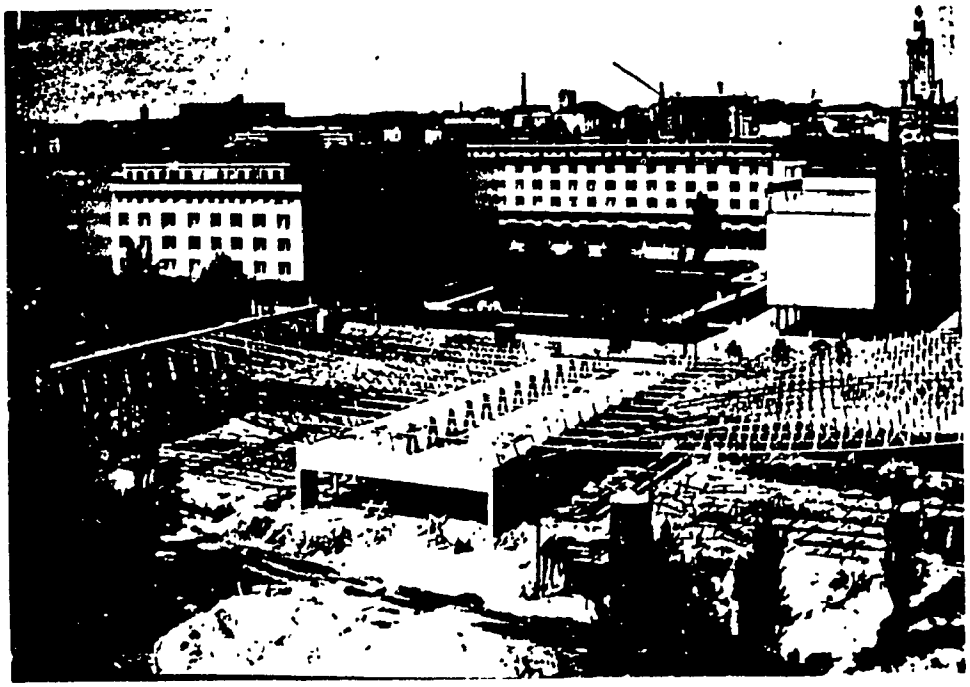

Figure 2.12. Tendon placement of the roof of the Super Sam shopping centre, Poland.

2.7. LOSSES OF PRESTRESSING

The initial prestressing force induced in the tendons is reduced due to the effect of steel relaxation, end anchorage slip, prestressing jacks and saddle frictions. The prestressing losses may be compensated by inducing additional initial prestressing force.

2.7.1. STEEL RELAXATION

The loss of prestress due to relaxation of steel girder and the tendon should be measured. The measured relaxation of ordinary steel sections indicate 3% increase in length subjected to stress of about 60% of its yield strength, [91].

The steel relaxation of the stretched tendon is a time dependent progressive loss which decreases the strength of the tendons. Figure 2.13 illustrates the strength loss versus time. Equation (2.3) with sufficient accuracy provides the relaxation loss for stress relieved wires and strands [45].

$$(2.3) \qquad \Delta f_{sr} = f_{ip} \frac{\log_{10}(t')}{10} \left(\frac{f_{si}}{f'_{Yt}} - 0.55 \right)$$

Δf_{sr} = steel relaxation stress at time t' hours after prestressing

f_{ip} = the initial prestressing stress , f_{si} = the initial stress

and the reduced yield strength of the tendon due to the offset stress $f'_{Yt} = f_{Yt} - 0.1\, f_{Yt}$, where f_{Yt} is the yield stress of the tendon.

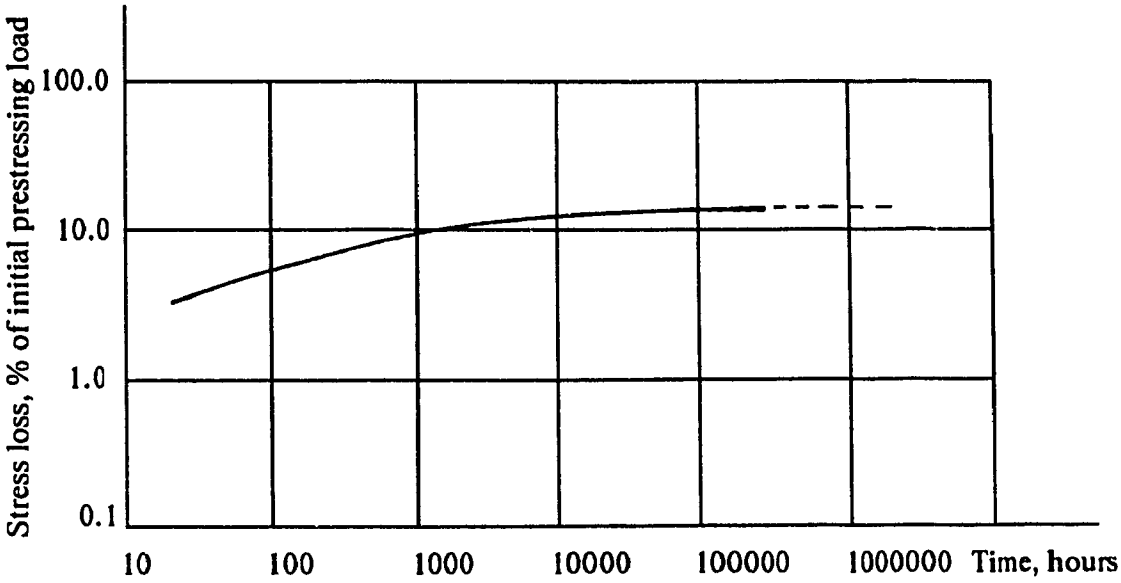

Figure 2.13. Prestressing loss due to steel relaxation.

The other proposed equation to compute the steel relaxation losses is given by the following equation, [46].

$$\Delta P_{sr} = \alpha (F_{Yt}\ A_t) \tag{2.4}$$

where ΔP_{sr} is the loss of the prestressing force due to the steel relaxation and α is a function of f_{Pi} / f_{Yt} and A_t is the cross sectional area of the tendon.

Both equations show that the effect of steel relaxation on the prestressed member depends on the initial prestressing force. Experiments show that up to the point where the initial stress f_{Pi} equals to 60 % of the yield stress f_{Yt} the loss due to steel relaxation is not significant and any increase in the initial prestressing force will accordingly and almost equally increase the value of the induced effective stress. The efficiency is progressively reduced due the the effect of relaxation such that at above 90% virtually no gain in effective stress is realized for increase in the initial prestressing force, Figure 2.14 [47].

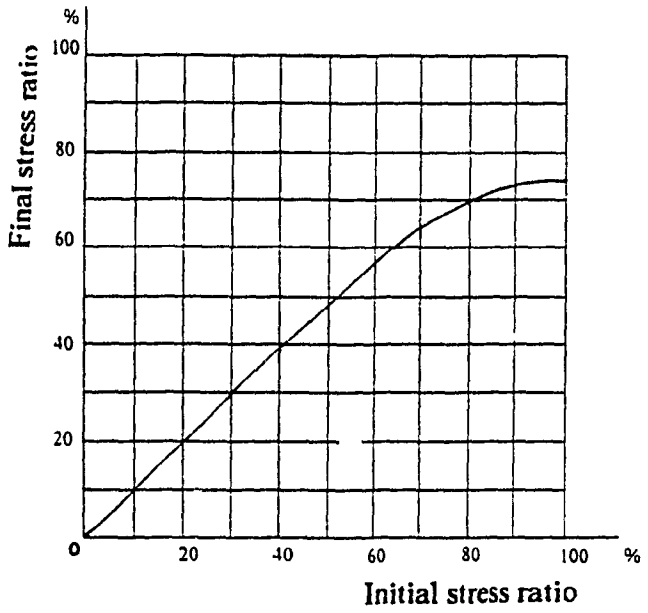

Figure 2.14. Final stress ratio versus initial stress r· · ·· tendons.

2.7.2. ANCHORAGE SLIPAGE

The prestressing force is applied to the tendons by prestressing jacks and transferred to the member through the end anchorages after the jacks are released. As soon as the jacks are released the end anchorages slips in to transfer the prestressing force to the member and as a result the cables are shorten and the initial prestressing force is reduced accordingly. The loss due to the slip in of the end anchorage ΔP_{sa} is equal to:

$$(2.5) \qquad \Delta P_{sa} = \frac{E_t \ \Delta_a \ A}{l}$$

E_t, A and l are the modulus of elasticity, the area and the length of the tendon, respectively and Δ_a is the slip length of the the anchorage. The value of Δ_a is equal to 1 mm to 5 mm depending on the type of the anchorage, [48].

2.7.3. FRICTION LOSS

Cables are placed at the tension zone of the girder and where necessary the tendon slopes have to be changed according to the required tendon configurations. At the points where the slope of the cables change, saddles or cable guides are provided. Friction forces occur at the points where the cables are transferred over the saddles, when the cables are stretched along the girder by prestressing jacks, Figure 2.15.

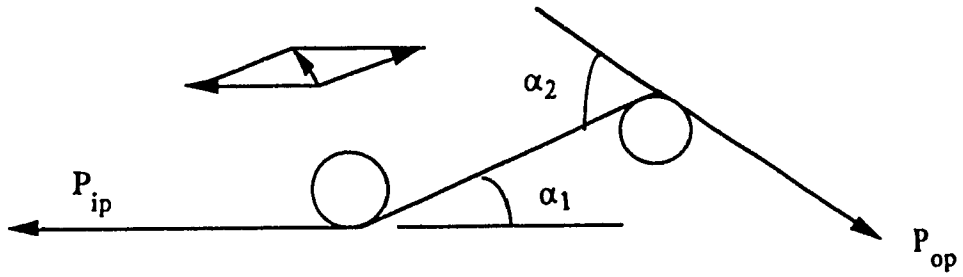

Figure 2.15. Friction Loss

The friction forces will impose a reduction in the initial prestressing force (incoming force along the tendon length) versus the prestressing force at the portion of the tendon just after the saddles (outgoing forces). The friction loss can be evaluated by the following equations.

$$(2.6) \qquad \Delta P_f = P_{ip} - P_{op} = 0.5\ \mu\ \text{arc}\ \Delta\alpha\ (P_{ip} + P_{op})$$

where P_{iP} and P_{iP} are the incoming and outgoing forces, μ is the friction coefficient, $\Delta\alpha = \alpha_1 + \alpha_2$ and the total friction loss is equal to the summation of the losses in each saddle[49].

The losses due to friction between tendons and the saddles has two major effect, the

primary curvature (draping) and the secondary curvature which is the deviation of the tendons at the bent points. Equation (2.7) includes the above effects [50].

$$(2.7) \qquad P_{ip} = P_{op}\, e^{(\mu\alpha + k x)}$$

P_{ip} and P_{op} are the incoming and the outgoing prestressing force in the tendon, respectively, μ and k are primary and secondary coefficients provided by reference[39]. α is the total angle change in radians, x is the distance from the jacking end to the point under consideration. The ratio of the frictional loss to the initial prestressing force (percentage of prestressing) can be defined by equation (2.8).

$$(2.8) \qquad \frac{\Delta P_f}{P_{ip}} = 1 - \frac{P_{op}}{P_{ip}} = 1 - e^{-(\mu\alpha + kx)}$$

CHAPTER III. STRUCTURAL ANALYSIS

3.1. INTRODUCTION

The static analysis of steel box girders prestressed by tendons cover the stress analysis in elastic range where the principle of superposition of forces and displacements is valid.

However the structural analysis of steel box girders prestressed by tendons is more complicated than non prestressed girders. The complication factors include:

a)The variable tendon position induces moment along the girder which changes in accordance to the eccentricity of the prestressing force from the neutral axis,

b)Elongation of tendons under service loads applied to the girder after the prestressing process is completed, causes an increase in the initial value of the prestressing force (incremental prestressing force),

c)Negative bending moments at the intermediate supports are reduced which makes the conventional non-prestressed continuous girders different in comparison with prestressed girders.

The prestressing force increment or self-increased prestressing force occurs when the prestressing process is completed and the girder is subjected to superimposed dead and live loadings. The initial prestressing force is increased. The prestressing force increment adds to the indeterminancy of the structure.

The analyses of bending moment and the prestressing force increment for simply supported spans has already been performed in details [17, 19, 51 & 52]. Brodka et al has presented the analysis of prestressing force increment for two and three continuous span girders, where the loads are applied at certain distances along the span, for example at mid spans [53].

The generalized analysis of prestressed continuous steel girders having variable span lengths and under arbitrary loading intensity and position is presented in this chapter.

The analysis is based on flexibility and virtual work methods. The indeterminate structure is converted to the determinate by assuming the redundants as the incremental prestressing force and the negative bending moments at the middle supports. The simultaneous equations of unknown redundants are written (flexibility method), and the deformation coefficients are calculated by the virtual work method. Matrix analysis is employed for the solution of redundants.

In particular, the incremental prestressing force and the negative bending moments (the unknown redundants) are formulated for various tendon configurations of two and three spans continuous girders. The bending moments and the shear forces at any section along the girder can then be calculated by the application of static equations of equilibrium. The incremental prestressing force for tensile members and simply supported girders are also presented in this chapter.

3.2. BASIC ASSUMPTIONS

a)Analysis of prestressed steel girders is performed in elastic range, assuming that stresses at each section are linearly distributed across the section. The principle of superposition of forces and deformations and other general assumptions applicable to elastic analysis are valid.

b)Draped tendon is placed at the tension zone along the girder.

c)Position of the neutral axis is assumed to be in the same level along the girder (constant cross-sectional properties throughout the girder).

d)Various spans are so loaded that the maximum bending moments either positive or negative are reached. The maximum incremental prestressing force occurs when all the

spans are loaded.

e)Negative bending moment induces tension at the top fibers of the section and compression at the bottom fibers, whereas the positive moment has a reverse effect on the girder.

f)The selected sign convention indicates a negative sign for compression and a positive sign for tension stresses.

3.3. PRESTRESSING FORCE INCREMENT

The prestressing force increment corresponds to the supplementary elongation of tendons caused by partial service loads (generally superimposed dead and live loads) applied to the structural member after the prestressing process is completed.

3.3.1. TENSILE MEMBERS

Prestressing is accomplished by the application of jacking force induced to tendons to counterbalance with the axial tensile forces in the member due to external loading. In practice the prestressing is completed prior to the application of superimposed dead and live loads. Accordingly, the initial effective prestressing force (considering the initial prestressing force reduced by prestressing losses) will be increased due to the cable elongation caused by these loadings. The system of prestressed member is structurally indeterminate by one degree, Figure 3.1. The prestressing force increment is the unknown.

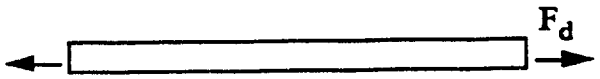

a. Tensile member prior to prestressing

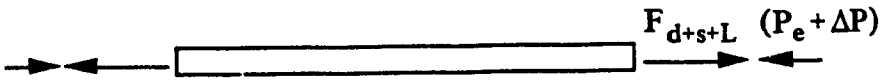

b. Prestressed system

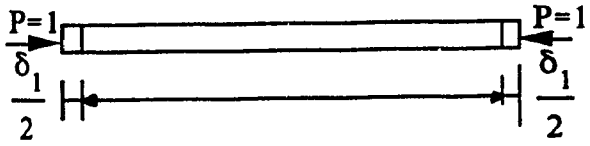

c. Released system under unit prestressing force

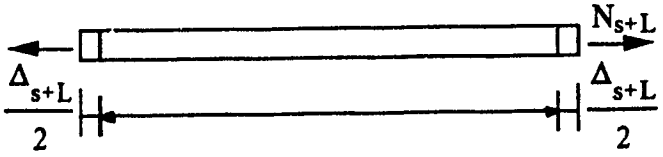

d. Released system subjected to applied service loads

Figure 3.1. Prestressed Tensile Members

The system is released and the compatibility equation for deformation (elongation of the cable and shortening of the tensile member) is written as Equation (3.1):

$$\delta_1 \Delta P - \Delta_{s+L} = 0. \qquad (3.1)$$

ΔP is the prestressing force increment, δ_1 and Δ_{s+L} are the elongation and shortening of the tendon and the member caused by unit prestressing force and partial service loads (superimposed dead and live loads), respectively. By virtual work method the values of these deformations are formulated as:

$$(3.2) \qquad \delta_1 = \int_L \frac{P_1^2}{E_t A_t} \, dx$$

$$(3.3) \qquad \Delta_{s+L} = \int_L \frac{P_1 N_{s+L}}{E A} \, dx$$

P_1 is a unit prestressing force along the tendon and N_{s+L} is equal to the superimposed dead and live loads (F_{s+L}) reduced by ΔP, ($F_{s+L} - \Delta P$).

Substitute for P_1 and N_{s+L} in Equations (3.2) and (3.3) to evaluate δ_1 and Δ_{s+L}. Solving Equation (3.1) for ΔP is formulated as Equation (3.4).

$$(3.4) \qquad \Delta P = - \frac{N_{s+L} E_t A_t}{E A + E_t A_t}$$

E and A and E_t and A_t are the moduli of elasticity and the cross sectional area of the member and the tendons, respectively. The negative sign indicates the compressive action of the prestressing force increment.

The value of the effective prestressing force P_e after applied service load is equal to:

$$(3.5) \qquad P_e = P_i + \Delta P \ , \qquad \text{(Note, } P_e = P_i \text{ when } N_{s+L} = 0 \text{)}$$

P_i is the initial prestressing force reduced by the prestressing losses (steel relaxation, anchorages slip in, etc.).

3.3.2. BENDING MEMBERS

3.3.2.1. SIMPLY SUPPORTED GIRDERS

Application of part of the service loads to a bending member already prestressed by tendons will cause additional elongation of the tendons. Accordingly the initial effective prestressing force P_e will increase by the value of the prestressing force increment ΔP.

The prestressed single span girder is structurally indeterminate (one degree of indeterminancy) due to the additional self increased prestressing force. To analyze the girder the structure is released and ΔP is taken as the redundant. The values of the deformations are evaluated by the virtual work method. The compatibility equation for the deformations along the girder is formulated as Equation (3.6). The corresponding flexibility values due to a unit prestressing force in the tendon and a unit vertical force applied to the girder at a distance x from the left support are presented in Equations (3.7) and (3.8), respectively, Figure 3.2. It should be noted that the effect of shear and torsion in the flexibility equations has been neglected due the insignificant contributions they may have in the calculation of the prestressing force increment.

$$(3.6) \qquad \delta_1 \, \Delta P + \Delta_{s+L} = 0. \qquad \text{or} \qquad \Delta P = - \frac{\Delta_{s+L}}{\delta_1}$$

$$(3.7) \qquad \delta_1 = \int_L \frac{m_x^2}{E\,I} \, dx + \int_L \frac{p_x^2}{E\,A} \, dx + \int_L \frac{p_x^2}{E_t\,A_t} \, dx$$

$$(3.8) \qquad \Delta_{s+L} = \int_L \frac{m_x \, M_x}{E\,I} \, dx + \int_L \frac{p_x \, N_{s+L}}{E\,A} \, dx$$

in which δ_1 and Δ_{s+L} are the deformations due to the unit prestressing force and the unit concentrated load, respectively. m_x and M_x are the bending moments at an arbitrary

distance x from the left support along the girder corresponding to the prestressing force and the superimposed dead and live loads. m_x is equal to a unit prestressing force by the value of the eccentricity at any section x, $m_x = 1 \cdot e_x$.

p_x and N_{s+L} are the axial loads due to unit prestressing force and applied service loads, however for simply supported bending members $N_{s+L} = 0$ and $p_x = 1.0$.

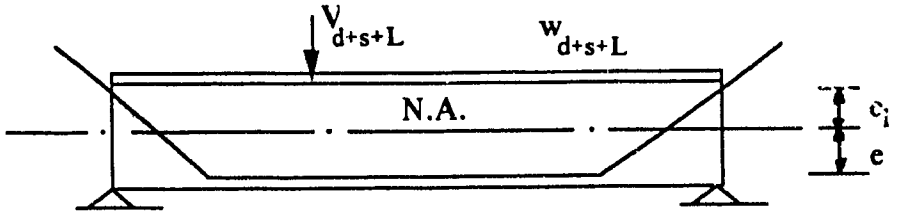

a. Prestressed system

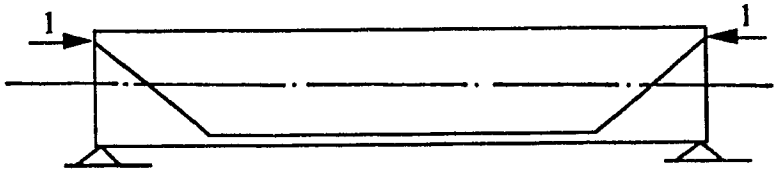

b. Released system under unit prestressing force

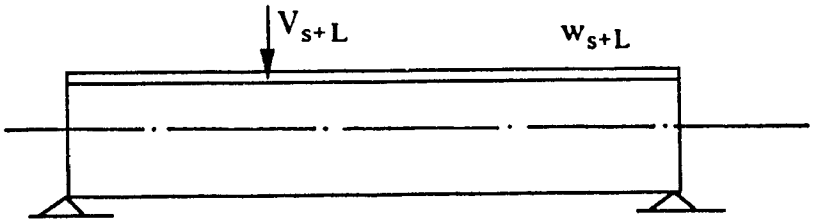

c. Released system under applied service loads

Figure 3.2. Prestressed simply supported girder

For the purpose of analysis the values of the bending moment and the axial forces can be formulated along the girder and substituted in the Equations (3.7) and (3.8) to obtain the flexibility coefficients δ_1 and Δ_{s+L}.

The value of the prestressing force increment can be calculated from Equation (3.6) for a concentrated load V_{s+L} at a section m from the left support and a prestressed draped tendon stretched along the girder with the bottom and top eccentricities e and e_1 from the neutral axis of the member, as shown in Figure 3.2, by substituting for the flexibility coefficients from the following equations. l, l_1, m and α are shown in Figure 3.2.

$$(3.9) \qquad \delta_1 = \frac{2}{EI}\left[\frac{l_1}{3}(e_1^2 - 2e^2 - ee_1) + \frac{l}{2}(e^2)\right] + \frac{l}{EA} + \frac{1}{E_t A_t}\left(l - 2l_1 + \frac{2l_1}{\cos^3\alpha}\right)$$

$$(3.10) \qquad \Delta_{s+L} = \frac{V_{s+L}}{2EI}\left[e\left(m^2 - ml + \frac{l_1^2}{3}\right) + e_1\left(\frac{l_1^2}{3}\right)\right]$$

Similar equation can be developed for the effect of a uniformly distributed load w_{s+L} on the girder, Equation (3.11):

$$(3.11) \qquad \Delta_{s+L} = \frac{w_{s+L}}{12EI}\left\{e\left[l^3 + l_1^2(2l - l_1)\right] - e_1 l_1^2(2l - l_1)\right\}$$

The total value of the incremental prestressing force can be obtained by the summation of ΔP for various loading cases. The prestressing force increment is dependent on the loading and geometrical properties of the girder and the tendons but it is independent of the initial effective prestressing force.

3.3.2.2. PRESTRESSING FORCE INCREMENT OF CONTINUOUS SPAN GIRDERS

The analysis presents the most general approach for the calculation of the prestressing force increment of a continuous span girder prestressed by draped tendons at the tension regions (fixed at the two ends only) and having variable span lengths and under arbitrary loading intensity and position.

The static analysis covers the elastic range and the principles of linear distribution of stresses and superposition of forces and deformations are valid. The analysis is based on flexibility and virtual work methods. The indeterminate structure is converted to the determinate by assuming the redundants as the incremental prestressing force and the negative bending moments at the middle supports, Figure 3.3. The simultaneous equations of unknown redundants are written (flexibility method), and the deformation coefficients are calculated by the virtual work method. Matrix analysis is employed for the solution of redundants.

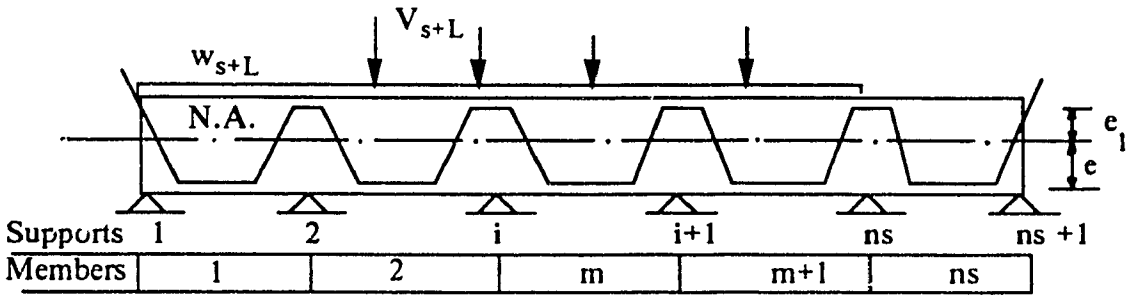

a. Prestressed continuous girder

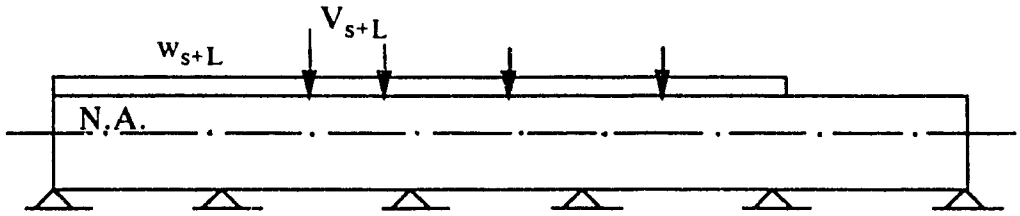

b. Released system under partial service loads

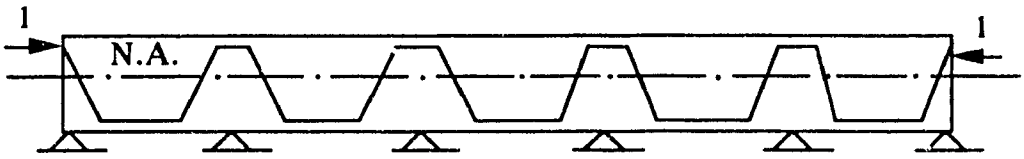

c. Released System Due to a Unit Prestressing Force

Figure 3.3. Prestressed continuous span girder, prestressing tendon and superimposed loading.

The application of variable prestressing forces and then service load (superimposed dead and live loads) along the girder increases the degree of indeterminancy of the structure by one due to the effect of the self-increased prestressing force. The flexibility method simplifies the analysis of such indeterminate structures. The redundants are taken as:

a)The incremental prestressing force.

b)Bending moments at the middle supports (negative bending moments).

The flexibility equations can be written using the principle of superposition of deformations at the points of interest. Considering a continuous girder of (ns -1) intermediate supports, the sum of deformations at the point of redundant number 1 (at the first middle support from the left), is given as:

$$(3.12) \quad \delta_{11} . M_1 + \delta_{12} . M_2 + ...+ \delta_{1,ns} . \Delta P = \Delta_{1L} ,$$

Where:

ns = number of spans

- M_i is the bending moment at support i and δ_{1i} is the deformation at point 1 caused by a unit load corresponding to M_i at i $(1 \leq i \leq ns - 1)$

- Δ_{1L} is the deformation at point 1 corresponding to the applied service loads (superimposed dead and live loads).

- ΔP is the incremental prestressing force and $\delta_{1,ns}$ is the elongation caused by a unit load corresponding to ΔP

Similarly additional equations are written as the simultaneous Equations (3.13).

$$\delta_{11} \cdot M_1 + \delta_{12} \cdot M_2 + \ldots\ldots + \delta_{1j} \cdot \Delta P = \Delta_{1L}$$

$$\delta_{21} \cdot M_1 + \delta_{22} \cdot M_2 + \ldots\ldots + \delta_{2j} \cdot \Delta P = \Delta_{2L} \qquad (3.13)$$

$$\ldots\ldots\ldots\ldots\ldots\ldots\ldots\ldots\ldots\ldots\ldots\ldots\ldots\ldots\ldots\ldots\ldots\ldots\ldots\ldots$$

$$\delta_{i1} \cdot M_1 + \delta_{i2} \cdot M_2 + \ldots\ldots + \delta_{ij} \cdot \Delta P = \Delta_{iL}$$

where $i = 1, ns$, and $j = 1, ns$

The simultaneous Equations (3.13) in a matrix form is shown as Equation (3.14).

$$\begin{bmatrix} \delta_{11} & d_{12} & . & . & \delta_{1j} \\ \delta_{21} & \delta_{22} & . & . & \delta_{2j} \\ . & . & . & . & . \\ \delta_{i1} & \delta_{i2} & . & . & \delta_{ij} \end{bmatrix} * \begin{Bmatrix} M_1 \\ M_2 \\ . \\ \Delta P \end{Bmatrix} = \begin{Bmatrix} \Delta_{1L} \\ \Delta_{2L} \\ . \\ \Delta_{iL} \end{Bmatrix} \qquad (3.14)$$

Equation (3.14) can be written in simplified form as follow:

$$[\ \delta_{ij}\ ] .\{\ M_{ns-1}, \Delta P\ \} = \{\ \Delta_{iL}\ \} \qquad i = 1 \text{ to } ns \qquad j = 1 \text{ to } ns \qquad (3.15)$$

$$\{\ M_{ns-1}, \Delta P\ \} = [\ \delta_{ij}\ ]^{-1} . \{\ \Delta_{iL}\ \}, \qquad (3.16)$$

where $i = 1$ to $ns - 1$, $j = 1$ to $ns - 1$, $k = ns$, and $[\ \delta_{ij}\ ]^{-1}$ is the inverse flexibility matrix.

The variable (ns) represents the number of spans, (ns -1) indicates the number of intermediate supports, M corresponds to the negative bending moment at supports, and (ΔP) correspond to the incremental prestressing force. The subscript L relates to the deformations caused by the applied service loads.

The flexibility coefficients δ_{ij}, and Δ_{iL} can be calculated by virtual work method. By equating the internal work performed by the internal induced stresses along the girder, and the external work done by a unit load and the corresponding deformations. The expression for the flexibility coefficients (neglecting the shear and torsion effects) is derived as:

$$(3.17) \quad \delta_{mn} = \int_L \frac{M_m M_n}{E I} dx + \int_L \frac{N_m N_n}{E A} dx$$

where, M_m is the bending moment at an arbitrary position on the entire length of the m^{th} span due to the partial service loadings, and N_m is the axial force of the same span.

For analysis of the flexibility coefficients (δ_{ij} and Δ_{iL}), the general equations for bending moments and axial forces at any section x, over the entire length of the span must be written considering the variation of the cross sectional properties of the girder and of the tendons, [54].

The corresponding bending moment and the axial force diagrams for a three span continuous girders having constant cross sectional areas and prestressing force intensity are illustrated in Figures 3.4 and 3.5. Figure 3.4 shows the geometry of the assumed girder and the tendon configurations. The released structure is shown in Figure 3.4.b. Figures 3.4.c and 3.4.d demonstrate the bending moment diagrams of the released structure due to a concentrated load at distance m and a uniformly distributed load over a typical span. Figures 3.5.a through 3.5.c illustrate the bending moment diagrams due to a unit arbitrary load at the corresponding redundant. The effect of a unit prestressing axial force along the entire girder is shown in Figures 3.5.d and 3.5.e.

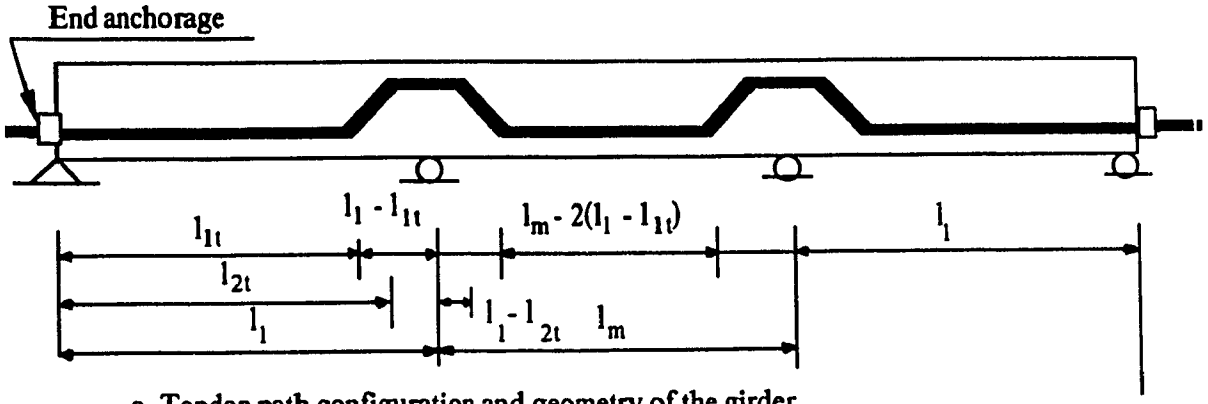

a. Tendon path configuration and geometry of the girder

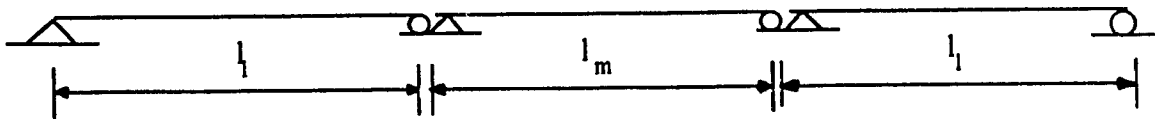

b. Indeterminate continuous beam is transformed to determinate (released system)

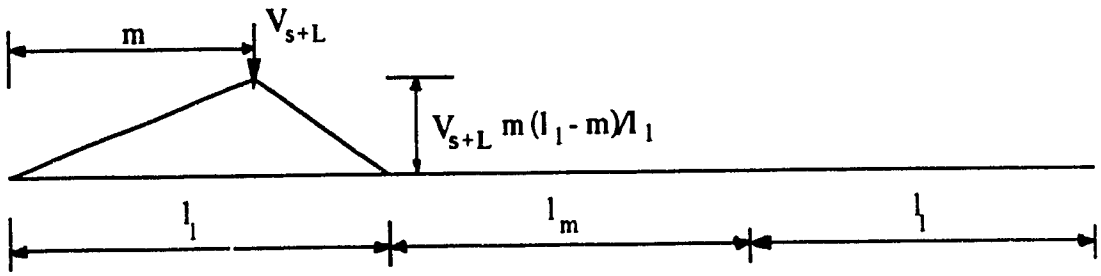

c. Typical bending moment diagram due to concentrated load at distance m, on any arbitrary span, e.g. span l_1

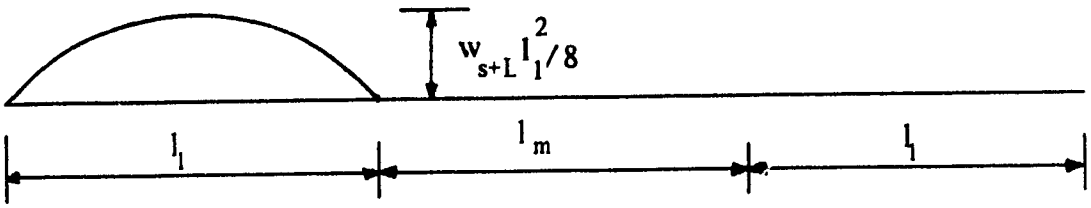

d. Typical bending moment diagram due to a uniformly distributed load on any arbitrary span, i.e. span l

Figure 3.4. A general tendon path configuration and bending moment diagrams for prestressed steel continuous girders.

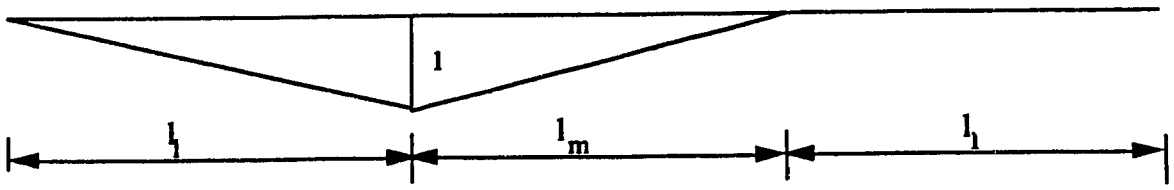

a. Unit moment at intermediate support 1.

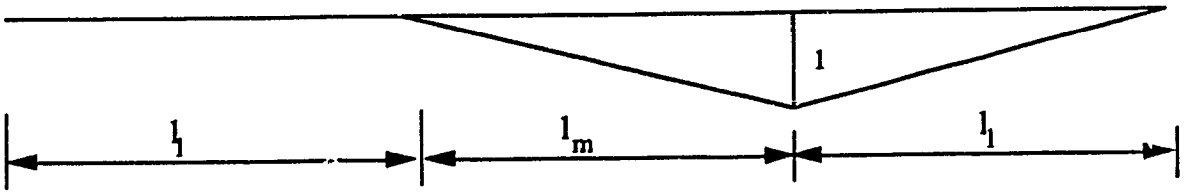

b. Unit moment at intermediate support 2

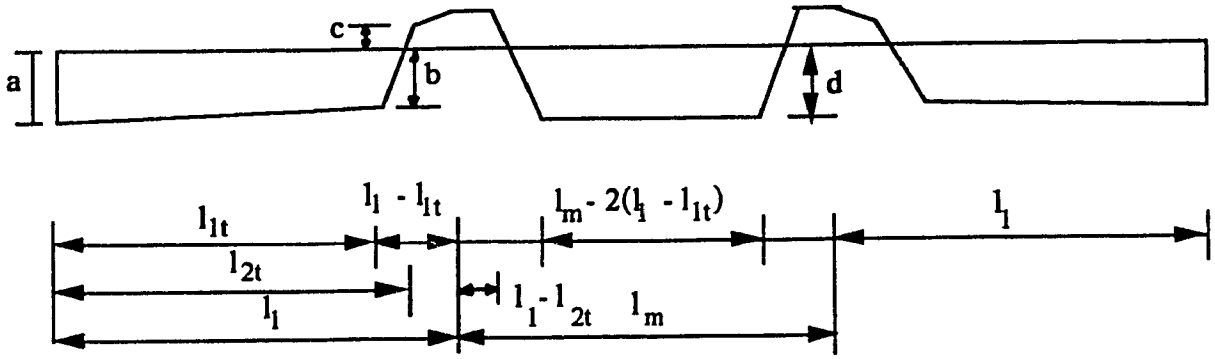

c. Prestressing moment due to a unit prestressing force in the tendon

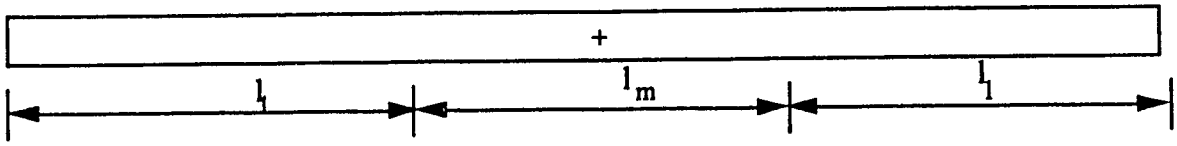

d. Axial force diagram due to a unit force along the girder

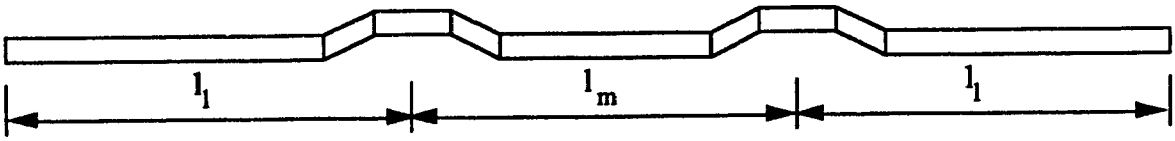

e. Axial force diagram due to a unit force along the tendon

Figure 3.5. Bending moment diagrams.

Equations (3.18.a) and (3.18.b) indicate the moments at any section x from the left support along the two adjacent spans on the released structure and caused by a unit negative moment at the i^{th} internal support, where, $i = 1$ to $ns - 1$.

(3.18)

$$M_i = -\frac{x}{l_i} \qquad \text{for the interval} \qquad 0 \geq x \geq l_i \qquad (a)$$

$$M_i = -\left(1 - \frac{x}{l_{i+1}}\right) \qquad \text{for the interval} \qquad 0 \geq x \geq l_{i+1} \qquad (b)$$

Equations (3.19.a) through (3.19.h) illustrate moments for various intervals along the girder corresponding to a unit prestressing axial force applied by the tendons. M_1 is the equation for the moment distribution along the first span and the last one ($M_{ns-1} = M_1$). Whereas, M_k indicates the moment equations for any span (k). The length of the straight tendons over the internal supports ($l_1 - l_{2t}$) and the inclined part of tendons ($l_{2t} - l_{1t}$) are equal for all spans.

(3.19)

$$M_1 = -\left(a + \frac{b-a}{l_{1t}} \cdot x\right) \qquad 0 \geq x \geq l_{1t} \qquad (a)$$

$$M_1 = -\left[b - \frac{b+c}{l_{2t} - l_{1t}}(x - l_{1t})\right] \qquad l_{1t} \geq x \geq l_{2t} \qquad (b)$$

$$M_1 = -\frac{c}{l_1 - l_{2t}}(x - l_1) \qquad l_{2t} \geq x \geq l_1 \qquad (c)$$

$$M_k = 0. \qquad 0 \geq x \geq l_1 - l_{2t} \qquad (d)$$

$$M_k = -\frac{d}{l_{2t} - l_{1t}}\left[x - (l_1 - l_{2t})\right] \qquad l_1 - l_{2t} \geq x \geq l_1 - l_{1t} \qquad (e)$$

$$M_k = -d \qquad l_1 - l_{1t} \geq x \geq l_k - (l_1 - l_{1t}) \qquad (f)$$

$$M_k = -\frac{d}{l_{1t} - l_{2t}}(x - l_k + l_1 - l_{2t}) \qquad l_k - (l_1 - l_{1t}) \leq x \leq l_k - (l_1 - l_{2t}) \qquad (g)$$

$$M_k = 0 \qquad l_k - (l_1 - l_{2t}) \leq x \leq l_k \qquad (h)$$

in which, $k = 2$ to $ns - 1$, $a = e_{1b}$, $b = e_{1b} + e_{1t}\,(I_{1t}/I_1)$, $c = e_{1t}(1 - I_{2t}/I_1)$ and $d = e_{kb} + e_{kt}$. e_t and e_b are the top and bottom tendon eccentricities from the neutral axis.

The moment equation (3.20.a) demonstrates the change in moment over span (j) due to the uniformly distributed load of unit intensity, w_{s+L}. Similarly Equations (3.20.b) and (3.20.c) specifies the moments for span (j) caused by the concentrated load, V_{s+L}, at distance m from the support (n - 1). The spans are loaded such that the maximum negative moment is created at the intermediate supports.

$$M_{kL} = \frac{(I_k\, x - x^2)}{2} \qquad \text{for the interval} \quad 0 \geq x \geq I_k \qquad (a)$$

(3.20)
$$M_{kL} = \frac{(I_k - m)\,.\,x}{I} \qquad \text{for the interval} \quad 0 \geq x \geq m \qquad (b)$$

$$M_{kL} = \frac{m\,.\,(I_k - x)}{I_k} \qquad \text{" " "} \quad m \geq x \geq I_k \qquad (c)$$

For all values of $k = 1$ to ns.

The flexibility coefficients for continuous span girders prestressed by tendons can be derived by substituting the values of the variables, the bending moment and the axial loads, into Equation (3.17) and integrating the expression over the span length L. For variable cross sectional properties of the tendons and the girder (area and section modulus) the integration of the expression are complicated and the use of an approximate method such as Simpson's rule and a computer program seems inevitable. However, such equations for the case of constant cross sectional area of tendons and girder are generalized for multiple span continuous girders. The flexibility coefficients for a multiple span girder of ns spans - each having various lengths and cross-sectional properties as indicated by the subscript m which defines the respective properties of the m^{th} intermediate span - can be formulated as:

(3.21) $$\delta_{11} = \frac{l_l}{3 . E . I_l} + \frac{l_m}{3 . E . I_m}$$

(3.22) $$\delta_{22} = \frac{2 . l_m}{3 . E . l_m}$$

(3.23) $\delta_{kk} = \delta_{22}$ where k = 2, ns - 2 and for ns ≥ 4

(3.24) $\delta_{jj} = \delta_{11}$ " j = ns - 1

(3.25) $$\delta_{12} = \frac{l_m}{6 . E . I_m}$$

(3.26) $\delta_{13} = 0$

(3.27) $\delta_{1j} = 0$, where j = 3, ns - 1

(3.28) $\delta_{ij} = \delta_{ji}$ for all values of i = 1, ns and j = 1, ns

(3.29) $$\delta_{1,ns} = \frac{1}{6 . E . I_l . l_l} [a\, l_{1t}^2 + b\, l_{2t}^2 + b\, l_{1t} l_{2t} + c(l_{1t}^2 - l_l^2 + l_{1t} l_{2t} - l_l l_{2t})] + \frac{d}{2 . E . I_m} (l_m - 2 l_l + l_{1t} + l_{2t})$$

(3.30) $\delta_{j,ns} = \delta_{1,ns}$ for j = ns - 1

(3.31) $$\delta_{k,ns} = \frac{d}{E . I_m} (l_m - 2 l_l + l_{1t} + l_{2t})$$

where k = 2, ns - 2 for all values of ns ≥ 4

(3.32) $$\delta_{ns,ns} = \frac{2}{3 . E . I_l} [l_{1t} (a^2 + b^2 + a b) + (l_{2t} - l_{1t}) (b^2 + c^2 - b c) + c^2 (l_l - l_{2t})] + \frac{d^2}{E . I_m} [\frac{2}{3} (l_{2t} - l_{1t}) + l_m - 2 (l_l - l_{1t})] + 2 l_l (\frac{1}{E A_l} + \frac{1}{E_t A_t}) + l_m (ns - 2) (\frac{1}{E A_m} + \frac{1}{E_t A_t}) + \frac{2 (ns - 1)}{E_t A_t} (\frac{1}{\cos a^3} - 1)$$

The flexibility coefficients δ_{ij} are the deformations at section j due to a unit load at

section i. The subscript ns is equal to the number of spans and at the same time it refers to the incremental prestressing force ΔP as the last redundant. The integers i through k are chosen as variable subscripts increasing by step one.

The deformations at the corresponding redundants i due to the actual loadings including the service loads and the prestressing force are defined as Δ_{iL}. The subscript U stands for uniformly distributed loads and C refers to a concentrated load.

$$(3.33) \quad \Delta_{1LU} = -\left(\frac{l_1^3}{24 \cdot E \cdot I_1} + \frac{l_m^3}{24 \cdot E \cdot I_m}\right) w_{s+L}$$

$$(3.34) \quad \Delta_{jLU} = -\left(\frac{2 \cdot l_m^3}{24 \cdot E \cdot I_m}\right) w_{s+L} \quad \text{for } j = 2,\ ns-2 \quad \text{and } ns \geq 4$$

$$(3.35) \quad \Delta_{jLU} = \Delta_{1LU} \quad , \qquad \text{for } j = ns-1$$

$$(3.36) \quad \Delta_{1LC} = -\left[\frac{m(l_1^2 - m^2)}{6 \cdot E \cdot I_1 \cdot l_1} + \frac{n(l_m - n)(2 \cdot l_m - n)}{6 \cdot E \cdot I_m \cdot l_m}\right] V_{s+L}$$

$$(3.37) \quad \Delta_{jLC} = -\frac{V_{s+L}}{6 \cdot E \cdot I_m \cdot l_m} \cdot \left[n(l_m^2 - n^2) + n(l_m - n)(2 \cdot l_m - n)\right] ,$$

where $j = 2,\ ns-2$ for $ns \geq 4$

$$(3.38) \quad \Delta_{jLC} = \left[-\frac{n(l_m^2 - n^2)}{6 \cdot E \cdot I_m \cdot l_m} - \frac{m(l_1 - m)(2 \cdot l_1 - m)}{6 \cdot E \cdot I \cdot l_1}\right] V_{s+L}$$

for $j = ns - 1$

$$(3.39) \quad \Delta_{iL} = \Delta_{iLU} + \Delta_{iLC} , \qquad \text{for } i = 1,\ ns$$

where Δ_{iL} is the sum of deformations due to concentrated and distributed loadings.

$$(3.40)\quad \Delta_{ns,\,LU1} = -\frac{w_{s+L}}{2EI}\left\{\left[\frac{l_1 l_{1t}^2}{6}(2b+a) - \frac{l_{1t}^3}{12}(3b+a)\right] + \frac{l_{1t}+l_{2t}}{2}\left[b\left(l_1 l_{2t} + \frac{l_{1t}^2+l_{2t}^2}{2}\right) + c\left(l_1 l_{1t} + \frac{l_{1t}^2+l_{2t}^2}{2}\right)\right] + \left(\frac{l_{1t}^2+l_{2t}^2+l_1 l_2}{3}\right)\left[-b(l+l_2) - c(l+l_1)\right] + c\left[\frac{2l_1}{3}(l_1^2+l_{2t}^2+l_1 l_{2t}) - \left(\frac{l_1+l_{2t}}{4}\right)(3l_1^2+l_{2t}^2)\right]\right\}$$

where $\Delta_{ns,\,LU1}$ corresponds to deformations in tendons due to a uniformly distributed load, w_{s+L}, applied on the side spans.

$$(3.41)\quad \Delta_{ns,\,LC1} = -\frac{V_{s+L}}{E.I}\left[m.a\left(-\frac{m}{2} + \frac{m^2}{6.l_1} + \frac{l_1}{2} - \frac{l_1^2}{6.l_1}\right) + m.b\left(-\frac{m^2}{6.l_1} + \frac{l_2}{2} - \frac{l_2^2+l_1.l_2}{6.l_1}\right) + m.c\left(\frac{l_2}{6} + \frac{l_1}{2} - \frac{l_1^2+l_1.l_2}{6.l_1} - \frac{l_1}{3}\right)\right]$$

Similarly, $\Delta_{ns,\,LC1}$ defines the deformations in tendons due to a concentrated load at distance m from the extreme left and right supports, V_{s+L}.

$$(3.42)\quad \Delta_{ns,\,LUm} = -\frac{d.w_{s+L}}{12.EI_m}\left\{4(l_m - l_1 - l_{2t})\left[(l_1-l_{1t})^2 + (l_1-l_{2t})^2 + (l_1-l_{1t})(l_1-l_{2t})\right] - 3(2l_1 - l_{1t} - l_{2t})\left[(l_1-l_{1t})^2 + (l_1-l_{2t})^2 + 2l_m(l_1-l_{2t})\right] + (l_m - 2l_1 + 2l_{2t})\left[l_m^2 + 2l_m(l_1-l_{1t}) - 2(l_1-l_{1t})^2\right]\right\}$$

The coefficient $\Delta_{ns,\,LUm}$ represents the deformation of the m^{th} intermediate span under the application of a unit uniformly distributed load.

$$(3.43) \qquad \Delta_{ns,\,LC\,m} = -\frac{d.V_{s+L}}{6\,E\,I_m}\left[(l_{2t}-l_{1t})(3l_1-2l_{1t}-l_{2t})+3n(l_m-n)-3(l_1-l_{1t})^2\right]$$

$\Delta_{ns,\,LCm}$ is the corresponding deformation of the prestressing tendons due to a unit concentrated load.

When the unknown redundants, the bending moments at the intermediate supports and The incremental prestressing force is calculated, then the bending moment, the shear and the axial force along the girder can be analyzed by using the static equations of equilibrium.

A computer program has been written on the basis of the given equations for the analysis of the prestressed steel continuous span girder with variable tendon and girders cross sectional properties. The input data of such program is the geometry of the girder and the tendon configurations including the cross sectional properties of the girder. The program is designed to compute the negative bending moments and the incremental prestressing force for continuous steel girders having three or more spans, Appendix C.

The flexibility coefficients for the two equal span continuous girders are given in Section 5.3. Numerical examples for two and three span steel girders prestressed by tendons are provided in Appendix A.

3.4. BENDING MOMENTS

The values of bending moments at any section along the girder are the sum of moments due to service loadings and the prestressed tendons. The prestressed tendons are placed along the girder in such a manner that they induce moments at any arbitrary section opposite in effect to those caused by the service loads. The tendons' path configurations, cross sectional area and its eccentricities from the neutral axis of the girder demonstrate the

rate of efficiency of prestressing techniques which increase the strength and the load carrying capacity of the member. The larger the value of the eccentricity e and of the cross sectional area of the tendons, the greater will be the counterbalancing effect of the prestressing moment. However there exist limits beyond which the effect of prestressing will be reversed, that is discussed in Section 4.4. Prestressing Limits.

In general, the effective bending moment for a girder prestressed by tendons can be expressed by Equation (3.44).

(3.44) $$M = M_{d+s+L} + (P_e + \Delta P)\cdot e$$

Where M_{d+s+L} is the bending moment due to the dead, superimposed dead and the live loads (total service loads). P_e, ΔP and e are the effective prestressing force after deduction of the losses, the prestressing force increment and the eccentricity of the tendon, respectively. The value of eccentricity e varies along the girder in accordance with the cable configuration. For a straight tendon e is constant whereas for a draped tendon it is variable and at any case it is defined as the distance between the neutral axis of the girder and the center of gravity of the prestressing tendons.

For simply supported flexural members the value of M at any section can be calculated from the static equations of equilibrium and the incremental prestressing force from the equations given in Section 3.3. Figure 3.6 illustrates the bending moment diagram for straight and draped tendons.

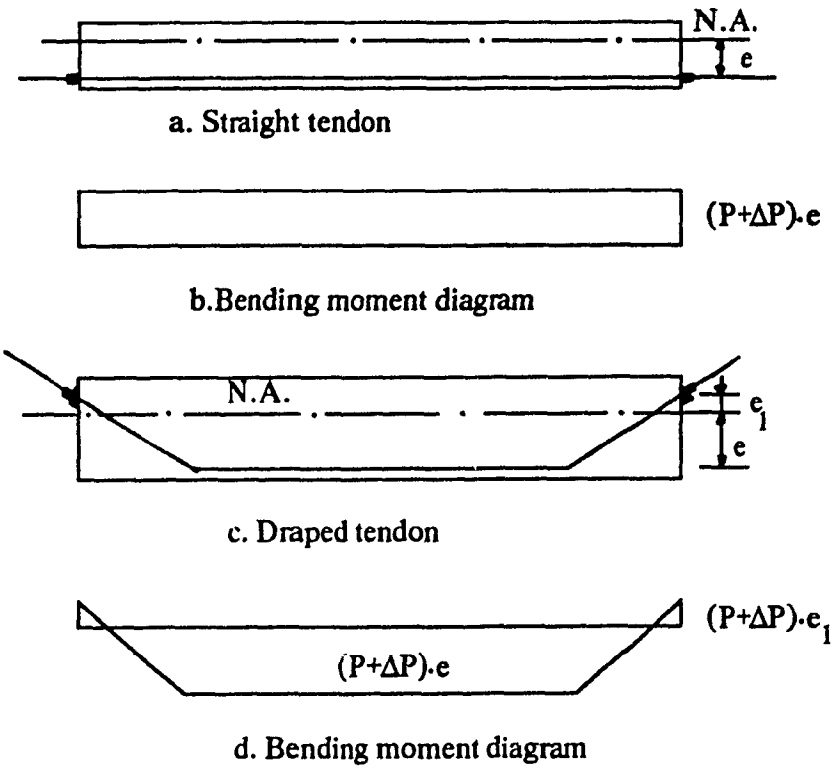

Figure 3.6. Bending moment diagrams due to prestressing forces

In the case of continuous multi-span girders the calculations of the bending moment at any arbitrary section consist of the sum of three terms:

1) moment due to the partial service loading (depending on the prestressing procedure, generally dead loads, M_d) applied to the girder prior to the implication of the prestressing force while the prestressing jacks are not released

2) the second term refers to the moments caused by the superimposed dead and live loads which are applied after the prestressing forces are induced to the girder (the jacks are released), M_{s+L}

3) the bending moment due to the prestressing effects, $(P_e + \Delta P)\cdot e$

The first term M_d can be computed by conventional methods of analysis of

continuous span girders. However for the calculation of the second term M_{s+L} the effect of prestressing should be considered. Solving the simultaneous Equations (3.13), expressed in matrix form as Equation (3.18), gives the bending moments at the intermediate supports. These equations show that negative bending moments at the intermediate supports M_{s+l} are dependent on the cross sectional areas of the tendons and the girder as well as on the eccentricity of the prestressing cables.

CHAPTER IV. DESIGN CONCEPTS AND STRESS DISTRIBUTION

4.1. INTRODUCTION

The load carrying capacity of a girder can be substantially increased when efficiently prestressed by tendons. The tendons are high strength steel cables placed at the extreme possible distance from the neutral axis in the tension region of the girder. The configuration, total cross-sectional area, the eccentricity from the neutral axis and the strength of the cables are the main characteristics to be considered in the design of prestressed steel girders. On the part of the girder a proper choice of the cross sectional properties can greatly contribute toward the efficiency of prestressing.

The combined stresses at any arbitrary section along the girder including stresses caused by the service loads and that of the prestressed tendons at various stages of loading should not exceed the required allowable stress limits. Therefore the prestressing process should be defined and followed accordingly in the construction period. In general, prestressing is defined as the case when the girder, under its own weight only, is prestressed by cables. The cables are installed in accordance with the desired trace configurations and stretched by prestressing jacks up to predetermined forces. Stressing jacks are released when the end anchorages are fixed. The superimposed dead and the live loads are applied to the prestressed girder. For the purpose of stress control three distinct stages can be defined in accordance with the various loading cases as:

1) Non-prestressed girder under self weight (partial dead load)

2) Prestressed girder carrying the dead load and under prestressing effect (transfer stage)

3) Prestressed girder carrying the total service loads - dead, superimposed dead and live loads (final service load stage)

The term post-tensioning refers to the condition where the girder is under part of the service loads which include the dead loads. The tendons are placed according to the desired configuration, stretched by jacks and fixed to the girder by end anchorages. Then the jacks are released and as a result the stretched and anchored tendons induce the counterbalance stresses (compression) along the girder where the cables extend. Accordingly, three stages of loading in post - tensioned girders can be distinguished as:

1) Girder supporting the dead loads (including that of the deck and self weight)
2) Girder under the effect of counterbalance stresses due to post - tensioning and the dead loads, just after the jacks are released
3) Girder carrying total service loads and force induced by stretched tendons

The beneficial stress compensation by prestressing or post-tensioning is limited to certain values beyond which the prestressing efficiency diminishes. In some critical cases, for example when the cables are positioned in the compression zone, it may create additional stresses and has negative effect.

4.2. PRESTRESSED TENSILE MEMBERS

The stresses at any arbitrary section for a tensile member prestressed by tendons are assumed to be uniformly distributed across the section. An exception to this assumption is at the immediate vicinity of the end anchorages where the prestressed tendons are fixed to the member, which requires special design consideration. The induced stresses, due to prestressing effect and stresses due to the applied service loads, shall be controlled in the following loading stages [55]:

a) Girder under the application of partial service loads (mainly dead loads) prior to the effect of prestressing, non-prestressed, Figure 4.1.a.

$$(4.1) \qquad f_d = \frac{N_d}{A} \leq \text{the designed stress requirements}$$

Where f_d, N_d and A are the stress, the partial service load (dead load) and the cross sectional area of the member, respectively.

b) Girder under the effect of prestressing force and dead loads, when the prestressing process is completed and the jacks are released inducing forces normally in the opposite direction to the tensile forces in the member, Figure 4.1.b. In this case the stresses in the tendons and of the tension element should be controlled.

$$f_{Pt} = \frac{P_e}{A_t} \leq \text{Allowable stress in tendons} \tag{4.2}$$

$$f_d^{pre} = \frac{N_d - P_e}{A} \leq \text{The allowable stress in element studied (Compressive)} \tag{4.3}$$

In which, f_{pt}, P_e and A_t are the stress, the effective prestressing force and the area of the tendons, respectively. $P_e = P_i - P_l$ in which P_i is the initial prestressing force and P_l is the prestress losses. It should be noted that if $P_e > N_d$ the element should be checked for the compressive action of the prestressing force $(P_e - N_d)$, prior to the application of superimposed dead and live loads.

c) Finally the stresses of the member under prestressing force and full service loads, Figure 4.1.c. At this stage, the effective prestressing force will be increased by the value of prestressing force increment which was discussed in Section 3.3.1.

$$f_{d+s+L}^{pre} = \frac{N_d}{A_m} + \frac{N_{s+L} - (P_e + \Delta P)}{A} \leq \text{The allowable stress (Tensile)} \tag{4.4}$$

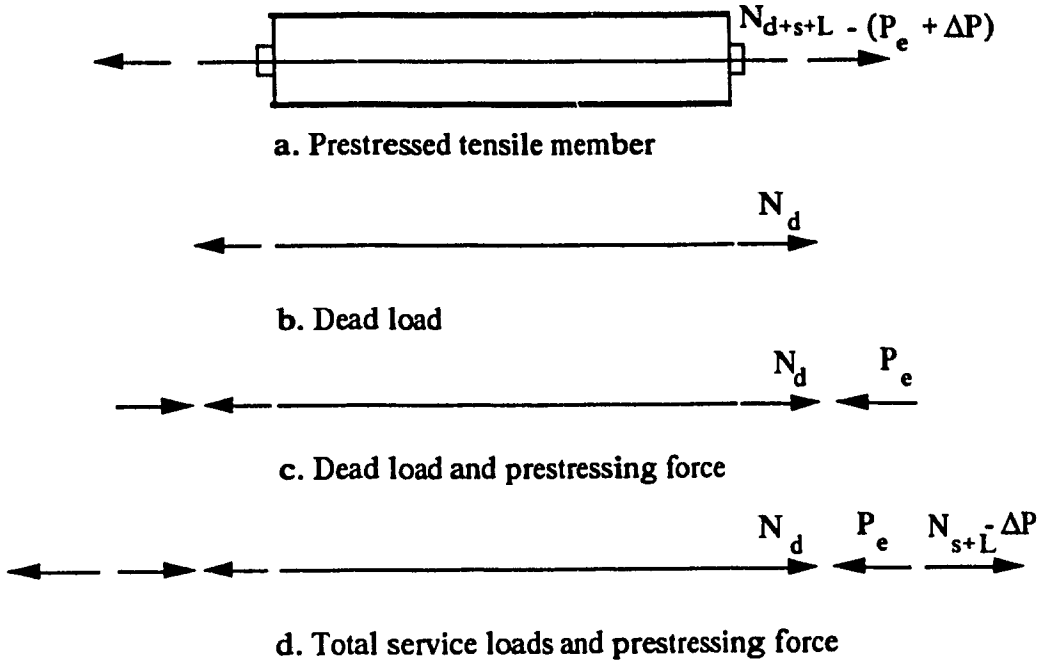

Figure 4.1. Loading stages of prestressed tensile members.

4.3. PRESTRESSED BENDING MEMBERS

The combination of the stresses due to the total service loads and the counterbalance prestressing effect is the final stress at any section along the girder. The stresses of the girder at various stages of loading should be accordingly controlled, i.e. non-prestressed girder, prestressed tendons, prestressed girder under partial dead load and total service loads. The magnitude of the stresses to be compensated by the effect of prestressing depends on various cross sectional properties of the girder and of the tendons, tendon configurations and the geometry of the girder.

In general the following stress expression can be developed for various loading cases when the bending moment at the desired section is calculated [56]:

a) girder under full or partial dead load, non-prestressed girder

$$(4.5) \qquad f_d = \pm \frac{M_d}{S}$$

Where f_d, M_d and S are the stress, the bending moment due to partial or total loads and the corresponding section modulus (top or bottom depending on the stress control position whether at the top or at the bottom of the section). The sign convention assumed negative (-) for compression and positive (+) for tension stresses. It is also assumed that the positive moment creates tension stresses at the bottom fibers and compression at the top, whereas the negative moment will induce stresses opposite, tension at the top and compression at the bottom.

b) Prestressing cables are fixed at the end anchorages (the jacks are released) and as a result the induced prestressing stress is added to the existing stresses due to dead loads for which the following equations can be derived:

- Stresses in the tendons:

$$(4.6) \qquad f_{Pt} = \frac{P_e}{A_t} \leq \text{The allowable tendon stress}$$

- For the tension zone:

$$(4.7) \qquad f_{d+pre}^{tens} = \frac{M_d - P_e e}{S_{tens}} - \frac{P_e}{A} \leq \text{The allowable stress (Tensile)}$$

- For the compression region of the section

$$(4.8) \qquad f_{d+pre}^{comp} = \frac{- M_d + P_e e}{S_{comp}} - \frac{P_e}{A} \leq \text{The allowable stress (Compression)}$$

Where S_{tens} and S_{comp} are the tension and the compression section moduli and A is the cross sectional area of the girder at the section under consideration.

c) The girder is under full service loads and the prestressing forces are induced, then the combined stresses due to the total service loads and the prestressing effect can be expressed as Equations (4.10) and (4.11).

- For the tendons considering the incremental prestressing force:

$$(4.9) \qquad f_{pt} = \frac{P_e + \Delta P}{A_t} \leq \text{allowable tendon stress}$$

- For the compression zone of the girder:

$$(4.10) \qquad f^{comp}_{d+s+L} = \frac{-M_{d+s+L} + (P_e + \Delta P)e}{S_{comp}} - \frac{(P_e + \Delta P)}{A}$$

- For the tension region of the girder:

$$(4.11) \qquad f^{tens}_{d+s+L} = \frac{M_{d+s+L} - (P_e + \Delta P)e}{S_{tens}} - \frac{(P_e + \Delta P)}{A}$$

Where M_{d+s+L} is the total service loads including dead, superimposed dead and live loads.

The stress distribution at any section along the girder is illustrated in the following sketches, Figure 4.2.

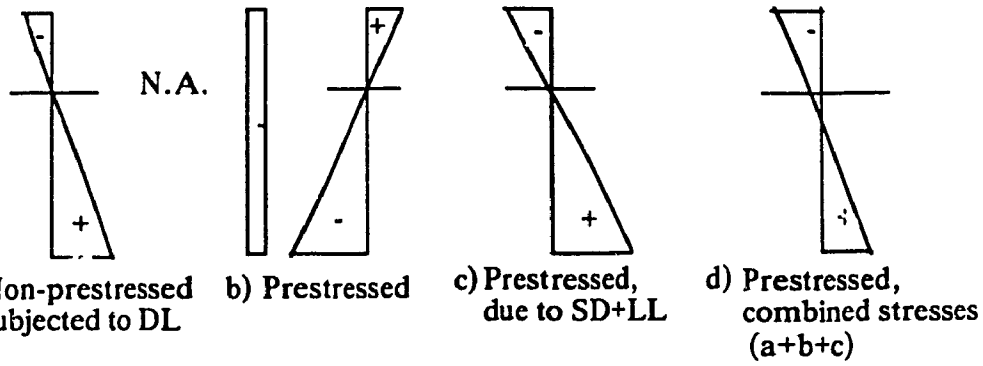

Figure 4.2.A general stress distribution for bending members at the positive moment region

Equation (4.11) indicates that the stress terms corresponding to the prestressed tendons counterbalance the effect of the stresses due to the applied loads. Any increase in the strength of the cables will proportionally increase the load bearing capacity of the girder at the tension zone. However at the compression region, Equation (4.10), certain tendon eccentricity and prestressing values should exist otherwise the prestressing effect will be reversed, see prestressing limits in Section 4.4.

4.4. PRESTRESSING LIMITATIONS

The limits of prestressing evaluate the maximum and minimum magnitude of stresses which may be compensated by prestressing. These limits depend on the cross sectional properties of the tendons and that of the girders, also on the eccentricity of the tendons from the neutral axis in the case of a flexural member.

4.4.1. TENSILE MEMBERS

The stresses of tensile members given by equation (4.3) indicates that the maximum counterbalance prestressing force is limited to the compressive strength of the member due to dead load and prestressing effect, while the member is prestressed but prior to the application of total service loads.

(4.12) $f_d^{pre} = \frac{N_d - P_e}{A} \leq$ The required compression stress

where in this case it is assumed that $P_e > N_d$

The minimum limit of prestressing depends on the economy comparison of prestressing gain and expenses. The economy gain is derived from reducing the weight of material by prestressing versus the expenses of the prestressing process. Other than these two major prestressing limits, the expressions for the stresses of tension members show that any increase in the prestressing force will proportionally increase the load bearing capacity of the member.

To calculate the increase in the load carrying capacity of a prestressed tension member the expressions for the stress of a non-prestressed member subjected to the dead, superimposed and live load is compared with similar member which is prestressed by high strength steel tendons under the application of total axial forces N_R.

(4.13) $$f_{d+s+L} = \frac{N_d + N_{s+L}}{A_m}$$

(4.14) $$f_{d+s+L}^{pre} = \frac{N_d - P_e}{A_m} + \frac{(N_R - N_d) - \Delta P}{A}$$

Where A is the cross sectional area of the system (the member including the prestressed tendons), A_m is the cross sectional area of the member only and N_R is the maximum load bearing capacity of the prestressed tensile member. By equating the two Equations (4.13) and (4.14) and solving for N_R the expression for the increased load bearing capacity of the member can be derived as:

$$N_R = N_{s+L}\left(\frac{A}{A_m}\right) + N_d + P_e\cdot\left(\frac{A}{A_m}\right) + \Delta P$$

(4.15)

$$N_R - (N_d + N_{s+L}) = N_{s+L}\cdot\left(\frac{A_t}{A_m}\right) + P_e\cdot\left(\frac{A}{A_m}\right) + \Delta P$$

The expression for the stress gain is given in Equation (4.16), which compares the stresses of the prestressed versus non-prestressed member subjected to similar loadings.

$$f_{d+s+L} = \frac{N_d + N_{s+L}}{A_m}$$

(4.16)

$$f^{pre}_{d+s+L} = \frac{N_d - P_e}{A_m} + \frac{N_{s+L} - \Delta P}{A}$$

$$f_{d+s+L} - f^{pre}_{d+s+L} = N_{s+L}\cdot\left(\frac{1}{A_m} - \frac{1}{A}\right) + \frac{P_e}{A_m} + \frac{\Delta P}{A}$$

The stress compensation induced by the prestressed cables are proportional to the value of effective prestressing force (considering losses and the prestressing force increment) and up to the maximum prestressing limits.

4.4.2. FLEXURAL MEMBERS

The combined stress at the tensile region of the prestressed girder indicates that any increase in the effective prestressing force P_e and eccentricity e proportionally increase the magnitude of the counterbalance stresses induced by the tendons, Equation (4.11). The larger the cross sectional area of the cables and the eccentricity e - the distance of the center line of the tendons from the neutral axis of the girder - the larger will be the load bearing capacity of the girder. The maximum prestressing limit for the tension zone can be established from Equation (4.17) considering the control of stresses of the beam under dead load and prestressing force prior to the application of the total service loads, which may be of a reversed nature, namely compression. It is very unlikely that such a situation

occurs since the prestressing limit at the compression region of the girder governs the design.

$$(4.17) \quad f_{max.}^{comp} \geq \frac{M_d - P_e e}{S_{tens}} - \frac{P_e}{A}$$

$$(4.18) \quad P_e \left(\frac{1}{A} + \frac{e}{S_{tens}} \right) \leq f_{max}^{comp} - f_d^{tens}$$

$$(4.19) \quad f_d^{tens} = \frac{M_d}{S_{tens}}$$

To evaluate the prestressing limits of a bending member at the compression zone, Equation (4.10), the induced tension stresses caused by the prestressing effects which is aimed to reverse the action of compression stresses due to total service loads should be considered, also the compression stress due to the axial force implied by the prestressed tendons will have a reverse action. In other word the stresses due to the tendons prestressing should produce a positive value to counterbalance the compressive stresses due to the service loads, Equation (4.20).

$$(4.20) \quad \frac{(P_e + \Delta P)\, e}{S_{comp}} - \frac{(P_e + \Delta P)}{A} \geq 0.$$

Accordingly, the tendon's eccentricity e is limited to the following condition [57]:

$$(4.21) \quad (P_e + \Delta P)\left(\frac{e}{S_{comp}} - \frac{1}{A} \right) \geq 0.$$

$$(4.22) \quad e \geq \frac{S_{comp}}{A} \qquad \text{or} \qquad e \geq \frac{r^2}{y_{comp}}$$

Where y_{comp} and r are the distance of the compression fiber under consideration from the neutral axis and the radius of gyration of the cross sectional area of the girder, respectively. S_{comp} and S_{tens} are the respective compression and tension section modulus of the girder.

To compute the increase in the load carrying capacity of a prestressed girder versus a similar non-prestressed member, the values of the stresses at the tension and the compression zones of the girder due to the prestressing cables are compared with similar stress expressions in a non-prestressed bending member.

For the compression zone the increased load bearing capacity M_R at any arbitrary section is equal to:

$$(4.23) \quad \frac{M_{non\text{-}pre}}{S_{comp}} = \frac{M_R - (P_e + \Delta P)\, e}{S_{comp}} + \frac{(P_e + \Delta P)}{A}$$

$$(4.24) \quad M_R = M_{non\text{-}pre} + (P_e + \Delta P)\, e - \frac{(P_e + \Delta P)\, S_{comp}}{A}$$

In the tension region similar equations for the moments of resistance of a prestressed girder in comparison with the moments of non-prestressed can be developed as Equations (4.25) and (4.26).

$$(4.25) \quad \frac{M_{non\text{-}pre}}{S_{tens}} = \frac{M_R - (P_e + \Delta P)\, e}{S_{tens}} - \frac{(P_e + \Delta P)}{A}$$

$$(4.26) \quad M_R = M_{non\text{-}pre} + (P_e + \Delta P)\, e + \frac{(P_e + \Delta P)\, S_{tens}}{A}$$

In particular cases of strengthening or rehabilitation of an existing girder the load carrying capacity of the girder can be increased by post-tensioned tendons considering the prestressing limits particularly in the compression fibers of the section which is governing the design of such girders. Nevertheless, the stresses must be controlled independently under the service loadings. The stresses for the two main loading cases to be considered for strengthening of a girder include:

1) stresses due to the applied loads corresponding to the existing service loads (Non post-tensioned) and

2) Stresses corresponding to the combined loadings due to the total applied service loads and the effect of post - tensioning.

Since the design stresses in both cases remain unchanged the following expressions for the increase in the load bearing capacity of the girder can be derived.

In the tension fibers of the girder the gained bending moment induced by the Post-tensioned tendon is expressed as Equation (4.27).

$$(4.27) \qquad M_R - M_{non\text{-}pre} = (P_e + \Delta P)\left(e + \frac{r^2}{y_{tens}}\right)$$

The increase in the moment bearing capacity in the compression zone is given by Equation (4.28).

$$(4.28) \qquad M_R - M_{non\text{-}pre} = (P_e + \Delta P)\left(e - \frac{r^2}{y_{comp}}\right)$$

As an example, for the standard symmetrical cross sectional area of a rolled steel I

section the following expressions can be derived:

$$(4.29) \qquad S_{comp} = S_{tens} = \frac{I}{0.5\,d} = \frac{A\,d}{6}\,(3 - 2n) \qquad \text{where} \quad n = \frac{A_w}{A}$$

Substituting in Equations (4.27) and (4.28) the value of S from Equation (4.29), and considering that the value of the cable's eccentricity could be approximated as: $e = d/2$, the resisting moment increase of the girder due to the effect of post tensioning can be established as Equations (4.30) and (4.31) for the tension and the compression regions, respectively.

$$(4.30) \qquad M_R - M_{non\text{-}pre} = (P_e + \Delta P)\,2e\,(1 - \frac{n}{3})$$

$$(4.31) \qquad M_R - M_{non\text{-}pre} = (P_e + \Delta P)\,e\,(\frac{2n}{3})$$

In this case n vary from 0.3 to .57 depending on the weight of the standard steel I shapes. In the case of a rectangular section $A_W = A$ and $n = 1$, the increased moment capacity for the tension zone will be as twice the value for the compression zone.

In Equations (4.27) and (4.28) S_{comp} , S_{tens} and A are assumed constant, because they represent the cross sectional properties of the existing girder, whereas the cable eccentricity e and the post-tensioned force $(P + \Delta P)$ are the variables to be defined.

The benefit of post-tensioning may be greater in girders having asymmetrical sections, considering the increased relative value of the tendon eccentricity e.

For a composite section as shown in Figure 4.3, consisting of a steel beam W 24 * 68

and 7 inches of concrete at the top, post tensioned by 4 strands of 37 wires of Φ 5 mm, [56], the capacity gain is 35% in comparison to the non-post tensioned girder having similar cross-sectional geometry. The stress distributions of prestressed and post-stressed composite girder are shown in Figures 4.4 and 4.5.

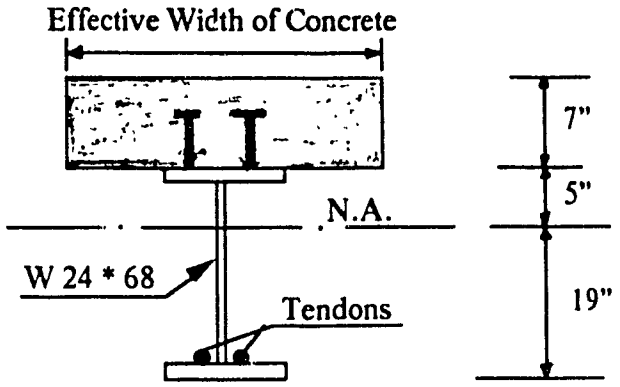

Figure 4.3.Prestressed composite section

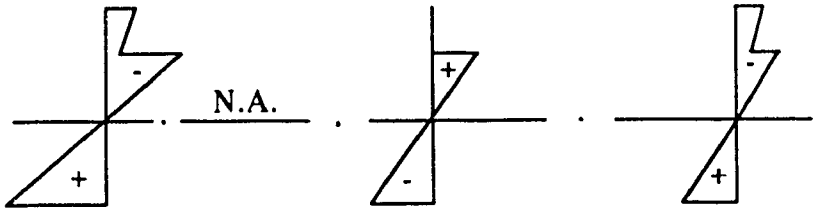

Figure 4.4. Stress distribution for composite prestressed girder.

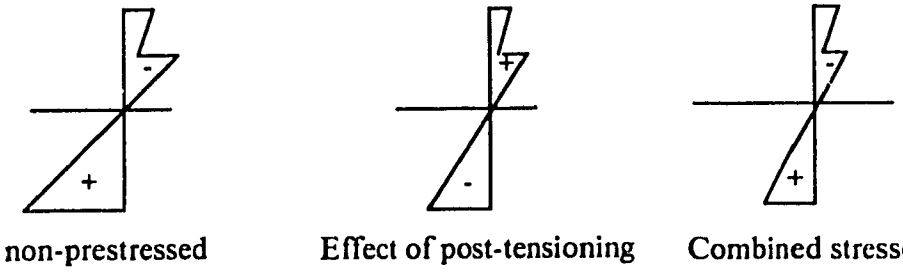

Figure 4.5. Stress distribution for composite post-tensioned girder.

Experiments performed on rolled W shapes simply supported and post tensioned by 2, 7 wire strands with nominal diameter of .6" and the rupture strength of 54 Kips, show the following increase in the load bearing capacity of the girder, [58 & 59].

Shape	Applied Stressing Force Kips	Increased Capacity %	
		Compression zone	Tension zone
W 14 * 74	8	2	19
Non-Composite	85	10	30
W 12 * 50 Composite	18	7	52

Table 4.1. Increase of the load carrying capacity by post-tensioning.

4.5. APPLICATION EXAMPLES

For rehabilitation of a parking structure in San Francisco post tensioning method were selected, [24]. The repair was performed due the water leaking, cracks in the concrete slabs and concrete spalling. Two strands were placed at the two sides of the girders and post tensioned by jacks. The tendons were extended continuously along the tensile regions on the girder, as shown in Figure 4.6.

In Montréal the Champlain bridge was strengthened by post tensioned cables placed externally along the prestressed concrete girders, Figure 4.7.

Based on test results on a scaled model of a steel truss bridge in United States, post tensioning by cables is considered as a potential alternative for bridge rehabilitation, [60 & 61]. Experiments performed by Klaiber and Dunker et al show the potential advantages in increasing the flexural strength of single span, composite steel beam and concrete deck

bridges post tensioned by tendons, [62, 63 & 64].

In England, a steel truss bridge built in 1906 had to be restored, because the corroded cross beams and the bottom chord girders were weakened. The post-tensioned tendons were used to rehabilitate the bridge [65].

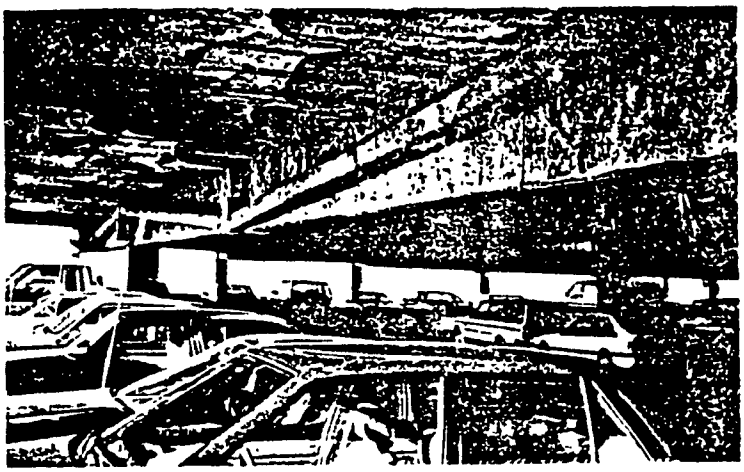

Figure 4.6. Pier 39 Parking structure in San Francisco.

Figure 4.7. Rehabilitation of Champlain Bridge in Montréal.

4.6. DESIGN CONCEPTS OF PRESTRESSED STEEL BOX GIRDERS

4.6.1. INTRODUCTION

The static analysis of prestressed steel box girders under the application of service loads and the prestressing forces, establish stresses which include axial compression, bending and shear stresses. The linear stress distribution across any arbitrary section is assumed to be valid. However, in the design of steel box girders it is essential to consider the effect of torsional stresses and the secondary stresses. The torsional stresses may occur due to asymmetrical loading of the section. The secondary stresses (residual stresses) are caused by the initial imperfection of thin plates used in fabrication of such girders and residual stresses caused by welding of thin plates. Also, the longitudinal and transverse stability of the girder and the local stability of the box elements (thin plates) should be checked under critical service loads and prestressing force.

Scordelis introduced the stress analysis of continuous steel box girders by the methods of Folded Plate, Finite Segment method, and Finite Element method [66]. Heins contributed significantly to the design of box girders, by introducing the proportional dimensions for the preliminary design of short and medium span girder bridges (up to 50m spans), [67, 68 & 69].

The effects of the residual stresses, the initial imperfection of thin plates and welding, under the application of compression forces have been already studied in detail [70 & 71].

Steel box sections are composed of deck plate, webs and bottom plate. Steel deck plate is stiffened by stringer ribs and transverse beams to support local heavy vertical loads (total service loads) and transfer them to the webs. Deck plate may be also a reinforced or prestressed concrete slab. The cross sectional area and the spacing of the longitudinal stiffeners and transverse beams should be properly designed to safely transfer the applied

service loads to the webs and to prevent local buckling in the stiffening elements [72, 73, 74, etc.].

The webs are the connecting elements between the top deck and the bottom flange resisting the shear and bending stresses transferred by the deck. The webs may be strengthened by longitudinal and transverse stiffeners at fairly short distances (normally half the depth of the box) securing its resistance against local and longitudinal buckling.

The bottom flange is under tension at the region of positive moments and in compression corresponding to the applied negative moments. In the case of the latter it should be accordingly stiffened, similar to the deck plate. The bottom flange of a steel box section prestressed at the tension zone by the cables of high strength steel is considered as compression plate and should be stiffened against the application of eccentric prestressing forces, where necessary.

Other stresses of important influence in the design of box girders are:

a) Residue stresses due to the welding of thin plates composing the box section.

b) Initial imperfections of the plates.

c) Non-uniform warping, mainly due to non-uniform torsional stress distribution in the cross section, causing the appearance of normal warping and shear stresses [71].

d) Part of the flanges closer to the webs is effected by the shear stresses transmitted by the webs. This will cause a non-uniform distribution of bending and shear stresses (shear lag).

e) Effect of eccentric loads, causing transverse deformations accompanied by transverse bending at the joint of web to the flanges.

4.6.2. STRESSES IN BOX GIRDERS

In general the cross section of a prestressed box girder is subjected to flexural, torsional and distortional stresses [67].

a) Flexural stresses are due to bending and shear, when the girder is subjected to a symmetrical loading across its top flange, Equation (4.32).

$$(4.32) \qquad f_b = \pm \frac{M}{S} \quad \text{and} \quad \tau = \frac{V\,Q}{I\,t}$$

The distributions of these stresses are illustrated in Figure 4.8.

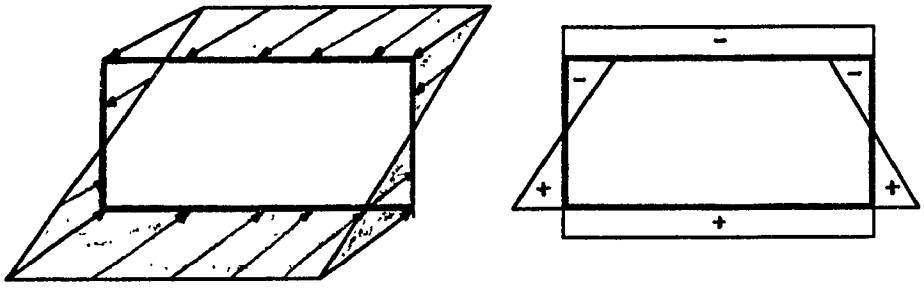

Stress distribution due to bending moment

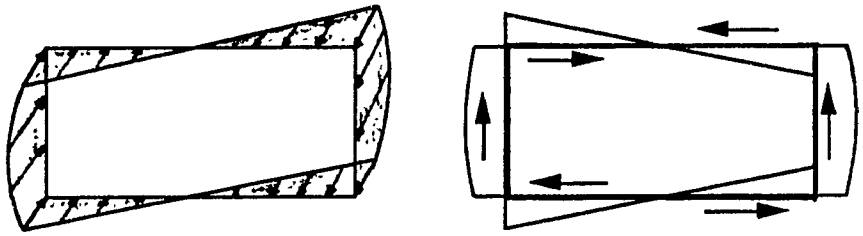

Stress distribution due to shear

Figure 4.8. Distribution of flexural stresses

b) Pure torsion: Torsional stresses occur when the applied loading is eccentric to the shear center of the cross section, Figure 4.9. The asymmetrical load P applied to the box section can be resolved into flexural force P and torsional force P.e, where e is the eccentricity of the force P from the shear center. The torsional force is also divided into pure torsion and distortion [75].

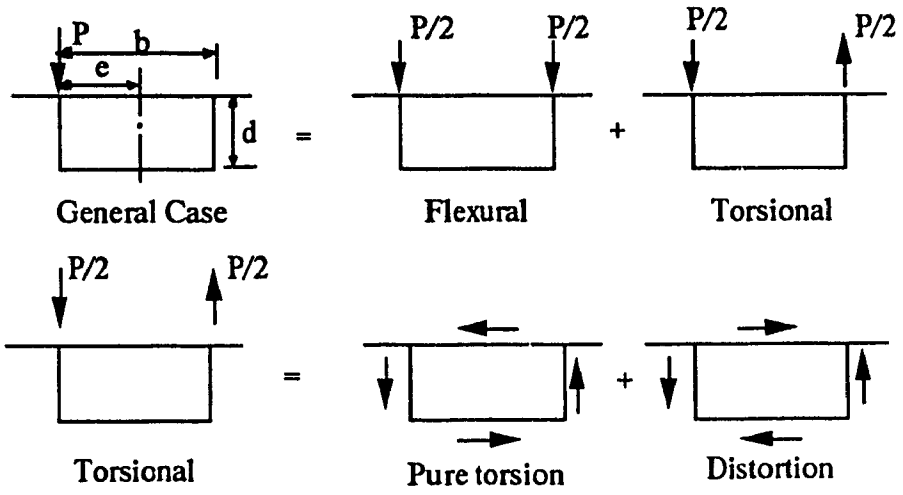

Figure 4.9. Force components of asymmetrically loaded box sections.

The shear stress due to pure torsion τ_s, for open sections and closed sections are given in Equations (4.33) and (4.34), respectively.

$$\tau_s = \frac{T}{J} . t \qquad (4.33)$$

$$\tau_s = \frac{T}{2 . A_o . t} \qquad (4.34)$$

where, T is the applied torque, J is the torsion constant, A_o is the enclosed area of the box section (i.e. b.d) and t represents the plate thickness. Figure 4.10 demonstrates the shear stress distribution due to pure torsion.

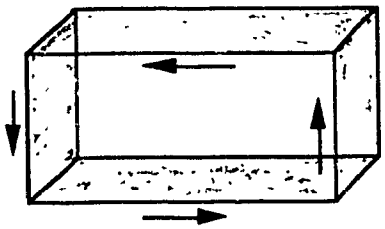

Figure 4.10. Shear stresses due to pure torsion

The torsional resistance of a section is equal to:

$$(4.35) \quad T = G\,J\,(\frac{\Phi}{L})$$

Where G is the shear modulus, Φ is the angle of twist and L is the length of the girder. The value of J for open and closed sections are expressed in Equations (4.36) and (4.37), respectively [92].

$$(4.36) \quad J = \frac{1}{3} \sum (b\,t^3)$$

$$(4.37) \quad J = \frac{4\,A_0^2}{\int \frac{ds}{t}}$$

In which b presents the plate dimension, t is the plate thickness, ds = length of a given element with thickness t. For a box section the value of J can be derived as:

$$(4.38) \quad J = \frac{4.b^2.d^2}{\frac{b}{t_t} + \frac{2.d}{t_w} + \frac{b}{t_b}}$$

Where b, d are illustrated in Figure 4.11. The values of t_t, t_w and t_b are the thicknesses of the top flange, web and the bottom flange plates including the equivalent thickness of the stiffeners, respectively. Figure 4.11 illustrates the dimensions of the box girder.

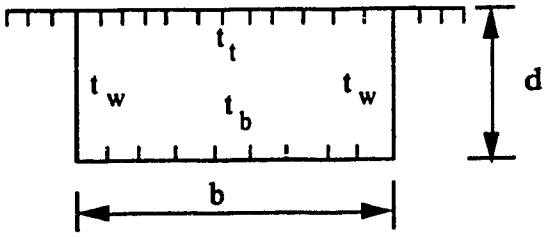

Figure 4.11. A typical box section stiffened at the top and bottom flanges.

The torsional moment and the torsional angle for the applied uniformly distributed or concentrated torque, applied to a section being fixed at the two ends against twist are expressed in the following equations in Table 4.2 [92].

	Torque	Torsional moment, T(z)	Angle of twist, Φ
(4.39)	m_T	$\frac{m_T.l}{2}(1-\frac{2.z}{l})$	$\frac{m_T.l^2}{2.G.J}(\frac{z}{l})(1-\frac{z}{l})$
(4.40)	M_T	$M_T(1-\frac{a}{l})$ $\quad 0 \le z \le a$	$\frac{M_T.l}{G.J}(1-\frac{a}{l}).\frac{z}{l}$
		$-M_T.\frac{a}{l}$ $\quad a \le z \le l$	$\frac{M_T.l}{G.J}(1-\frac{z}{l}).\frac{a}{l}$

Table 4.2. Equations of torsional moment and torsional angle.

Where a, z and l are the position of the concentrated torque, an arbitrary distance from the left end and the length of the member, respectively, Figure 4.12.

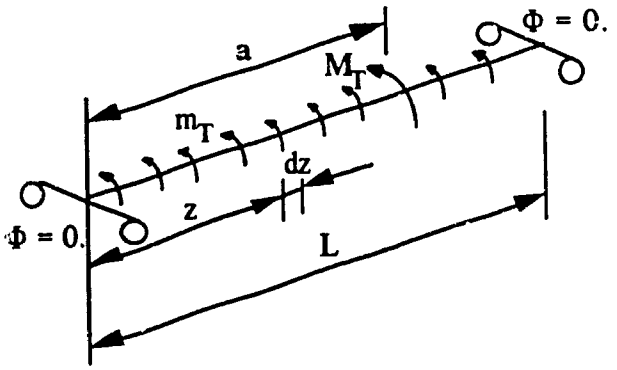

Figure 4.12. A typical member subjected to a concentrated or uniformly distributed torque

A comparison between the torsional constants of a closed section and an open section demonstrates the great torsional strength capacity of the closed section to a similar open section, $J_{closed} = 10^4 (J_{open})$ [67]. It can be readily shown that a closed section is much more stronger than an open section when the member is subjected to a torque. Consider the similar closed and slit box sections shown in Figure 4.13.

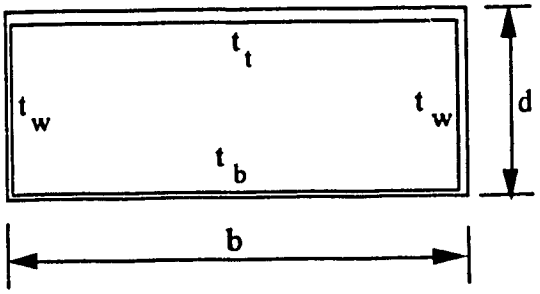

Closed box section

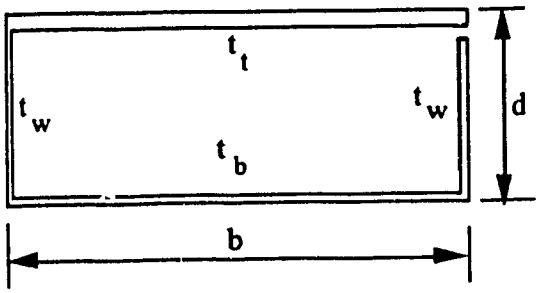

Open section (slit box)

Figure 4.13. Comparing the closed and open box sections

The respective shear stresses due to torsional moment T for the closed and open box sections are equal to:

$$(4.41) \qquad \tau_{closed} = \frac{T}{2.b.d.t}$$

$$(4.42) \qquad \tau_{open} = \frac{3.T}{b\,(t_t^3 + t_b^3) + 2.d.t_w^3} \,.\, t$$

If the thicknesses of the boxes are equal in all dimensions, the stress ratio of the open section to the closed section will be:

$$(4.43) \qquad \frac{\tau_{open}}{\tau_{closed}} = \frac{3.b.d}{(b+d).t}$$

For the specific case of a square box of dimension b, this ratio will be equal to 1.5 (b/t).

Torsional Warping: The slender plates used in the fabrication of steel box girders when subjected to a torque (torsional loading) will warp and accordingly will induce warping stresses to the section, Figure 4.14, which include a normal bending stress and shear stress, Equations (4.44) and (4.45) [67].

$$(4.44) \qquad f_w = \frac{B_w\, W_n}{I_w}$$

$$(4.45) \qquad \tau_w = \frac{E\, S_w}{t}\, \Phi$$

where B_w is the bimoment or the warping moment = $E\, I_w\, \Phi$

W_n = the normalized warping function

I_w = warping constant

Φ = angle of rotation

S_w = warping static moment

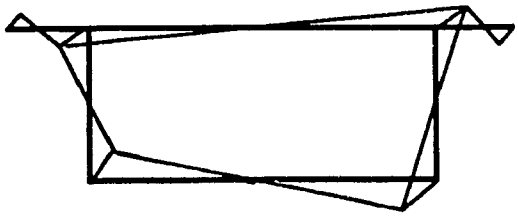

Longitudinal Warping

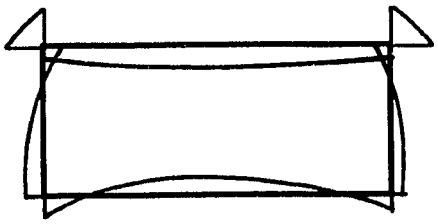

Shear Warping

Figure 4.14. Torsional warping stresses

A study by C.P.Heins has shown that for twisting angle Φ between 0 and 0.5 and $\varphi \geq 10 + 40\,\Phi$ warping can be disregarded, for $0.5 \leq \Phi \leq 1.0$ and $\varphi \geq 30$ warping is negligible, in which $\varphi = L\,(G\,J / E\,I_w)^{1/2}$. For single closed box sections $\varphi \geq 30$, therefore warping can be disregarded. Pure torsional stresses can be disregarded when $\varphi \leq 0.4$ [67].

c) Distortional stresses are secondary stresses which occur due to the creation of additional stresses in response to the deformed shape of the section. These stresses include, a normal stress, shearing stress and a corner bending stress. Figure 4.15, illustrates the stress distribution across the section caused by the distortional stresses.

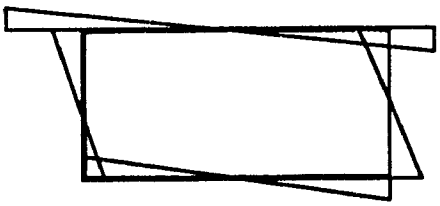

Normal Warping

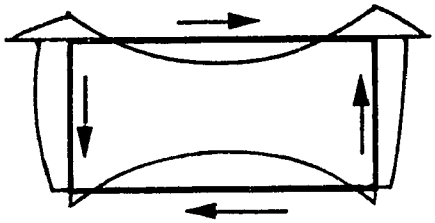

Shear Warping

Figure 4.15. Distortional stresses.

The effect of distortional stresses can be substantially decreased by introducing intermediate diaphragms or bracing. The design requirements for intermediate diaphragms and bracing considering the distortional stresses are provided by Heins [67].

The distortional warping stresses can be calculated from Equations (4.46) and (4.47) [92].

(4.46) $\sigma_{DW} = 1.8 \left(\frac{p_l . B . l_D^2}{16 . S_b} \right)$ for uniformly distributed load p_l (kN/mm^2)

(4.47) $\sigma_{DW} = 2.2 \left(\frac{P_l . B . l_D}{8 . S_b} \right)$ for knife edge load, P_l (kN/mm^2)

Where l_D is the spacing of the intermediate diaphragms, S_b is the section modulus at

bottom plate of box girder and B is the clear width of the top flange, Figure 4.16. p_l is the intensity of the asymmetrical distributed load applied to the half width of the box section.

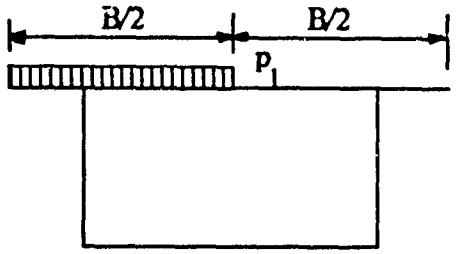

Figure 4.16. Half width of the box section is subjected to asymmetrical loading

4.6.3.STABILITY OF STEEL BOX GIRDERS

The plate elements of box sections (top and bottom flanges and webs) are subjected to axial, flexural and shear stresses. The Structural Stability Research Council specifies the following interaction equation for thin plates subjected to bending and compression [93].

$$(4.48) \qquad \left(\frac{f_a}{f_{a.cr}}\right) + \left(\frac{f_b}{f_{b.cr}}\right)^2 \leq 1.$$

Where f_a and f_b are the axial and bending stresses, while $f_{a.cr}$ and $f_{b.cr}$ are the critical axial and bending stresses of the section, respectively. Note that the effect of shear stress in the interaction equation is negligible at the center of the girder where flexural stress is maximum.

The critical elastic buckling stress for the plate in combined flexure and compression is given in Equation (4.49) [94].

$$(4.49) \qquad \sigma_{cr} = \frac{\pi^2 k.E.t^2}{12(1-\nu^2)h^2}$$

Where t, h, E and ν are the thickness, dimension, modulus of elasticity and the Poisons ratio of the plate, respectively. k is the critical buckling coefficient given in Table 4.2. The value of k is a function of the panel edge conditions and relative magnitude of flexural and compression stresses α given in Equation (4.50) [94].

$$(4.50) \qquad \alpha = \frac{h}{y}\left[1 - \frac{f_a + f_b(1 - \frac{y}{h})}{f_a + f_b}\right]$$

α	A	B	C
2	23.9	39.6	36
1.33	11.0		17
1	7.8	13.56	12
0	4.0	7.0	6

Table 4.3 Magnitudes of k, the critical buckling coefficient

A= all edges simply supported

B= Top and bottom edges fixed, sides simply supported

C= Practical conditions (80% fixity at the top and bottom edges)

The working stress criteria for the design of steel box girders specifies the width to thickness ratio of compression flange with stiffeners and the corresponding value of the allowable stress as proposed by Heins [68].

4.7. TRANSVERSE LOADINGS OF BOX SECTIONS

The transverse symmetrical loading on the top deck of a steel box girder assumed to be uniformly distributed across the width of the section and transferred to the webs, Figure 4.17. The effect of symmetrical transverse loading can be expressed as:

1) Longitudinal bending and shear

2) Transverse axial stresses caused by the rate of change of the longitudinal shear, which implies compression and tension in top and bottom flange and in the webs [75].

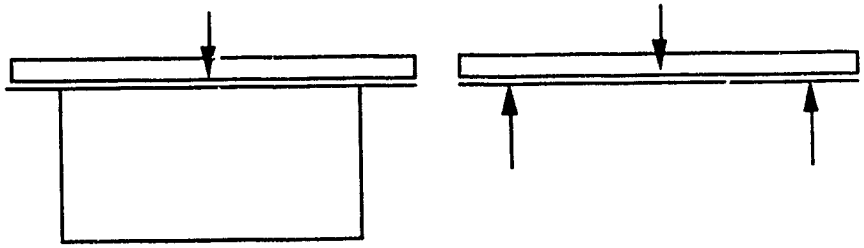

Figure 4.17. Symmetrical uniformly distributed and concentrated loadings

In the case of asymmetrical loadings, torsional and distortional stresses due to the eccentric applied loads are also induced in addition to the longitudinal stresses, Figure 4.18. The effect of asymmetrical loadings can be divided into two components: 1) symmetrical loading and 2)torsional forces [75].

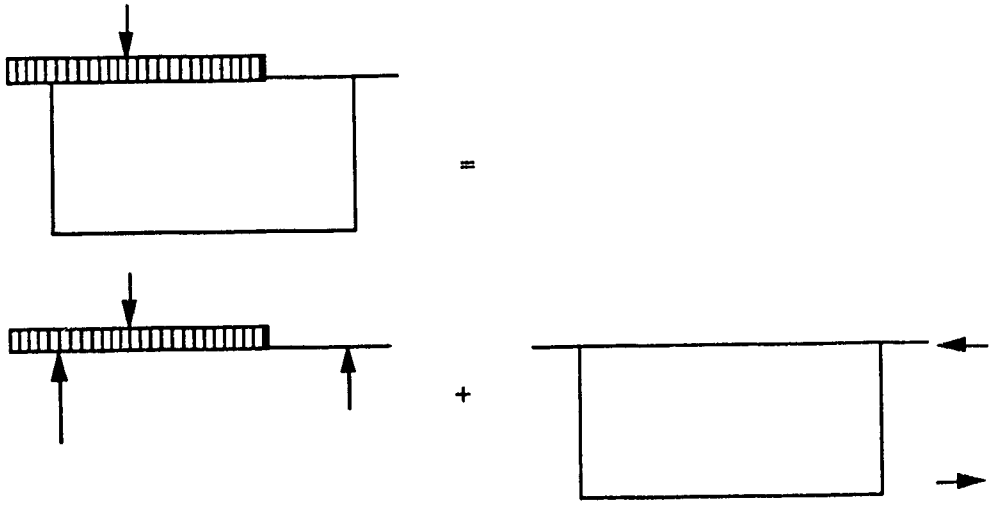

Figure 4.18. Asymmetrical distributed and concentrated loadings.

V. INFLUENCE LINES FOR THE PRESTRESSING FORCE INCREMENT AND BENDING MOMENT

Prestressed girders subjected to moving loads can be analyzed by drawing the influence lines in two separate stages, non-prestressed and prestressed. The first case is when the girder is not prestressed in which the influence lines for the bending moment and shear can be formulated by conventional methods. In the case of prestressed girders, in addition to the influence lines for the bending moment and shear, influence line for the prestressing force increment may also be considered. The bending moments at the interior supports are reduced in comparison to non-prestressed similar girders. The prestressing force increment corresponds to the additional elongation of cables caused by the external loadings (superimposed dead loads and live loads), applied to the girder after the prestressing is completed. The influence lines for the bending moment at the intermediate supports and prestressing force increment of prestressed girder are presented in this section.

5.2. INCREMENTAL PRESTRESSING FORCE OF SIMPLY SUPPORTED GIRDER

An approximate solution to the problem was presented by Belenya [77]. In this approach the prestressed force increment (ΔP) is approximated for a simply supported girder prestressed by short tendons. An exact solution within elastic limits can be obtained by considering the equation of flexibility [78]. The analysis is within the elastic limits where the principle of linear stress - strain relation (Hooke's Law) and superposition of stresses and deformations are considered to be valid. The assumed single span girder is prestressed by short tendon of length L_t, placed at the same distance $(L - L_t)/2$ from the end supports, Figure 5.1. The cross-sectional geometry of the girder and the tendon is assumed constant along the girder. The prestressed girder is indeterminate by one degree. The redundant is the incremental prestressing force ΔP. The unit concentrated loads are

placed at x_1, x_2 and x_3 from the left support, while girder is already prestressed. Also x_1 and x_3 are parts of the span length where no prestressed tendon exists, $0 \le x_1 \le (L - L_t)/2$ and x_2 defines the position of the short tendon, $(L - L_t)/2 \le x_2 \le L_t + (L - L_t)/2$, Figure 5.1.

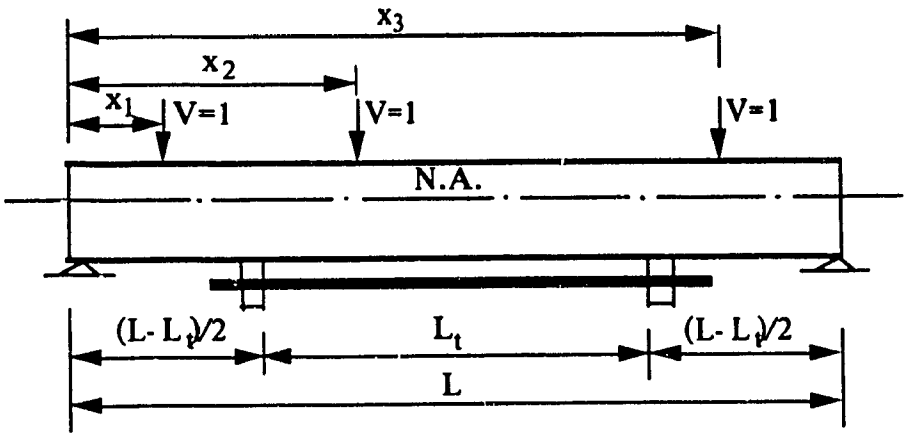

Figure 5.1. Typical girder prestressed by short tendons, subjected to an arbitrary unit load.

The compatibility equation for the deformations along the girder due to the applied unit force and a virtual unit prestressing force formulated in Equation (5.1) presents the intensity of the prestressing force increment of the beam.

$$(5.1) \qquad \delta_1 \, \Delta P + \Delta_{s+L} = 0. \qquad \text{or} \qquad \Delta P = - \frac{\Delta_{s+L}}{\delta_1}$$

The corresponding deformations along the girder can be defined by virtual work method, Equations (5.2) and (5.3)

$$(5.2) \qquad \delta_1 = \int_{L_t} \frac{m_x^2}{E\,I}\,dx + \int_{L} \frac{p_x^2}{E\,A}\,dx + \int_{L_t} \frac{p_x^2}{E_t\,A_t}\,dx$$

$$(5.3) \qquad \Delta_{1L} = \int_L \frac{m_x M_x}{E I} dx + \int_L \frac{p_x N_{s+L}}{E A} dx$$

δ_1 and Δ_{1L} are the deformations due to the unit prestressing force and the unit applied concentrated load, respectively.

m_x is the bending moment due unit prestressing force (m_x = 1.e), and M_x is the moment caused by unit applied concentrated force at arbitrary distances x_1 and x_2 from the left support along the girder.

p_x and N_x are the axial loads due to unit prestressing force (p_x = 1.0) and applied axial load (for simply supported bending members N_x = 0).

For the purpose of analysis, the equations for bending moments and the axial force are derived for two distinct loading positions, at $0 \le x_1 \le (L - L_t)/2$ and $(L - L_t)/2 \le x_2 \le (L + L_t)/2$. Equations (5.4) and (5.5) are the moments at any section x within the given intervals when the unit load moves along the girder.

$$(5.4) \qquad M_x = \frac{x(L - x_1)}{L} \qquad \text{for the interval} \qquad 0 \le x \le x_1$$

$$M_x = \frac{x_1(L - x)}{L} \qquad \text{for the interval} \qquad x_1 \le x \le L$$

$$(5.5) \qquad M_x = \frac{x(L - x_2)}{L} \qquad \text{for the interval} \qquad 0 \le x \le x_2$$

$$M_x = \frac{x_2(L - x)}{L} \qquad \text{for the interval} \qquad x_2 \le x \le L$$

Similar equations for the moment due to the unit prestressing force along length L_t placed at eccentricity e from the neutral axis can be formulated as the following equations:

(5.6) $m_x = 0$ for the interval $0 \le x \le \frac{(L - L_t)}{2}$

(5.7) $m_x = - e$ forthe interval $\frac{(L - L_t)}{2} \le x \le \frac{(L + L_t)}{2}$

(5.8) $m_x = 0$ for the interval $\frac{(L + L_t)}{2} \le x \le L$

The axial force p_x is given by Equations (5.9) and (5.10), while $N_x = 0$

(5.9) $p_x = 1$ for the interval $\frac{(L - L_t)}{2} \le x \le \frac{(L + L_t)}{2}$

(5.10) $p_x = 0$ for all other values of x

The corresponding moment diagrams, a) at x_1, b) at x_2 and c) due to the prestressing force are illustrated in Figure 5.2. The axial force diagrams for the girder and for the tendons are shown in Figure 5.3.

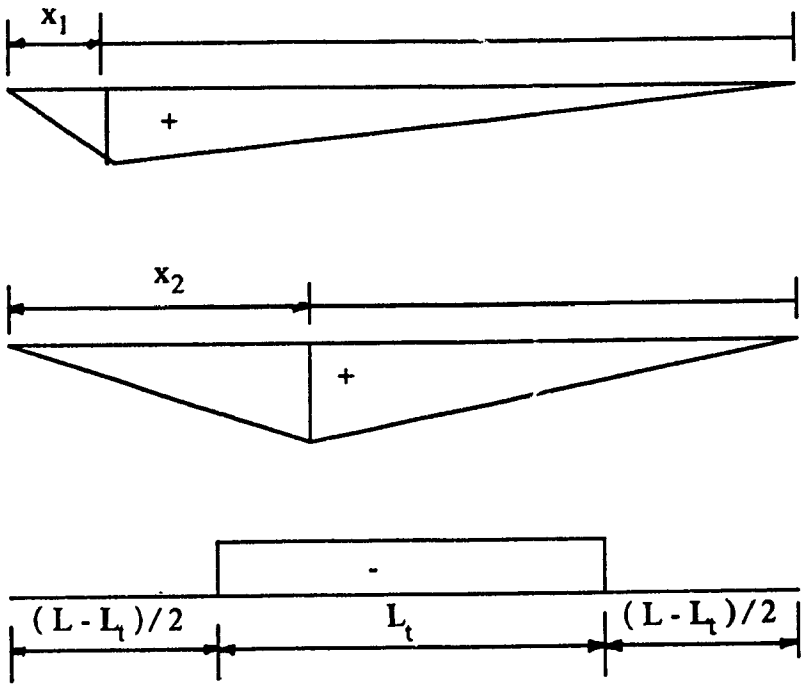

Figure 5.2. The bending moment diagrams due to an arbitrary unit vertical load and prestressing force.

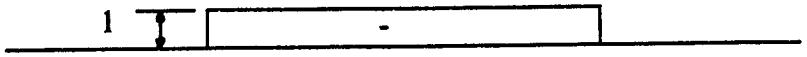

Axial compressive force diagram for the girder

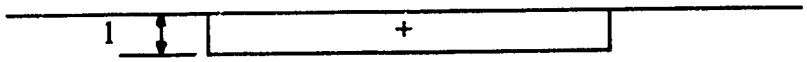

Axial tensile force diagram for the tendon

Figure 5.3. The axial force diagrams of the girder and the tendons

To obtain the expression for the flexibility coefficients δ_1 and Δ_{1L}, substitute for M_x and m_x and p_x in Equations (5.2) and (5.3) and integrate over the span length L.

$$(5.11) \qquad \delta_1 = \frac{L_t}{E\,I}\left(e^2 + \frac{I}{A} + \frac{E\,I}{E_t\,A_t}\right)$$

- For the unit load applied at x_2

$$(5.12) \qquad \Delta_{1L} = -\frac{e}{2EI}\left[\,L\,x_2 - x_2^2 - \frac{(L-L_t)^2}{4}\,\right]$$

- For the unit load at x_1

$$(5.13) \qquad \Delta_{1L} = -\frac{e\,x_1\,L_t}{2EI}$$

The value of the prestressing force increment is derived from Equation (5.1) for two different intervals, a) the load is located within the length where the tendon stretches, Equation (5.14), and b) at the two exterior segments where no prestressing tendon exists, Equation (5.15).

$$(5.14) \qquad \Delta P = \frac{e\left[\,L\,x_2 - x_2^2 - \dfrac{(L-L_t)^2}{4}\,\right]}{2\,L_t\left(e^2 + \dfrac{I}{A} + \dfrac{E\,A}{E_t\,A_t}\right)}$$

$$(5.15) \qquad \Delta P = \frac{e\,x_1}{2\left(e^2 + \dfrac{I}{A} + \dfrac{E\,I}{E_t\,A_t}\right)}$$

For the case where a load is applied at x_3, Figure 5.1, the prestressing force increment could be evaluated by Equation (5.15) considering the load's distance from the right support.

Equations (5.14) and (5.15) constitute the influence line for the incremental prestressing force caused by the application of any arbitrary loads on the girder after prestressing process is performed. The influence line diagrams include:

a) A linear line for the intervals $0 \le x_1 \le (L - L_t)/2$ and $0 \le x_3 \le (L - L_t)/2$ where the load is moving along the non-prestressed part of the girder, Figure 5.4.

b) A parabolic shape when the applied unit load is moving along the prestressed portion of the girder, $(L - L_t)/2 \le x_2 \le (L + L_t)/2$, Figure 5.4.

The ordinates of the influence line for particular points are calculated as follow:

(5.16) $\Delta P = 0$ for the values of $x_1 = x_3 = 0$

(5.17) $\Delta P = \dfrac{e\, L_t (L - L_t)}{4\, E\, I\, \delta_1}$ for $x_1 = x_2 = x_3 = \dfrac{(L - L_t)}{2}$

(5.18) $\Delta P = \dfrac{e\, L_t (2L - L_t)}{8\, E\, I\, \delta_1}$ for $x_2 = \dfrac{L}{2}$

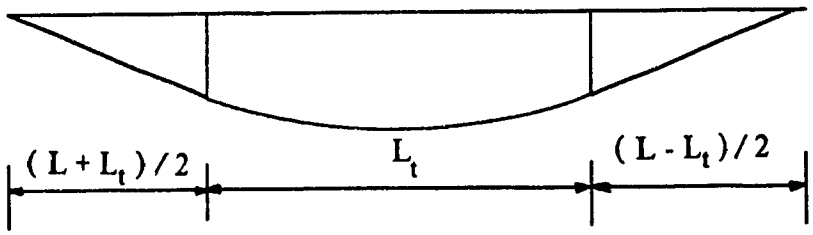

Figure 5.4. Influence line for the incremental prestressing force.

To evaluate the value of the incremental prestressing force, the concentrated force P_n should be multiplied by the ordinate of the influence line under the load's position and for the uniformly distributed force with the intensity w and length L_m the respective area of the influence line has to be multiplied by the w. The summation of these forces gives

the total incremental prestressing force.

For the case of the application of several concentrated loads on the prestressed girder as shown in Figure 5.5, which includes m forces on the non - prestressed segments at both sides of the span with a distance x_m from the left and right supports within the interval $0 \le x_m \le (L - L_t) / 2$, and $(m - n)$ presents the number of loads on the prestressed part, $(L - L_t)/2 \le x_2 \le (L + L_t) / 2$. The given Equations (5.14) and (5.15) are modified as Equations (5.19) and (5.20).

$$(5.19) \qquad \Delta P = \frac{e\,(P_1 x_1 + P_2 x_2 + ... + P_m x_m)}{2\,(e^2 + \frac{I}{A} + \frac{E\,I}{E_t A_t})}$$

$$(5.20) \qquad \Delta P = \frac{e\left[L\,(P_{m+1} x_{m+1} + ... + P_n x_n) - (P_{m+1} x_{m+1}^2 + ... + P_n x_n^2) - (n-2)\,(\frac{L - L_t}{2})^2\right]}{2\,L_t\,(e^2 + \frac{I}{A} + \frac{E\,I}{E_t A_t})}$$

in which $m = 1, 2, ..., m$ and $n = m+1, m+2, ..., n$

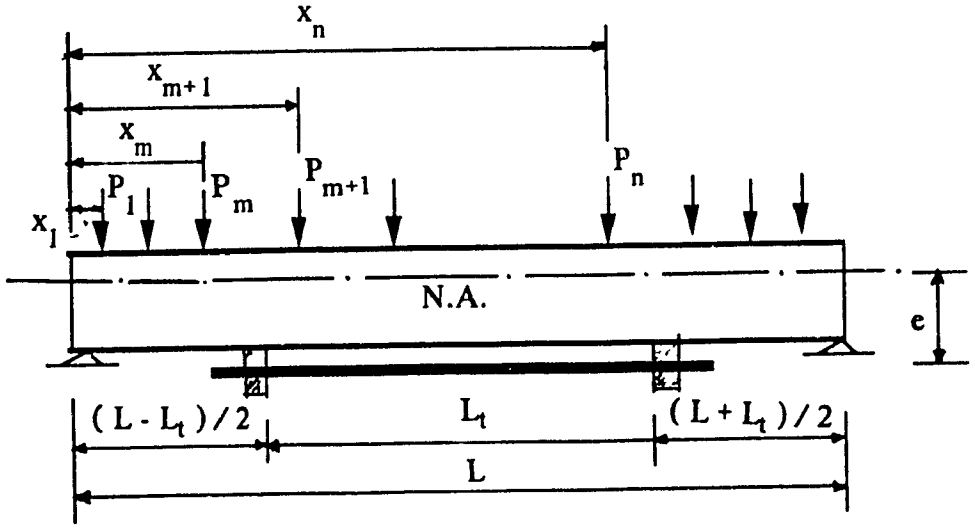

Figure 5.5. Typical loading on the girder

5.3. INFLUENCE LINE FOR TWO SPAN CONTINUOUS GIRDER

The two span steel girders prestressed by tendons is an indeterminate structure of second degree. For the purpose of analysis the two redundants are taken as:

1) Support bending moment (M)

2) Prestressing force increment (ΔP).

The compatibility equations corresponding to the deformations (flexibility equations) are written. The flexibility coefficients are computed by the integration of the external and internal work performed along the girder due to the applied loads and the arbitrary unit forces at the redundants. The analysis is limited to the elastic stage. The cross-sectional areas of the girder and the tendons are assumed constant. Three shapes of tendon configurations which present the most general cases are studied. The derived formulas are presented and the influence lines for the two assumed redundants are drawn. Based on the given equations, numerical examples are prepared for the analysis of the bending moment and the incremental prestressing force. The results are illustrated in diagrams and are compared with similar non-prestressed girders. A reduction in the value of negative bending moment is recorded in the case of prestressed girder.

For the purpose of analysis three types of tendon configurations are considered, namely as type I, type II and type III, shown in Figure 5.6 [79].

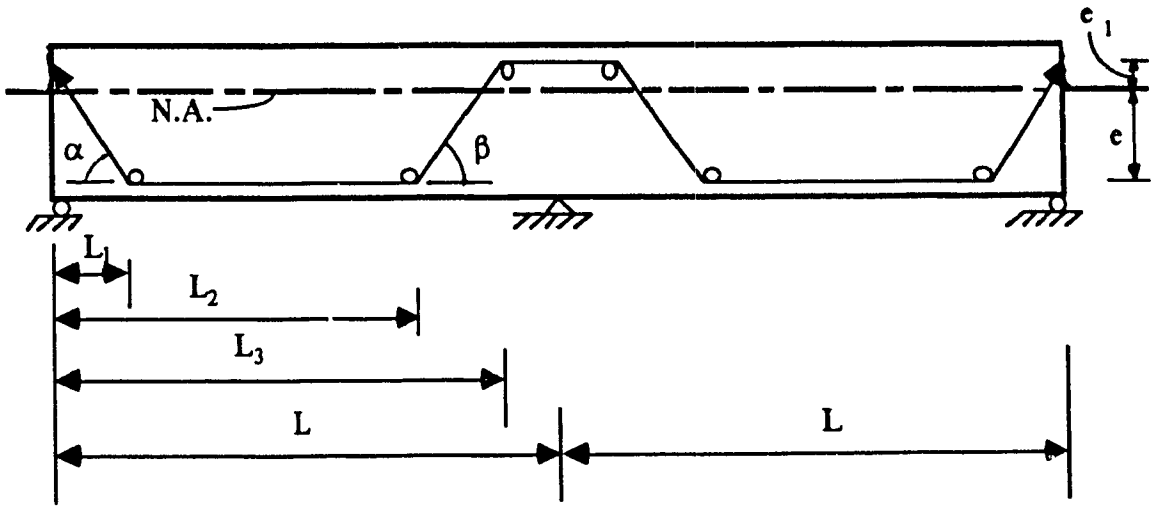

a) Tendon placement type I

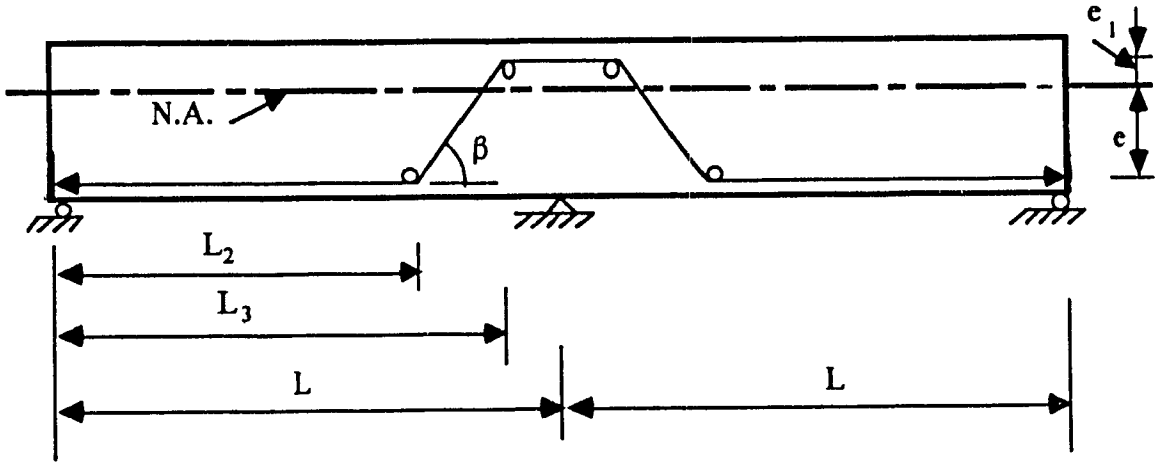

b) Tendon placement type II

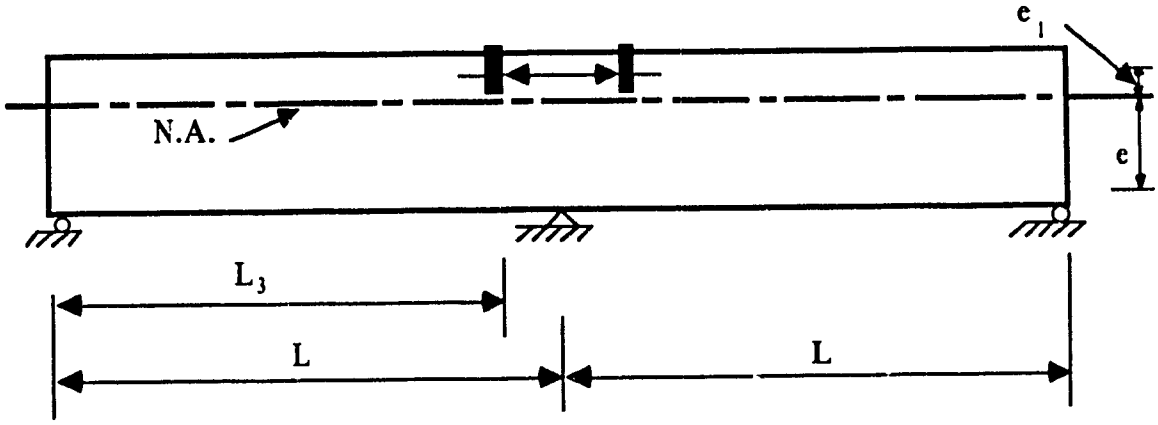

c) Tendon placement type III

Figure 5.6. Typical two span girders prestressed by tendons of various configurations.

The indeterminate structure is considered with the two redundants as:

1) Negative bending moment at the middle support (M)

2) Incremental prestressing force (ΔP).

The structure is subjected to the following loading cases, Figure 5.7,

a) a unit bending moment at the middle support,

b) a unit prestressing force through the tendon,

c) Applied loads (in this case a unit load at an arbitrary position representing the superimposed dead load and lives load).

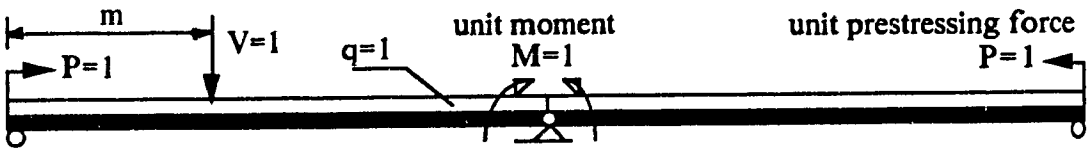

Figure 5.7. The released girder and the position of the unit forces (V=1, M=1, P=1)

The compatibility equations are formulated for the deformations caused by the negative bending moment at the middle support and by the incremental prestressing force [95]. To satisfy the compatibility conditions (continuity of the displacements) along the girder, Equations (5.21) and (5.22) are derived.

$$(5.21) \qquad \delta_{11} M + \Delta P\, \delta_{12} + \Delta_{1L} = 0$$

$$(5.22) \qquad \delta_{21} M + \Delta P\, \delta_{22} + \Delta_{2L} = 0$$

- δ_{ij} is the deformation at location i caused by the effect of a unit load at j,
- Δ_{iL} is the deformation at i due to the applied service loads L, in this case the superimposed dead load and live load.

-M and ΔP are the bending moment at the middle support and the prestressing force increment, respectively.

The δ_{ij} and Δ_{iL} are the flexibility coefficients which can be calculated by virtual work method equating the external and the internal work performed by a unit force applied in the direction of the two unknowns. The general equation for the deformation due to the arbitrary unit load is expressed in Equation (5.23) in which the integral terms due to torsion and shear are neglected.

$$(5.23) \qquad \delta_{ij} = \int_L \frac{M_i M_j}{E I} \, dx + \int_L \frac{N_i N_j}{E A} \, dx$$

- M_i and M_j are the equation of the bending moments along the girder,
- N_i and N_j are the axial forces along the tendon and the girder, respectively,
- E, I and A define the modulus of elasticity, the moment of inertia and the cross-sectional area of the girder, respectively.

To obtain the general bending moment and axial force equations for a typical two-span continuous girder prestressed by tendon of configuration type I, the relevant diagrams are considered, Figures 5.8 through 5.12. Accordingly, the bending moments and the axial forces of the released structure, corresponding to the various loading positions and at any distance x from the left support, can be derived as the following equations. The subscript 1 refers here to the first redundant which is the bending moment at the middle support and number 2 stands for the second unknown - the incremental prestressing force.

$$(5.24) \qquad M_1 = - \frac{x}{L} \qquad 0 \le x \le L$$

Where M_1 is the bending moment at any distance x from the side support caused by a virtual unit moment at the middle support, Figure 5.8.

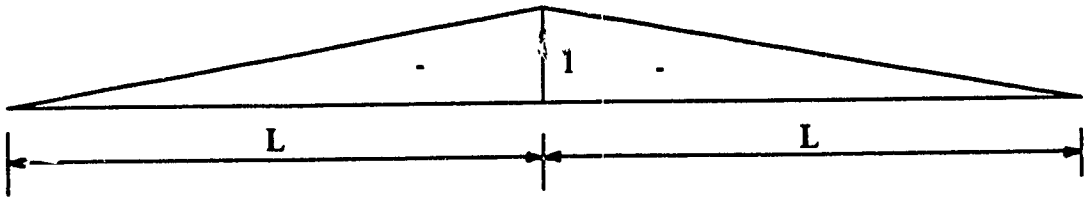

Figure 5.8. Moment diagram due to a unit moment at the middle support

In Figures 5.9.a and 5.9.b the typical moment diagram due to the application of concentrated load V = 1 kN and a uniformly distributed load q = 1 kN / m are shown. Accordingly, the corresponding bending moments at any section x along the girder are derived as Equations (5.25) through (5.27).

(5.25) $$M_p = \frac{P\,(L - m)}{L}\,x \qquad 0 \le x \le m$$

(5.26) $$M_p = \frac{P\,m}{L}\,(L - x) \qquad m \le x \le L$$

(5.27) $$M_q = \frac{q}{2}(L\,x - x^2) \qquad 0 \le x \le L$$

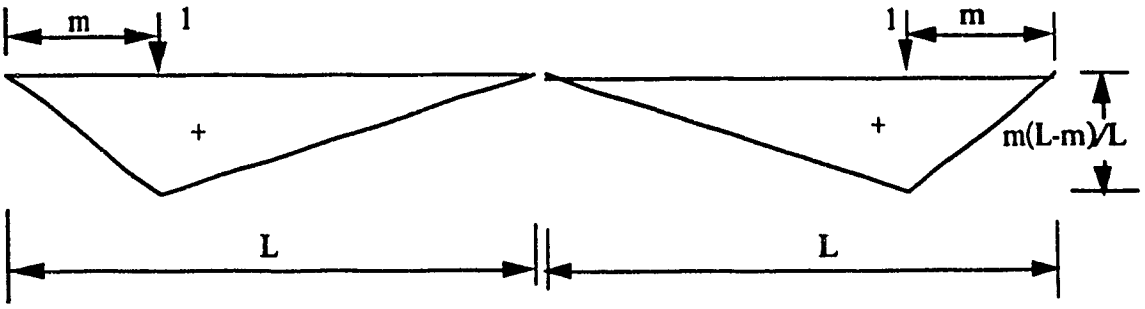

a. Moment diagram due to a concentrated load at distance m from the end supports

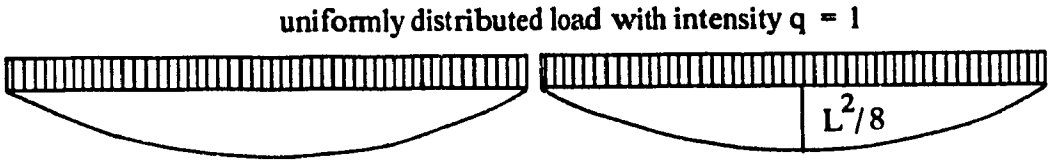

b. Moment diagram due to uniformly distributed load

Figure 5.9. Moment diagrams for girder released at mid support.

The bending moment due to the arbitrary unit prestressing force and in various intervals along the span is formulated in Equations (5.28) through (5.31). Figure 5.10.a illustrates the variation of the bending moment.

$$(5.28) \quad M_2 = -\frac{a+b}{L_1}\,x + a \qquad 0 \le x \le L_1$$

$$(5.29) \quad M_2 = \frac{b-c}{L_2-L_1}\,(x-L_1) - b \qquad L_1 \le x \le L_2$$

$$(5.30) \quad M_2 = \frac{c+d}{L_3-L_2}\,(x-L_2) - c \qquad L_2 \le x \le L_3$$

$$(5.31) \quad M_2 = -\frac{d}{L-L_3}\,(x-L) \qquad L_3 \le x \le L$$

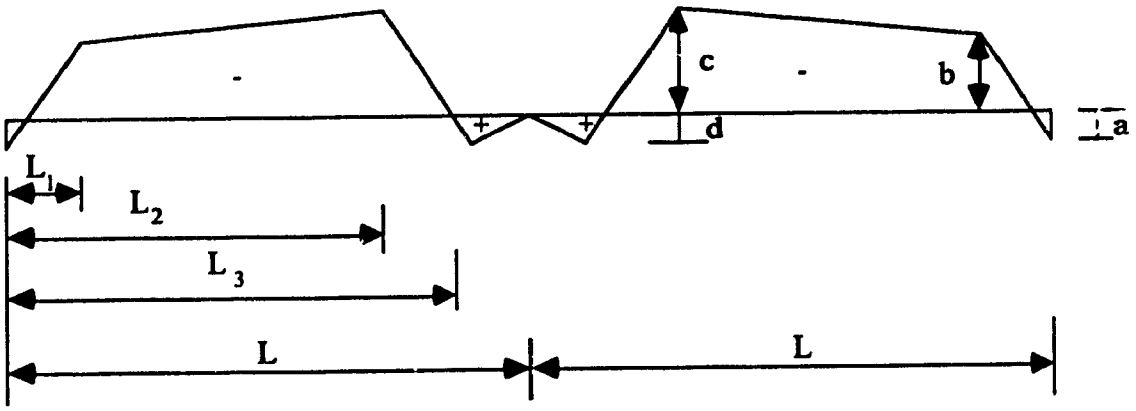

a) Tendon configuration type I

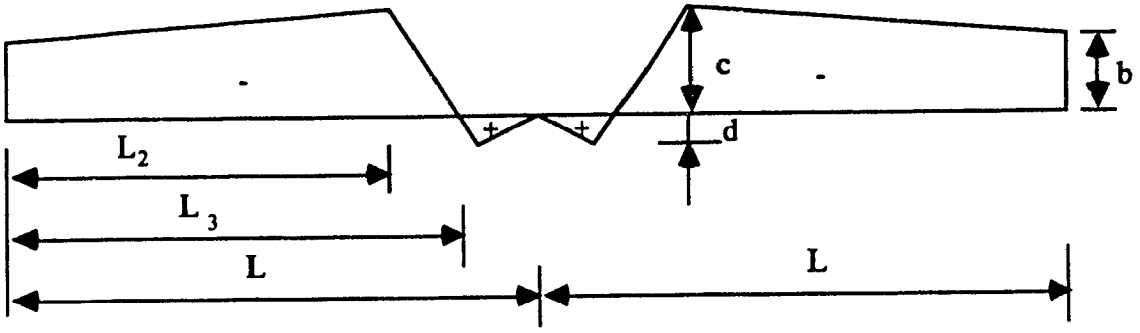

b) Tendon configuration type II

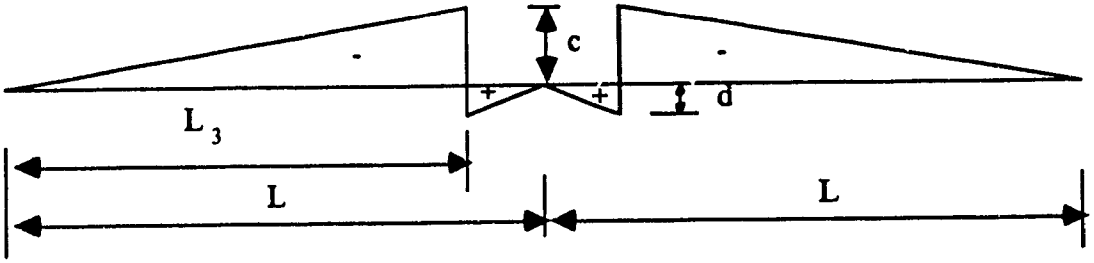

c) Tendon configuration type III

Figure 5.10. Bending moment diagrams due to a unit prestressing force

Equations (5.32) to (5.36) present the values of the axial force in various intervals along the girder and the draped tendons, Figures 5.11 and 5.12.

(5.32)	$N_1 = 1$	$0 \le x \le L$
(5.33)	$N_2 = 1 \cos \alpha$	$0 \le x \le L_1$
(5.34)	$N_2 = 1$	$L_1 \le x \le L_2$
(5.35)	$N_2 = 1 \cos \beta$	$L_2 \le x \le L_3$
(5.36)	$N_2 = 1$	$L_3 \le x \le L$

N_1 defines the axial force along the girder and N_2 describes similar axial force in tendons, α and β are the angles of the sloped tendons with the horizontal line, Figure 5.6.a.

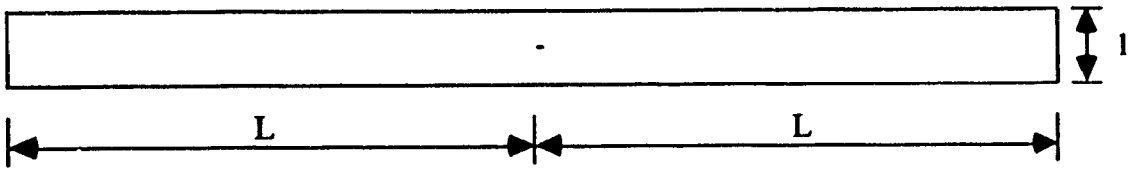

a & b. Tendon configurations type I and II.

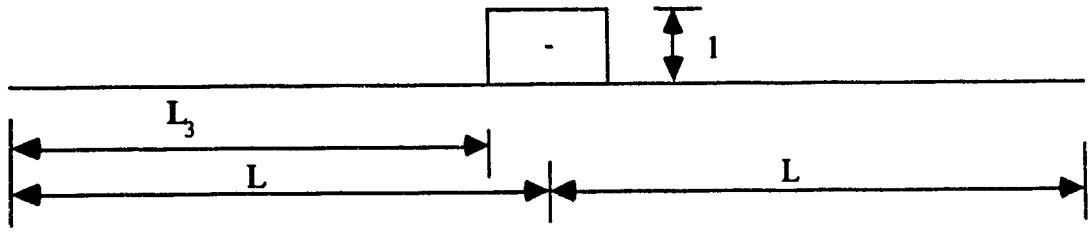

c. Tendon placement type III

Figure 5.11. Axial force diagram due to a unit force along the released girder.

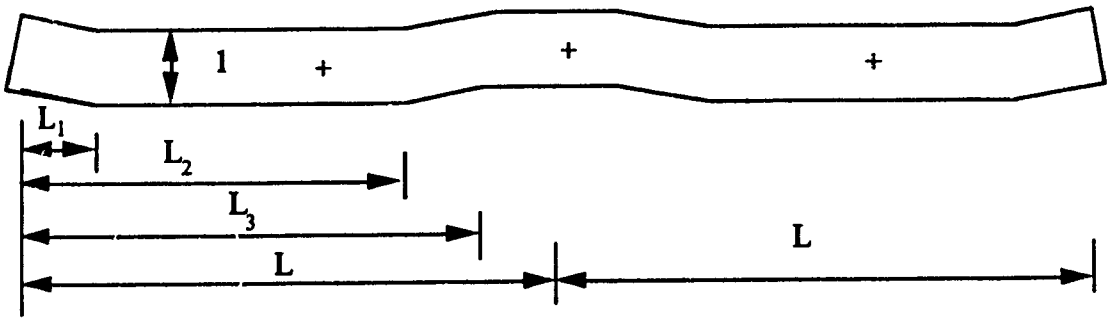

a. Tendon configurations type I.

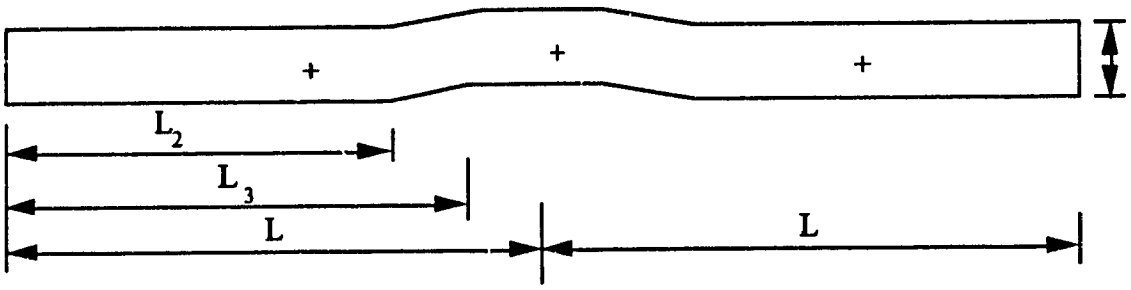

b. Tendon configuration type II.

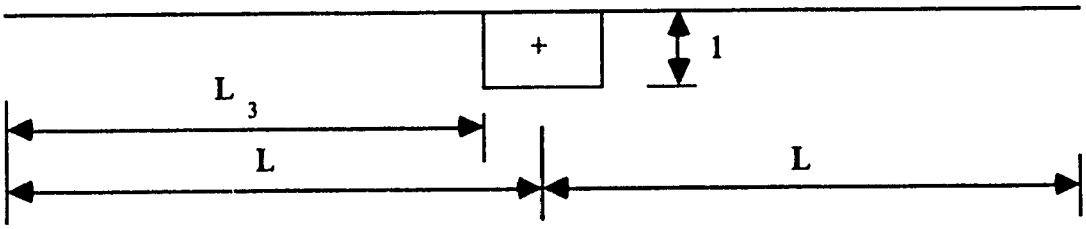

c. Tendon placement type III.

Figure 5.12. Variation of axial force in the tendon due to a unit prestressing force.

The values of the deformations δ_{ij} and Δ_{iL} derived from Equation (5.23) for various types of tendon placements are defined by the following equations:

I. Tendon configuration type I, Figure 5.6.a.

The rotation δ_{11} at the middle support caused by the application of a unit bending moment in the direction of the negative bending moment for the girder with span length L

is equal to:

$$(5.37) \qquad \delta_{11} = \frac{L}{3\,E\,I}$$

The rotation δ_{12} at the middle support due to a unit compressive axial force induced to the system by the prestressed tendons is equal to:

$$(5.38) \qquad \delta_{12} = \frac{1}{3\,EIL}\left[L_1^2(-a-c) + L_2^2(b+d) + L_3^2 c + L^2(-d) + L_1 L_2(b-c) + L_2 L_3(c+d) + L L_3(-d)\right]$$

- L_1, L_2 and L_3 are the distances of the draped cable measured from the left support, Figures 5.6.a, 5.6.b and 5.6.c.
- The parameters a, b, c and d, illustrated in Figure 5.10, are equal to:

$$a = e_1,\ b = e + e_1\frac{L_1}{L},\ c = e + e_1\frac{L_2}{L},\ d = e_1\left(1 - \frac{L_3}{L}\right)$$

- e and e_1 are the bottom and the top tendon eccentricities from the neutral axis, respectively.

The elongation of the girder and the tendons due to the applied unit axial force to the system equals to:

$$(5.39)\quad \delta_{22} = \frac{2}{EI}\left[\frac{L_1}{6}(2a^2-2ab+2b^2)+\frac{L_2-L_1}{6}(2b^2+2bc+2c^2)+\frac{L_3-L_2}{6}(2c^2-2cd+2d^2)+\frac{L-L_3}{6}(2d^2)\right]+\frac{2L}{EA}+\frac{2L_1}{E_tA_t\cos^3\alpha}+\frac{2(L_2-L_1)}{E_tA_t}+\frac{2(L_3-L_2)}{E_tA_t\cos^3\beta}+\frac{2(L-L_3)}{E_tA_t}$$

- A_t and E_t are the cross-sectional area and the modulus of elasticity of the tendons.
- α and β are the angles of the draped tendons with the neutral axis.

The rotations at the middle support caused by uniformly distributed load of unit intensity (q=1) and the concentrated load V=1 are derived from Equations (5.40) and (5.41). Value of Δ_{1LL} in Equation (5.42) defines the total rotation at the middle support.

$$(5.40)\quad \Delta^q_{1LL} = -\frac{L^3}{24EI}$$

$$(5.41)\quad \Delta^V_{1LL} = -\frac{1}{EIL^2}\left(\frac{m^3n}{3}+\frac{m^2n^2}{2}+\frac{mn^3}{6}\right)$$

$$(5.42)\quad \Delta_{1LL} = \Delta^q_{1LL} + \Delta^V_{1LL}$$

in which: $n = L - m$

The elongations of the girder and the tendons due to a uniformly distributed load of unit intensity, q=1 and a unit concentrated load, V=1, are similarly presented in Equations (5.43) and (5.44).

$$(5.43)\quad \Delta^{q}_{2\,LL} = \frac{1}{2EI}\left\{ aL_1^2\left(\frac{L}{6}-\frac{L_1}{12}\right) + b\left[(L_1+L_2)\left(-\frac{LL_2}{6}\right)+\frac{L_2}{12}(L_2^2+L_1L_2+L_1^2)\right] + c\left[(L_1+L_2)\frac{LL_1}{6}-\frac{L_1}{12}(L_1^2+L_1L_2+L_2^2)+(L_3+L_2)\left(-\frac{LL_3}{6}\right)+\frac{L_3}{12}(L_3^2+L_2L_3+L_2^2)\right] + d\left[(L_2+L_3)\left(\frac{-LL_2}{6}\right)+\frac{L_2}{12}(L_3^2+L_2L_3+L_2^2)+\frac{L}{12}(-L_3^2+L^2+LL_3)\right]\right\}$$

$$(5.44)\quad \Delta^{V}_{2LL} = \frac{1}{EIL}\left\{ n\left[(a-2b)\frac{L_1^2}{6}+\left(\frac{b-c}{L_2-L_1}\right)\left(\frac{m^3}{3}+\frac{L_1^3}{6}-\frac{L_1m^2}{2}\right)-\frac{b}{2}(m^2-L_1^2)\right] + m\left[\frac{(b-c)(L_2-m)}{L_2-L_1}\left((L_2+m)\left(\frac{L}{2}+\frac{L_1}{2}-\frac{L_2}{3}\right)-LL_1-\frac{m^2}{3}\right)+ b(L_2-m)\left(-L+\frac{L_2+m}{2}\right)+c(L_3-L_2)\left(-L+\frac{L_2+L_3}{2}\right)+ (c+d)\left((L_3+L_2)\left(\frac{L}{2}+\frac{L_2}{6}\right)-LL_2-\frac{L_3^2}{3}\right)+\frac{d}{3}(L-L_3)^2\right]\right\}$$

where $n = L - m$

The total elongation Δ_{2LL} is equal to:

$$(5.45)\quad \Delta_{2LL} = \Delta^{q}_{2LL} + \Delta^{V}_{2LL}$$

II. Tendon placement type II, Figure 5.6.b.

Similar equations as for the Type I are developed for type II. The derived equations are compared with the given flexibility coefficients for type I. The Equations (5.37) through (5.45) can be modified considering the following:

$$L_1 = 0, \quad a = 0, \quad \cos \alpha = 1$$

III. Tendon placement type III, Figure 5.6.c.

The same equations as for the type I can be considered assuming the following values for the given parameters:

$$L_1 = 0, \quad e = 0, \quad L_3 = L_2, \quad \cos \alpha = \cos \beta = 1$$

The proposed procedure for the analysis of the flexibility coefficients can be generalized for the prestressed two span girders having unequal spans, as well as for girders with variable cross-sectional areas.

The two unknowns M and ΔP are computed from Equations (5.46) and (5.47) with regard to the simultaneous Equations (5.20) and (5.22), considering $\delta_{12} = \delta_{21}$.

$$(5.46) \qquad M = \frac{\Delta_{1LL}\,\delta_{22} - \Delta_{2LL}\,\delta_{21}}{\delta_{12}^2 - \delta_{11}\,\delta_{22}}$$

$$(5.47) \qquad \Delta P = \frac{\Delta_{2LL}\,\delta_{11} - \Delta_{1LL}\,\delta_{12}}{\delta_{12}^2 - \delta_{12}\,\delta_{22}}$$

Calculated value of the incremental prestressing force ΔP has to be added to the initial effective prestressing force P reduced by the losses due to the relaxation of steel tendons, slip in end anchorages and friction of cable guides. The term $(P + \Delta P)$ corresponds to the total effective prestressing force induced to the girder. The term M signifies the modified negative bending moment at the middle support considering the effect of prestressing.

Based on the developed equations a computer program was written which includes the effect of various types of tendon configurations. For the analysis of prestressed girders subjected to moving live loads, the use of the influence lines can be considered as effective tool. The influence lines for the bending moment at the middle support and the prestressing force increment are presented for various span lengths. The influence lines have not been generalized because numerous variable parameters are involved. Influence lines may be provided for various span lengths. Figures 5.13 and 5.14, illustrate the influence lines for the bending moment and the prestressing force increment for a girder with two equal spans of 60 m length each, prestressed by continuous tendons type I, Figure 5.6.a., and subjected to a moving concentrated load equal to one. The ordinates of the middle support bending moment of a similar non-prestressed girder are also shown in Figure 5.13. Similar to the conventional influence lines, the negative bending moment and the incremental prestressing force for the girder, subjected to service loadings applied to the girder when prestressing is completed, can be evaluated as:

a) concentrated load; $\Sigma V \cdot$(the corresponding ordinates)

b) uniformly distributed load; $\Sigma q \cdot$(the corresponding area under the load).

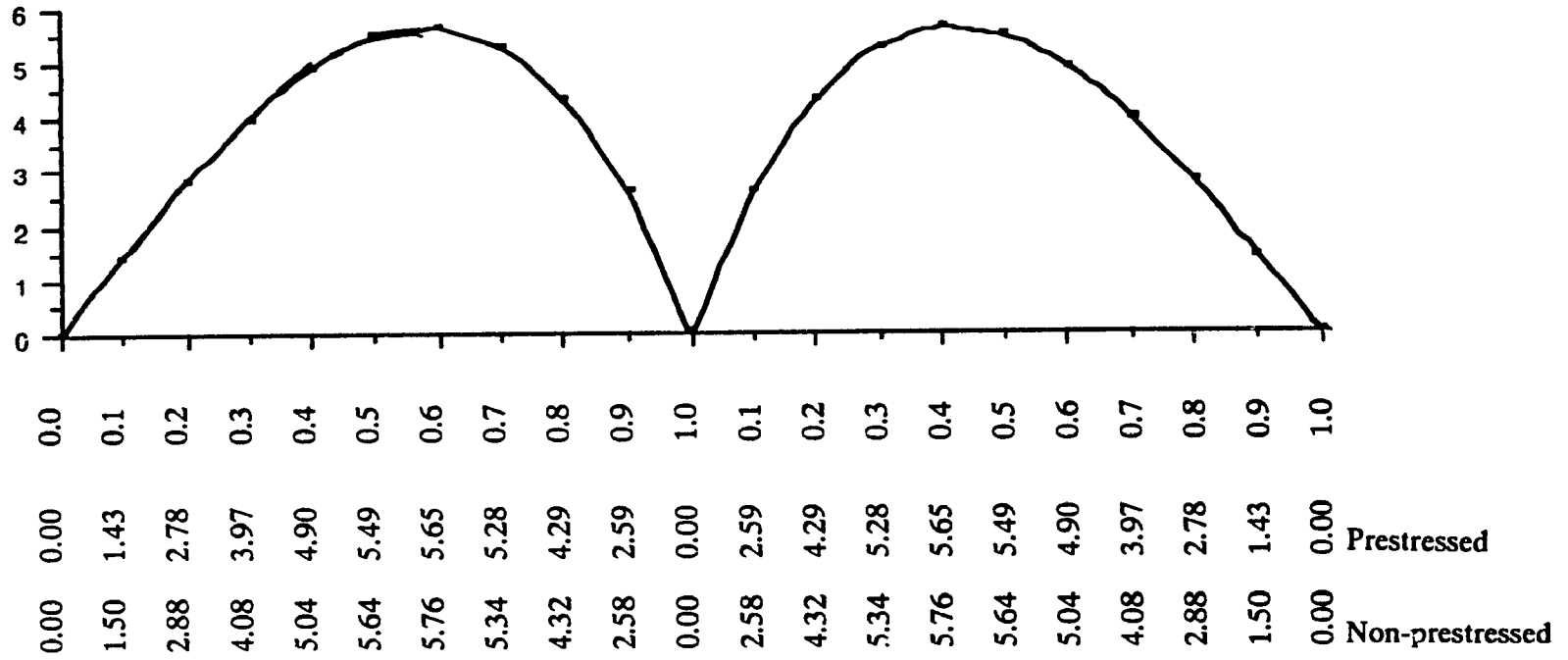

Figure 5.13. Influence line for the bending moment at the middle support, due to an arbitrary unit load, for a two span girder each of 60 m, prestressed by tendon configuration Type I.

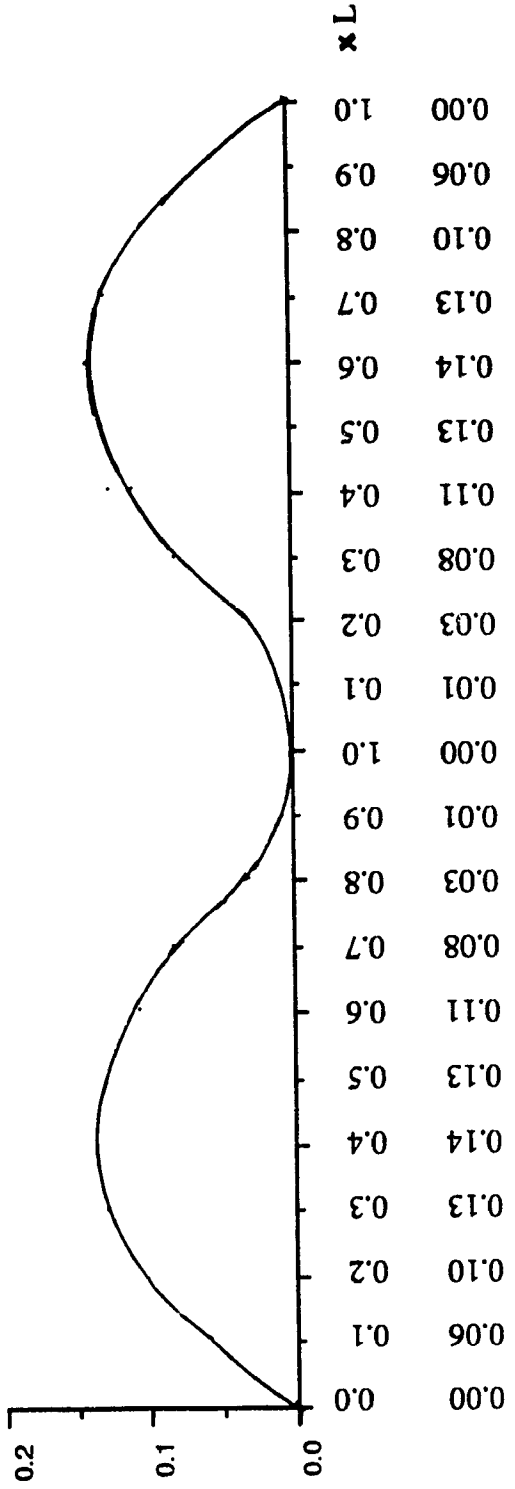

Figure 5.14. Influence line for the incremental prestressing force, due to an arbitrary unit load, for a two span girder each of 60 m, prestressed by tendon configuration Type I.

CHAPTER VI. EXPERIMENTAL MODEL STUDY

6.1. INTRODUCTION

To investigate the validity of the theoretical study and the feasibility of increasing the load carrying capacity of the steel box girders by prestressing, a series of tests was performed on a steel box girder model made at the Structural Laboratory at Concordia University. The model is a distorted similitude of the assumed prototype, both provide similar qualitative behavior and a quantitative stress relationship.

The assumed prototype is a two-equal-span continuous steel box girder having variable cross section along the girder.

The main objectives of the test can be described as:

- To investigate the stress distribution along and across the girder
- To compare the load carrying capacity of the prestressed and the non-prestressed model subjected to similar applied service loads.
- To verify the effect of the induced prestressing force.
- To evaluate the incremental prestressing force due to the application of loads after prestressing is done.
- To compare the stresses in the prestressed and non prestressed model under the application of variable loads.
- To evaluate the force and the stress results obtained from the model study for the prototype.

To achieve these objectives a box girder model was designed to accommodate the conditions under which the behaviors of the two systems are similar and the behavior of the prototype can be accurately predicted from the test results.

6.2. GEOMETRY AND CROSS SECTIONAL PROPERTIES OF THE PROTOTYPE

The prototype consists of a two-equal-span continuous steel box girder, the geometry and the design of which is presented in Appendix III. The plan, longitudinal and cross-sectional geometry of the girder is shown in Figure 6.1. The top deck is an orthotropic steel plate stiffened by longitudinal ribs. The webs are inclined plates welded to the top and bottom flanges. The height of the trapezoidal cross section varies along the two equal span lengths of 80.m each. The height is constant along L_1 = 58. m from the side supports at the vicinity of the positive bending moment, designated as section I. Within L_1 = 58. m to L_2 = 70. m the section has a variable height, increasing from 1.9 to 2.6 m, but the slopes of the webs are kept constant. From L_2 = 70. m to L = 80. m the height is constant at 2.6 m along the negative moment region over the middle support (Section II). The cross sectional properties of the prototype girder for the mid-span and the middle support zones are as follow:

Section I- Region of positive bending moment (Figure 6.2.a)

$A = .24\ m^2$	$y_{top} = .75\ m$	$y_{bot} = 1.15\ m$
$I = .162\ m^4$	$S_{top} = .216\ m^3$	$S_{bot} = .141\ m^3$

Section II- Region of negative bending moment (Figure 6.2.b)

$A = .28\ m^2$	$y_{top} = 1.32\ m$	$y_{bot} = 1.28\ m$
$I = .36\ m^4$	$S_{top} = .271\ m^3$	$S_{bot} = .282\ m^3$

The cross sectional area and the eccentricities of the tendon are:

$A_t = .005\ m^2$	$e = 1.0\ m$	$e_1 = 1.2\ m$

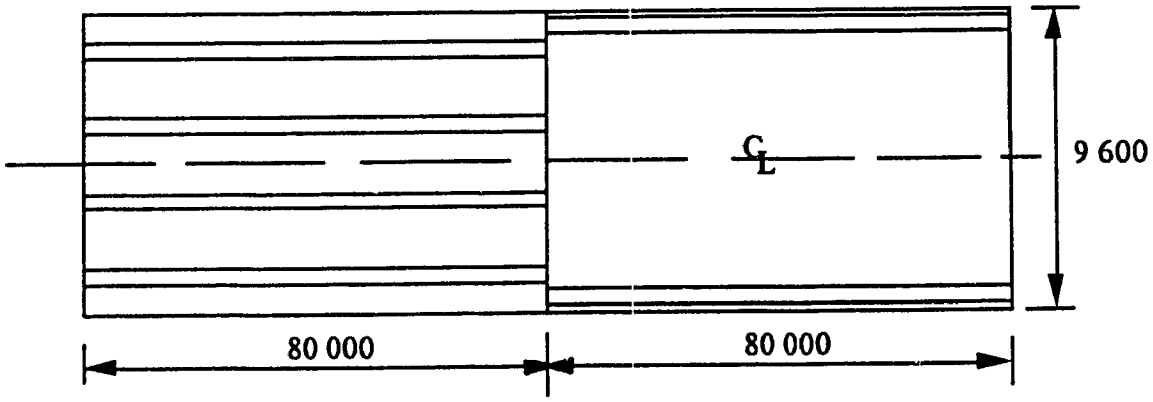

a. Plan of the prototype

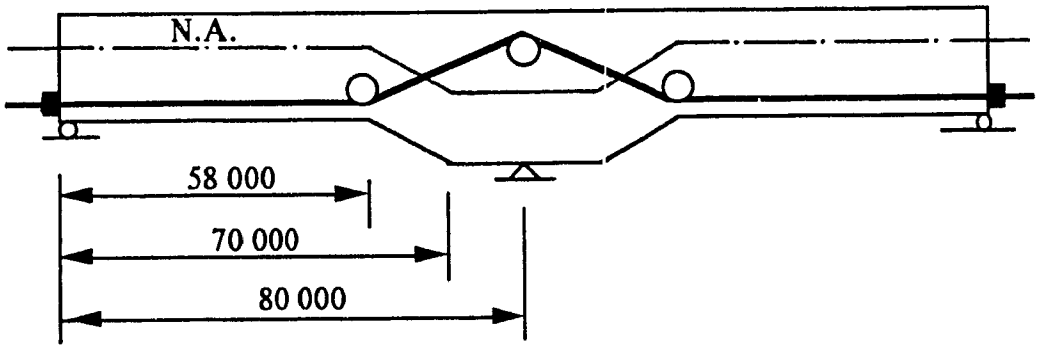

b. Longitudinal elevation

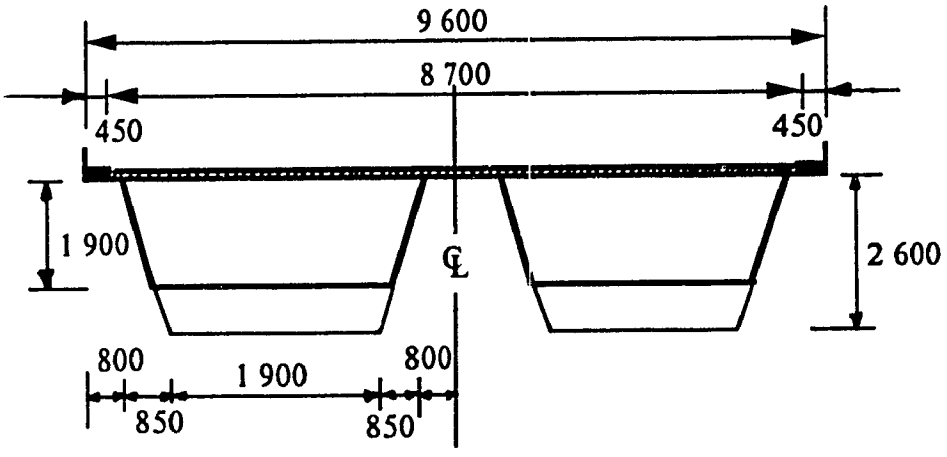

c. The cross section of the prototype

Figure 6.1. The geometry of the prototype box girder, all dimensions in mm

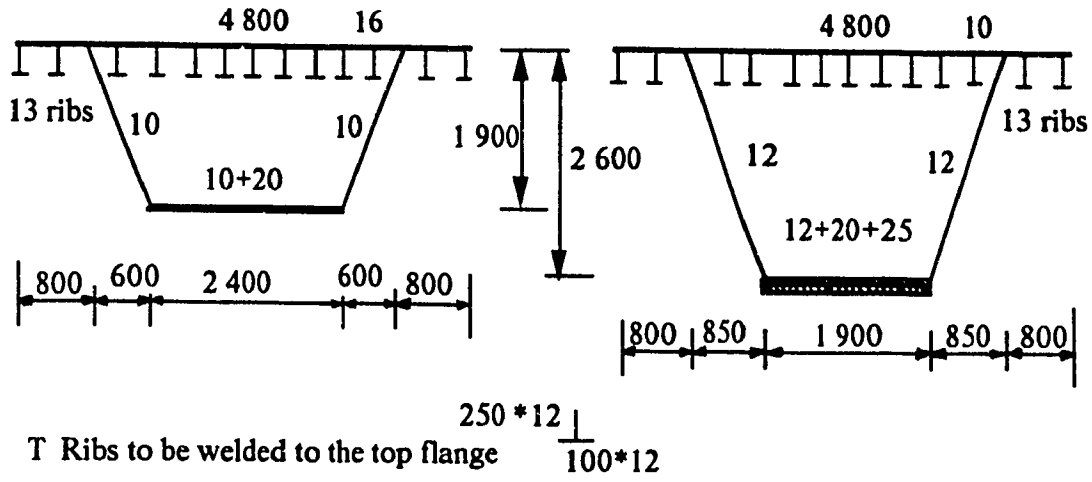

a. Cross section I

b. Cross section II

Figure 6.2. The cross sectional geometry of the prototype, all dimensions in mm

6.3. DESIGN AND FABRICATION OF THE MODEL

Several factors had to be considered in the fabrication of the model which include: the size, material and method of fabrication, as well as the cost and the space and testing equipment available in the structural laboratory.

Based on the above limitations the designed model will have various reducing scales for the length, width and thicknesses, result in a model which by definition is called distorted [80].

The model is made of steel plates of the same material as of the prototype. Therefore the behavior of the girder under loading will be comparable. The fabrication of the model is also very much the same as the fabrication of the prototype steel box girder could be. Shop welding and torch cut plates were to avoid large residual stresses due to welding and providing similar plate imperfections the model was fabricated using relatively thick plates. Due to the similarity of the cross sectional geometry of the prototype and the model, the performance of the former can be predicted accurately from the test results of the latter. The relatively thick plates used in the fabrication of the model contribute in preventing the undesired longitudinal and transverse buckling.

The tendons used are the standard prestressing strands of 7 Wires, representing the same behavior when prestressed as would be on the prototype.

6.3.1. SIMILITUDE CONDITIONS

In order to predict the behavior and response of the prototype from the test results on the model a specific relationship must be kept between the two, defined as the similitude conditions. Similitude conditions are expressed in the following formulas, considering that the moduli of elasticity of the model and of the prototype are equal since similar materials are selected for both [81].

Similitude in length, depth and plate thicknesses

$$\frac{L_p}{L_{hm}} = k \tag{6.1}$$

For Area

$$\frac{A_p}{A_{hm}} = k^2 z \tag{6.2}$$

For the Section Modulus

$$\frac{S_p}{S_{hm}} = k^3 z \tag{6.3}$$

Moment of Inertia

$$\frac{I_p}{I_{hm}} = k^4 z \tag{6.4}$$

Bending moment

$$\frac{M_p}{M_{hm}} = k^3 z \tag{6.5}$$

Concentrated load and prestressing force

$$\frac{P_p}{P_{hm}} = k^2 z \tag{6.6}$$

The strain at any arbitrary point along the prototype will be equal to the strain at similar point on the ideal homologous model considering scale down factor k for the length,

$$\frac{\varepsilon_p}{\varepsilon_{hm}} = 1. \tag{6.7}$$

k is the scale reduction factor and z is a factor allowing for more flexibility in selecting the size of the model. The subscripts p and hm represent the prototype and the homologous model, respectively.

6.3.2. FABRICATION OF THE MODEL

The similitude conditions defined in Section 6.3.1 are applied to scale down the dimensions of the prototype to find the geometry and properties of the homologous model. However the fabrication of a true model having equal scale down factors for the depth, length, width and the plate thicknesses is found to be impractical.

The scale down factors for various dimensions of the model based on space limitations and better workability are selected as: 28 for the length and 5 for the depth and width. The ideal material for the model is steel which represents the same behavior as the prototype under loading. The model's longitudinal and cross-sectional configuration and shape are similar to those of the prototype.

The plate thicknesses of the model are designed such that a) they are perfectly weldable (not too thin), b) the effect of the residual stresses due to welding and plate imperfections

are similar for the model and the prototype. c) In the compression region longitudinal stiffeners (ribs) are not required, since adequate top flange slenderness ratio is provided to prevent local buckling. The plate thicknesses are taken as 8 mm for all elements except at the top and bottom flange at the vicinity of the negative bending moment, as noted in Figure 6.3.c.

The height of the model is variable along the length, but the slopes of the webs are constant. Similar to the prototype two various sections with two different heights are connected by a variable height. Figure 6.3 illustrates the dimensions of the actual fabricated model. The variation of the two sections, positive moment region (Section I) and the negative moment region (Section II) are in proportion to the similar values of the prototype provided that the scales down factors are considered, therefore the prediction factors for the two sections will be equal.

The cross sectional properties of the actual model built along the two regions - positive and negative bending moment criteria - are given as follow:

Section I- Region of positive bending moment (Figure 6.3.b)

$A = 18 * 10^3$ mm^2 $\quad y_{top} = 150$ mm $\quad y_{bot} = 230$ mm

$I = .44 * 10^9$ mm^4 $\quad S_{top} = 2.93 * 10^6$ mm^3 $\quad S_{bot} = 1.91 * 10^6$ mm^3

Section II- Region of negative bending moment (Figure 6.3.c)

$A = 21 * 10^3$ mm^2 $\quad y_{top} = 265$ mm $\quad y_{bot} = 255$ mm

$I = .98 * 10^9$ mm^4 $\quad S_{top} = 3.11 * 10^6$ mm^3 $\quad S_{bot} = 2.86 * 10^6$ mm^3

The cross sectional area and the eccentricities of the tendons are:

$A_t = 3 * 138.7$ mm^2 $\quad e = 200$ mm $\quad e_1 = 240$ mm

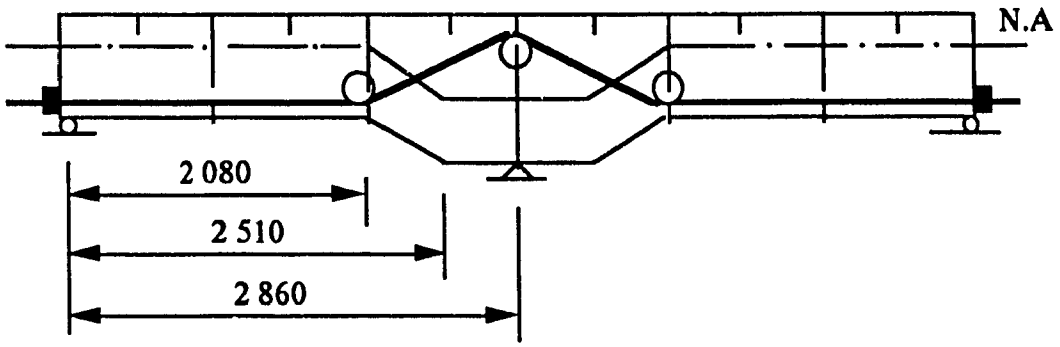

a. Longitudinal elevation

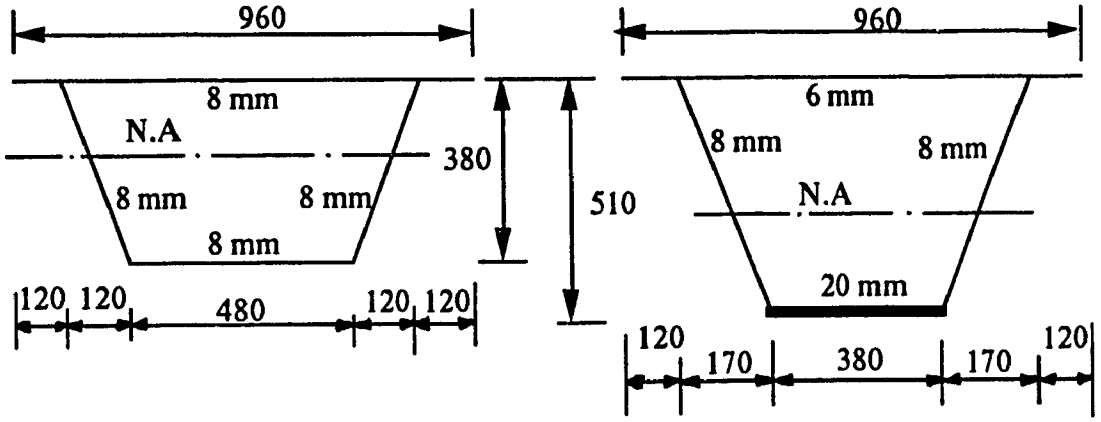

b. Cross section along positive moment

c. Cross section along negative moment

Figure 6.3. The geometry of the actual fabricated model, all dimensions in mm

The scale down factors and the properties of the ideal homologous model considering the similitude conditions can be calculated as:

For the depth and width,

$$\frac{d_p}{d_{hm}} = k = 5.0$$

In order to be consistent in the prediction of the stresses along the girder and allowing for more flexibility in the fabrication of the actual model the prediction factor z is

employed in further determination of the cross sectional dimensions of the model. Several trials were made to achieve a homologous model geometry for which the variation factors for the sections I and II are equal to similar factors along the prototype girder. The variation factors for the cross sectional properties of Section II divided by Section I are calculated as: For the depth 1.37, for the moment of inertia 2.22, for the cross-sectional area 1.17.

The value of the parameter z based on the moment of inertia of the actual fabricated model and the assumed prototype is equal to:

$$(6.8) \qquad \frac{I_p}{I_{hm}} = k^4 \cdot z = 625 \times z \quad \text{and} \quad \frac{I_p}{I_m} = \frac{.16 \times 10^{12}}{.44 \times 10^9} = 363.6 \;, \quad z = .58$$

For area

$$(6.9) \qquad \frac{A_p}{A_{hm}} = k^2 \cdot z = 25 \times .58 = 14.5$$

For the section modulus

$$(6.10) \qquad \frac{S_p}{S_{hm}} = k^3 \cdot z = 125 \times .58 = 72.5$$

6.3.3. PREDICTION FACTORS

The model is considered distorted since there are various reproduction scales for the length, the depth and the plate thicknesses. Two types of distortion are defined.

a) Geometrical distortion in which the shape of the model is similar to the assumed prototype, whereas the cross-sectional property of the model is scaled down from the prototype by the application of different factors.

b) Applied loadings' distortion in which the prestressing tendons and the vertical loads are scaled down by various factors. To prevent asymmetrical cross-sectional distortions the vertical loads have been distributed along the width of the model.

The structural behavior of the prototype can be predicted from the experimental results on the model by the introduction of correction factors. For instance the stresses at any arbitrary section can be ascertained for the prototype from the corresponding test results on the model considering the correction factors for the section modulus and the deviation of the cross sectional area of the actual built model to that of the homologous one. The correction factors are calculated based on the values obtained for the ideal homologous model (similitude conditions) and the actual fabricated model.

The corresponding correction factors for the cross sectional properties are gives as:

- The deviations of the section moduli of elasticity for the homologous model and the actual model at the top and bottom are equal to:

$$(6.11) \qquad CFS_{top} = \frac{S_{hm}}{S_m} = \frac{2.98\times10^6}{2.93\times10^6} = 1.015$$

$$(6.12) \qquad CFS_{bot} = \frac{S_{hm}}{S_m} = \frac{1.94\times10^6}{1.91\times10^6} = 1.015$$

- The correction factor for the cross sectional area is calculated as:

$$(6.13) \qquad CFA = \frac{A_{hm}}{A_m} = \frac{16555}{18000} = .92$$

The subscripts hm and m stand for the ideal homologous and the actual model.

The correction factors are valid along the girder because the variation of the geometry of the model along the girder has been proportionally introduced for Section 1 and Section 2 (similar correction factors are employed).

The relations between the loadings on the prototype and on the homologous model are expressed by the similitude conditions, Equations (6.5) and (6.6), considering the reduction factor for the length $K_1 = 28$. However to obtain reasonable results and to accommodate a better workability the calculated loadings for the ideal homologous model based on the similitude conditions are reduced.

The applied prestressing and vertical forces on the prototype and on the model have to be proportioned such that the bending moment due to the cable eccentricity (P.e) and the vertical loadings (M) have similar reduction factors, Equation (6.14).

$$(6.14) \qquad \frac{M_p}{M_m} = \frac{P_p \cdot e_p}{P_m \cdot e_m}$$

Considering the calculated bending moments at the middle support due to a unit vertical load on the model and on the prototype the relation between the prestressing force and the vertical loads are given as:

$$(6.15) \qquad \frac{8.13 \times V_p}{.29 \times V_m} = \frac{1.0 \times P_p}{.2 \times P_m} \quad \text{or} \quad 28 \frac{V_p}{V_m} = 5 \frac{P_p}{P_m}$$

$$(6.16) \qquad \frac{P_p}{P_m} = 5.6 \times K_1^2 \cdot z_1 = 4390.4 \times z_1 \qquad \text{where} \quad K_1 = 28$$

Substituting for $P_p = 4846$ kN and $P_m = 142.6$ kN gives $z_1 = 7.74 \times 10^{-3}$.

- The reduction factor for the vertical load

$$(6.17) \qquad \frac{V_p}{V_m} = k_1^2 \cdot z_1 = 6.07$$

The values of the vertical force on the model and on the prototype are equal to:

$$V_p = 438 \text{ kN} \quad \text{and} \quad V_m = 72.11 \text{ kN}$$

- The reduction factor for the bending moment

$$(6.18) \qquad \frac{M_{hm}}{M_m} = k_1^3 z_1 = 170.0$$

- The reduction factor for the prestressing force

$$\frac{P_p}{P_m} = 5.6 \; k_1^2 z_1 = 34.0$$

The recorded strains of the model under loading are the combination of strains due to the axial loads and flexural stresses. It is necessary to separate the components of these two strains so that the individual correction factors can be applied for the axial and flexural strains. Note that the term stress and strain can be interchanged since the modulus of elasticity of the model and the prototype is equal.

In Figure 6.4 the typical linear stress distribution has been shown at a positive moment region.

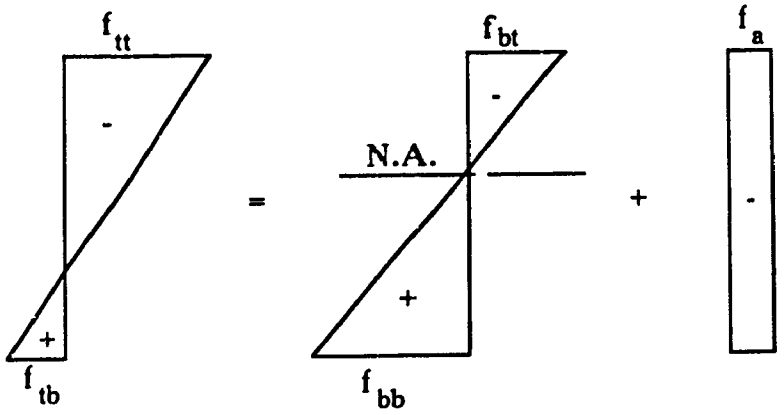

a) Total combined stresses b) Bending stress c) Axial stress

Figure 6.4. The stresses are resolved into bending and axial stress.

By proportioning the linear bending stress distribution, Figure 6.4.b, the top and bottom stresses due to bending can be expressed as Equations (6.19) and (6.20).

$$(6.19) \quad -f_{bt} = (-f_{bt} + f_{bb}) \frac{d_{top}}{d} = f_b \frac{d_{top}}{d}$$

$$(6.20) \quad f_{bb} = (-f_{bt} + f_{bb}) \frac{d_{bot}}{d} = f_b \frac{d_{bot}}{d}$$

where $f_b = -f_{bt} + f_{bb}$

The measured stresses at the top and at the bottom fibers of the section, Figure 6.4(a) are the sum of its constituents, bending and axial stresses, Equations (6.21) and (6.22). The expressions for the resolved stresses are obtained from the Equations (6.19), (6.20) and (6.23) with the corresponding value of f_b from Equation (6.24). The assumed sign convention, (-) for compression and (+) for tension.

$$(6.21) \qquad f_{tt} = f_{bt} + f_a = - f_b \frac{d_{top}}{d} + f_a$$

$$(6.22) \qquad f_{tb} = f_{bb} + f_{at} = + f_b \frac{d_{bot}}{d} + f_a$$

$$(6.23) \qquad f_a = f_{tt} \frac{d_{bot}}{d} + f_{tb} \frac{d_{top}}{d}$$

$$(6.24) \qquad f_b = - f_{tt} + f_{tb}$$

f is the stress, the first subscript letters a, b and t stand for the axial, bending and total stresses, where the second subscripts t and b correspond to the top and bottom fibers, respectively.

6.3.4. SUMMARY OF STRESS EVALUATION

To establish the stresses along the prototype girder the stresses obtained from the test results should be multiplied by the proper values of the correction factors. The procedure can be written as:

- Resolve the test results into axial and bending stresses, Equations (6.19), (6.20) and (6.23).
- Multiply the axial stress by

$$(6.25) \qquad \frac{(\frac{P}{A})_p}{(\frac{P}{A})_m} = \frac{34}{14.5 \times .92} = 2.55$$

- multiply the bending stress by

$$(6.26) \qquad \frac{(\frac{M}{S})_p}{(\frac{M}{S})_m} = \frac{170}{72.5 \times 1.015} = 2.31$$

6.4. INSTRUMENTATION

The employed measurement system consists of strain gages, load cells, data acquisition system and computer.

a) Strain gages - which are simple electrical resistors to measure the strains at predetermined specific locations on the model where strain gauges are bonded [82].

The structural critical points along the girder are selected for which the strains and eventually stresses have to be measured. Furthermore the strain gauges were bonded symmetrically on the girder to check the possibility of induced torsional stresses due to asymmetrical loadings and also as a matter of control of readings and double results. Figure 6.5 shows the location of the strain gauges bonded to the model at the top and at the bottom flange.

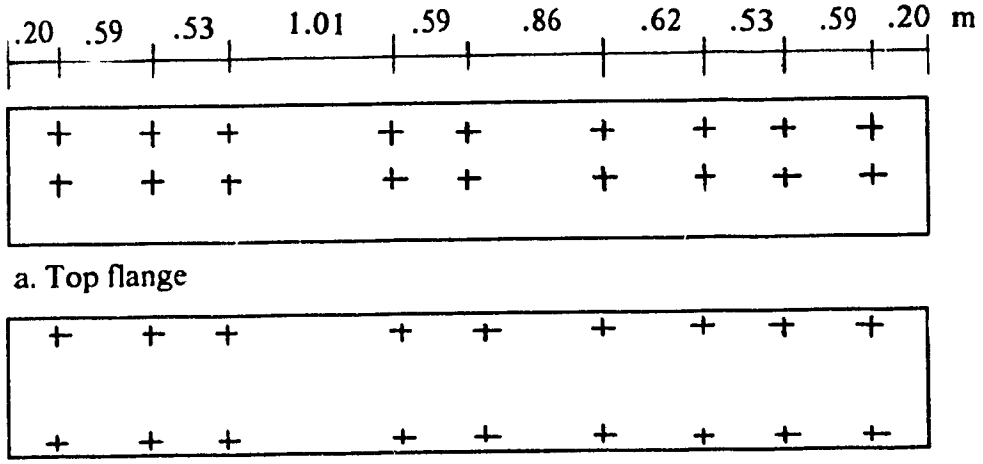

a. Top flange

b. Bottom flange

Figure 6.5. The position of the strain gauges

To achieve precise bond and accurate measurement the metal surface is properly prepared for the adhesion of the strain gauges. The recommended surface preparation included: degreasing, abrading, application of gauge layout lines, cleaning and conditioning and neutralizing [83].

b) Load Cells were installed to measure the applied axial loads, the vertical loads, the incremental prestressing force and the losses of prestressing. The jacks and load cells were calibrated prior to the experiment on Standard Test Machine. The load cells were placed between the hydraulic jacks and the portion of the girder where the loads are induced, see Figure 6.6 and 6.7.

c) Data Acquisition System. The advanced HP3852 S Data Acquisition System and control system were employed to read the signals from the strain gauges. The system is capable of reading of more than 100 gauges in a fraction of second. The system stores and saves the data and is able to send the data to computer for future recalls and assessments.

d) The Computer, was connected to the data acquisition system. The provided software receives the data from the data acquisition system and translates to strains.

6.5. FABRICATION OF THE MODEL

The plates were cut in precise required dimensions. The bottom flange and the webs were welded together and then the diaphragms were installed and welded. The desired tendons' path configurations were gained by installation of cable guides (Saddles) on the intermediate diaphragms at the tendons' slopes change. The saddles were greased in order to decrease the friction losses. The tendons were passed along the girder within the box section as shown in Figure 6.6.

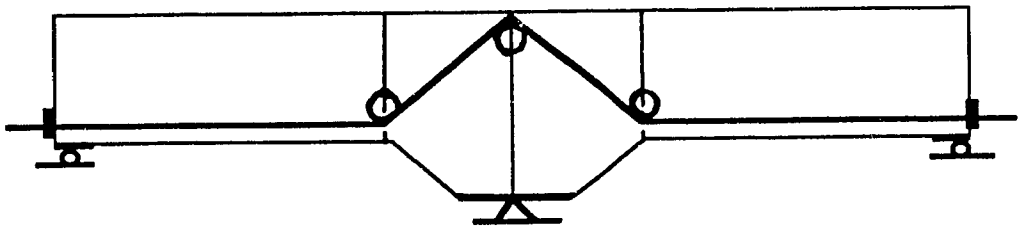

Figure 6.6. Tendon configuration of the model

The transverse flat plates are welded to the top flange and the fabricated piece is installed into the prearranged slotted webs. All the connections are thoroughly welded. The supports are two rollers at the two ends and a hinge at the middle support, Figure 6.9., to allow for horizontal movements. No downward settlement of the supports were permitted due the employment of strong seats and supports.

Vertical forces and prestressing forces are applied by hydraulic jacks which were calibrated prior to the experiment and were attached to the data acquisition system through the load cells. Several number of tests and strain readings were performed to ensure the validity and accuracy of the results. The strain readings were set to zero prior to the loadings, considering a redundant non-loaded strain gauge as the reference gauge. The reference gauge was installed at the vicinity of the middle support having similar environmental conditions - temperature, magnetic field, etc.- as of the other strain gauges. Figures 6.7 through 6.23 illustrate the fabrication of the model.

Figure 6.7. The plates are cut in the desired sizes.

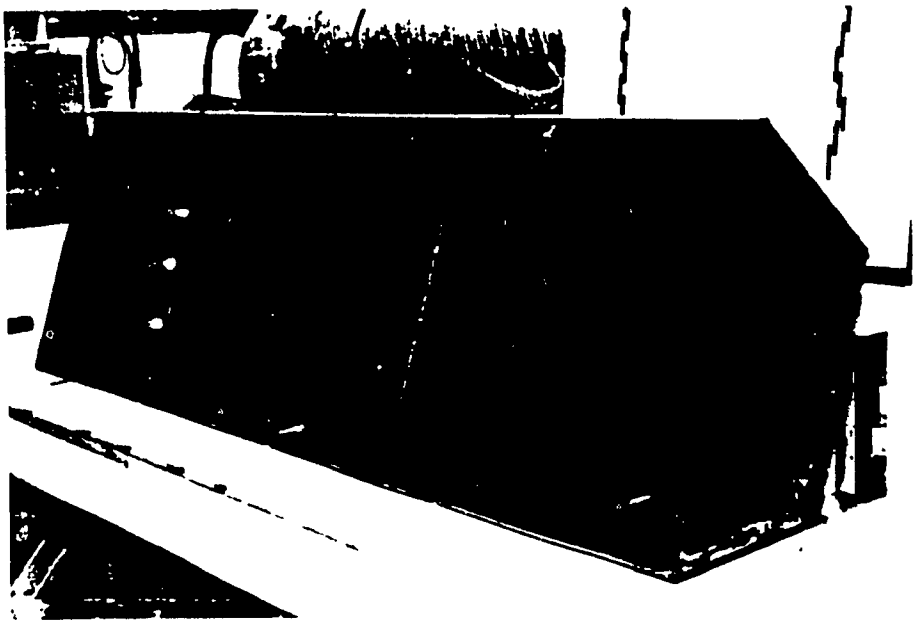

Figure 6.8. The girder is divided into three elements and welded separately, excluding the top flange.

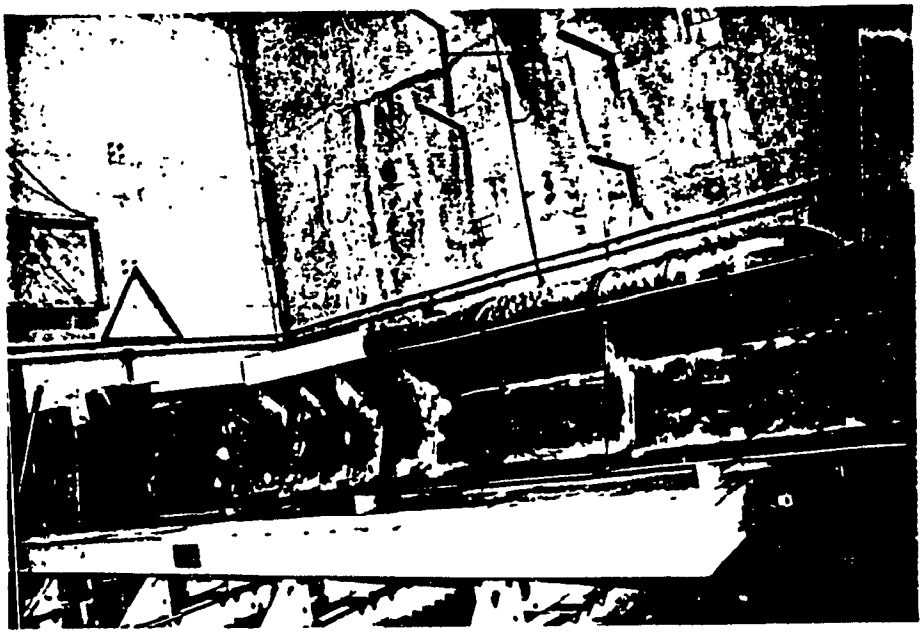

Figure 6.9. The three elements are assembled and welded together.

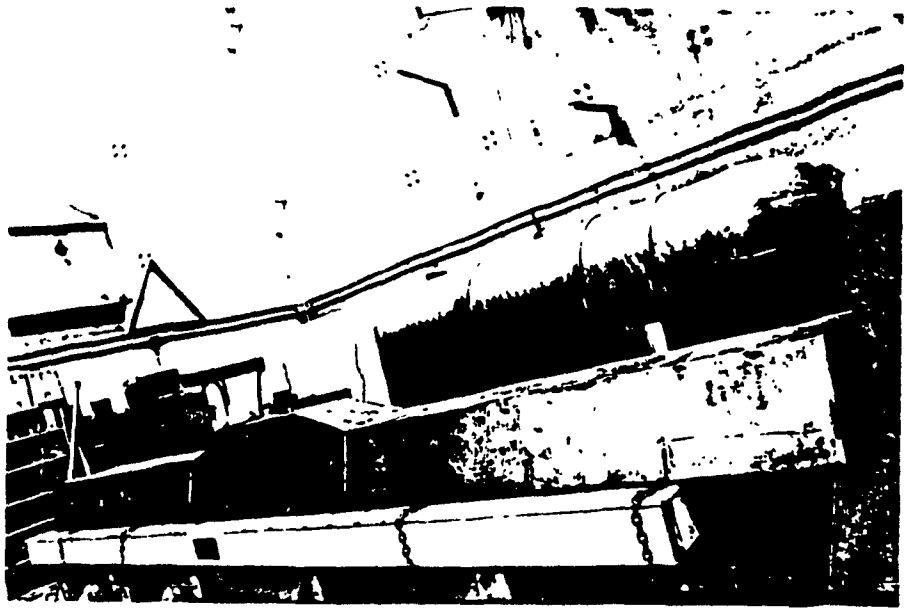

Figure 6.10. The weldings are completed on the outer side of the girder.

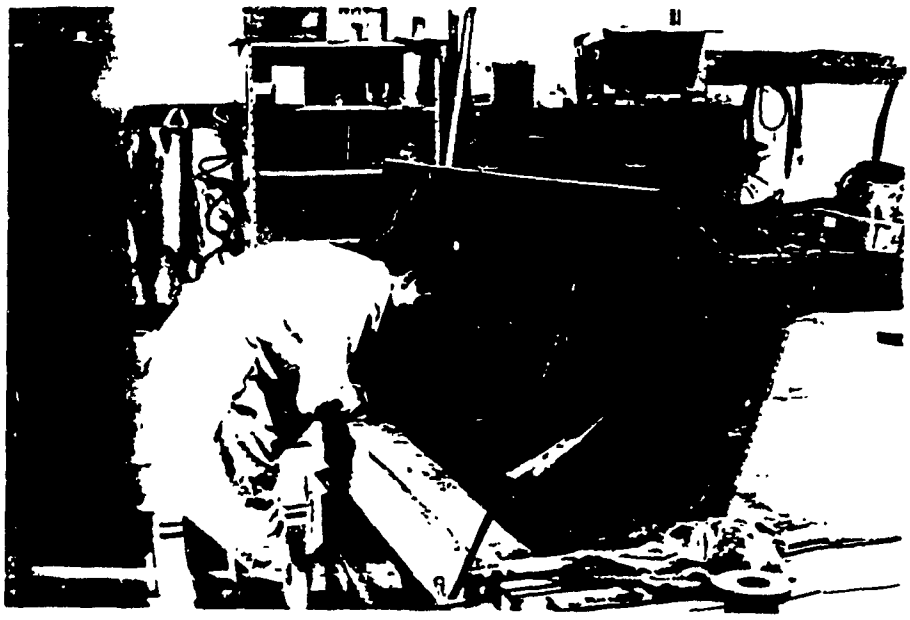

Figure 6.11. The diaphragms are placed and welded to the webs and bottom flange.

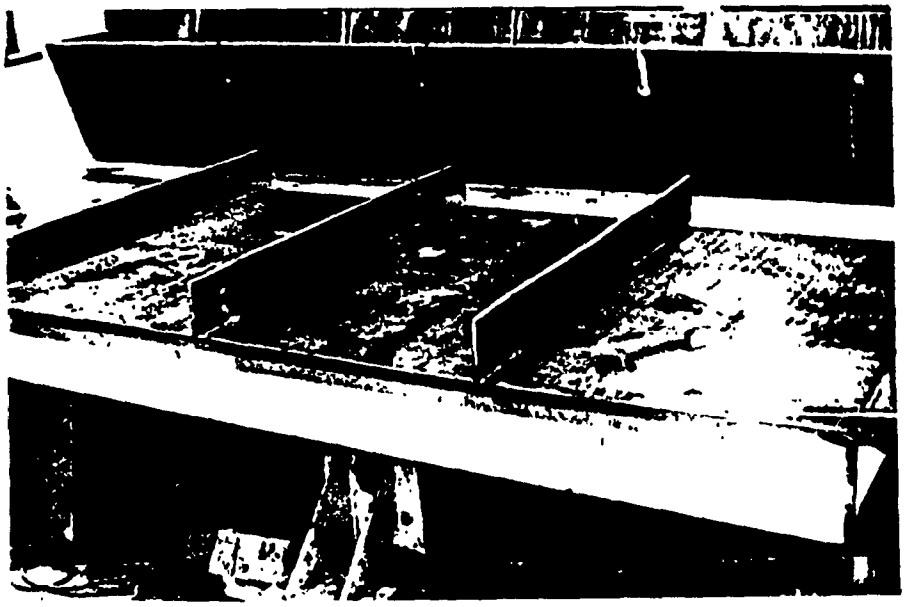

Figure 6.12. The transverse steel ribs are welded to the top flange.

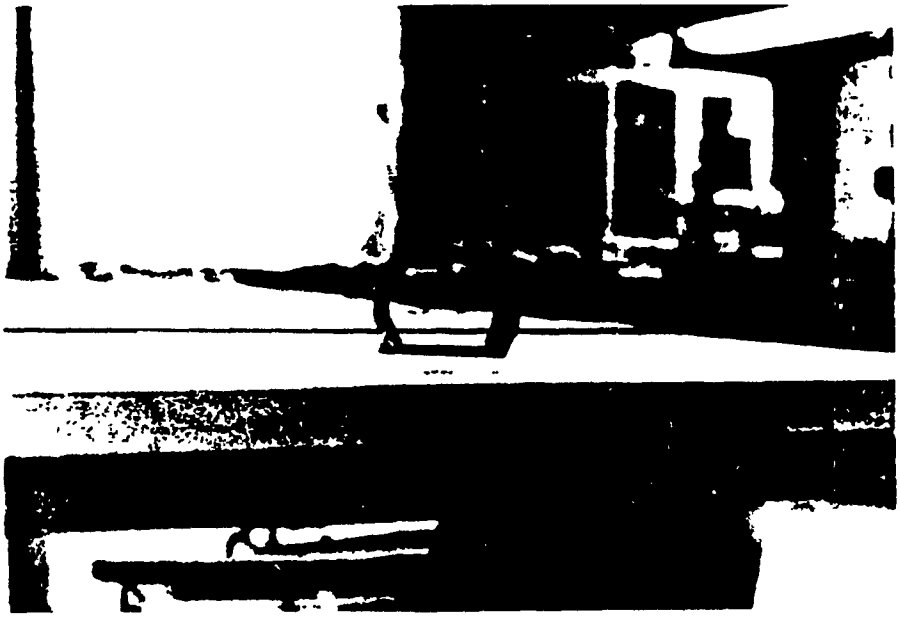

Figure 6.13. Cable guides.

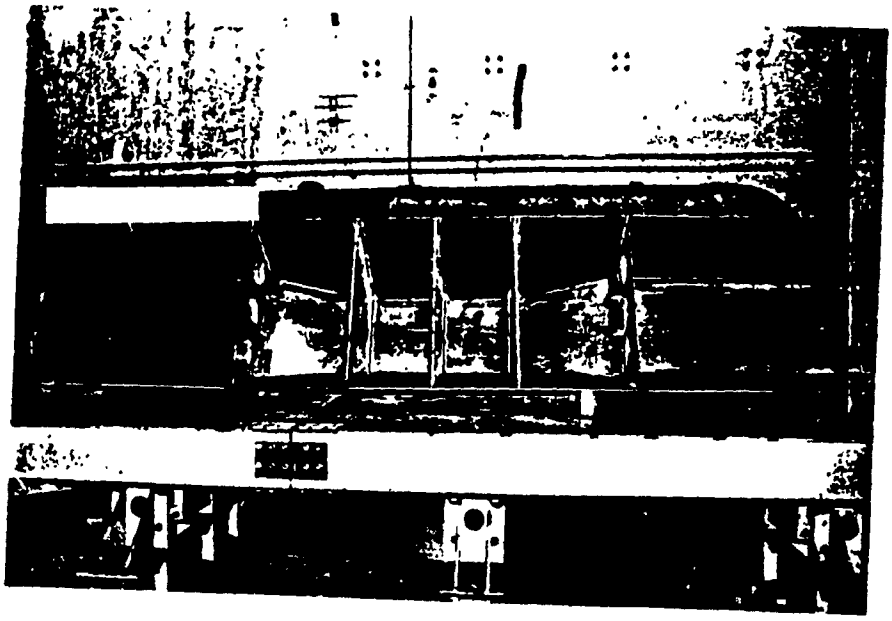

Figure 6.14. Cable guides are welded to the diaphragms at tendons'slope changes.

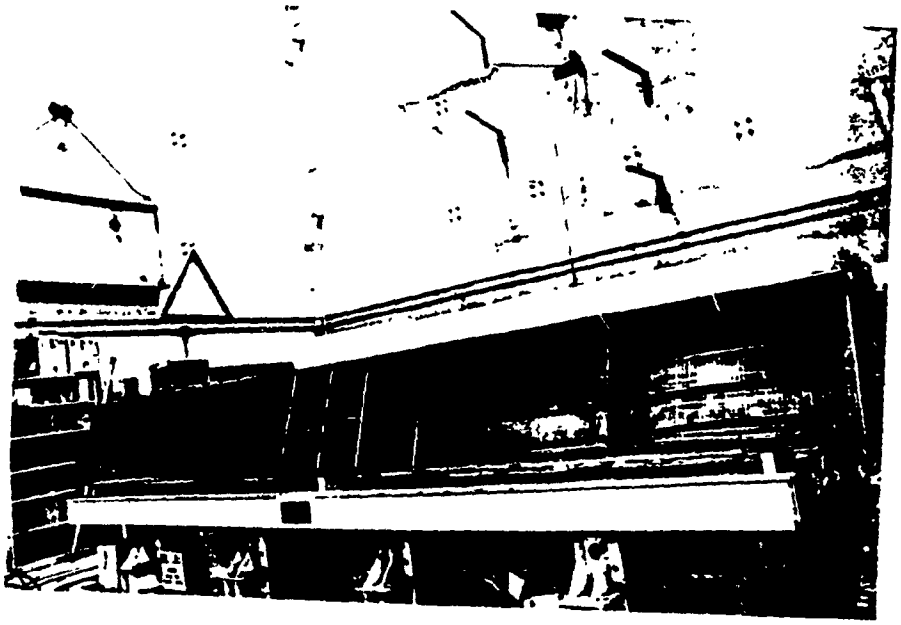

Figure 6.15. Tendons are passed through the box girder with the desired configuration.

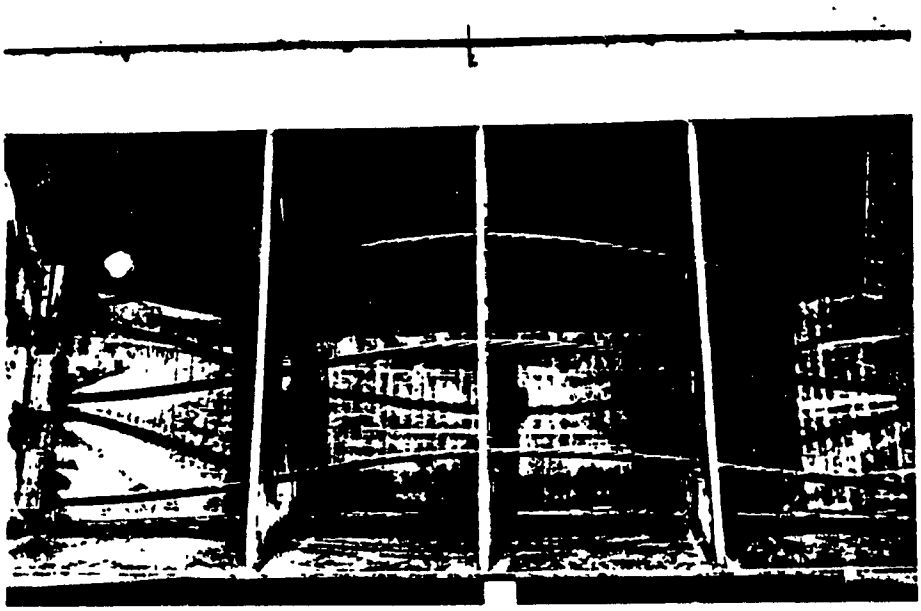

Figure 6.16. The peak height of the tendons at the middle support.

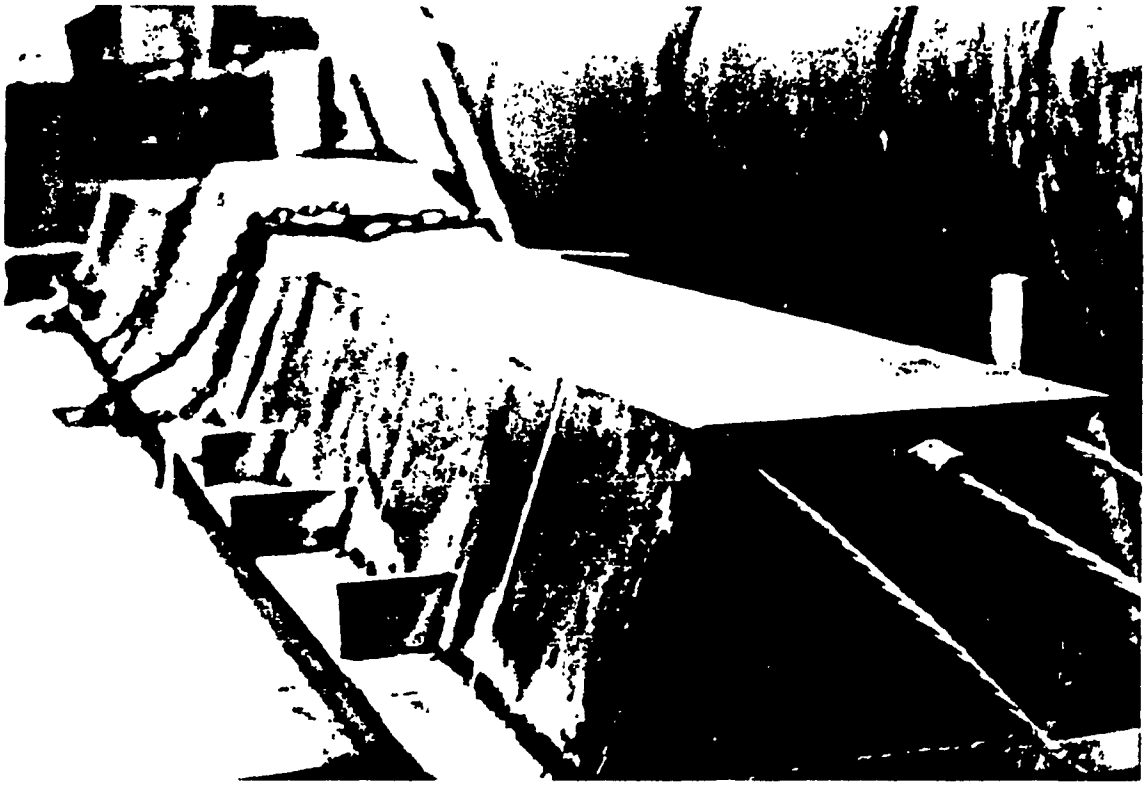

Figure 6.17.The trapezoidal box section is ready to be placed on the supports.

Figure 6.18. The type of steel plate is shown, G40.21-44W, F_y = 44 Ksi.

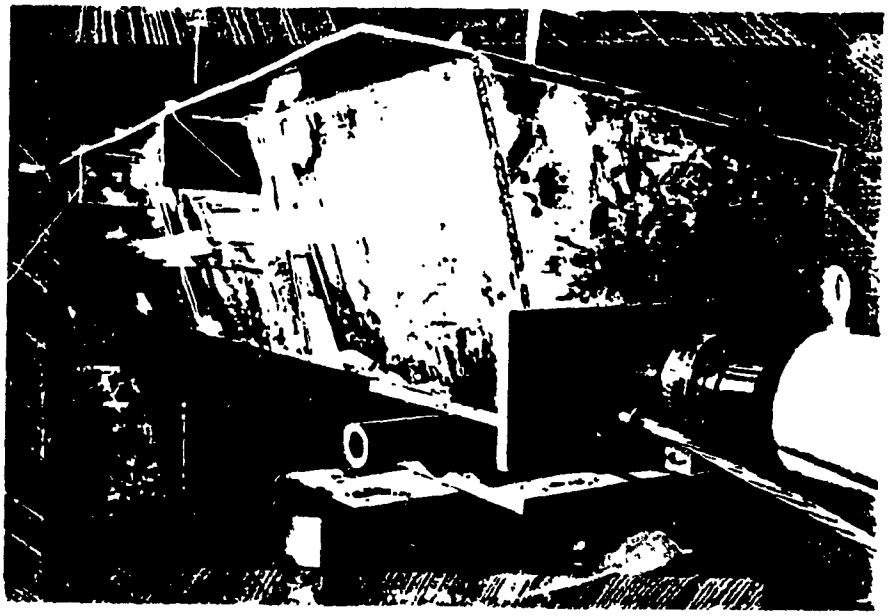

Figure 6.19. The girder is installed on the supports.

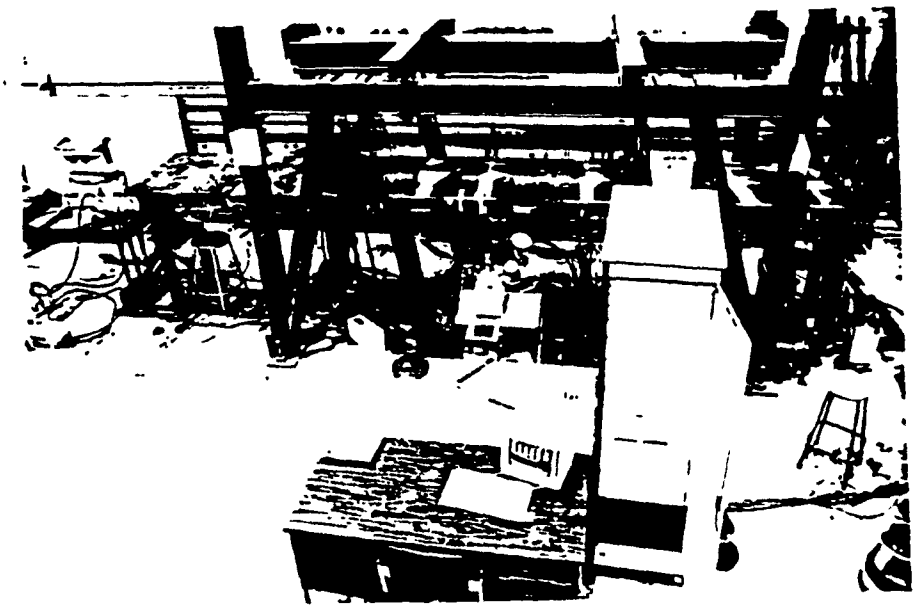

Figure 6.20. The strain guages are installed and connected to the data aquisition system.

Figure 6.21. Prestressing jacks are loaded.

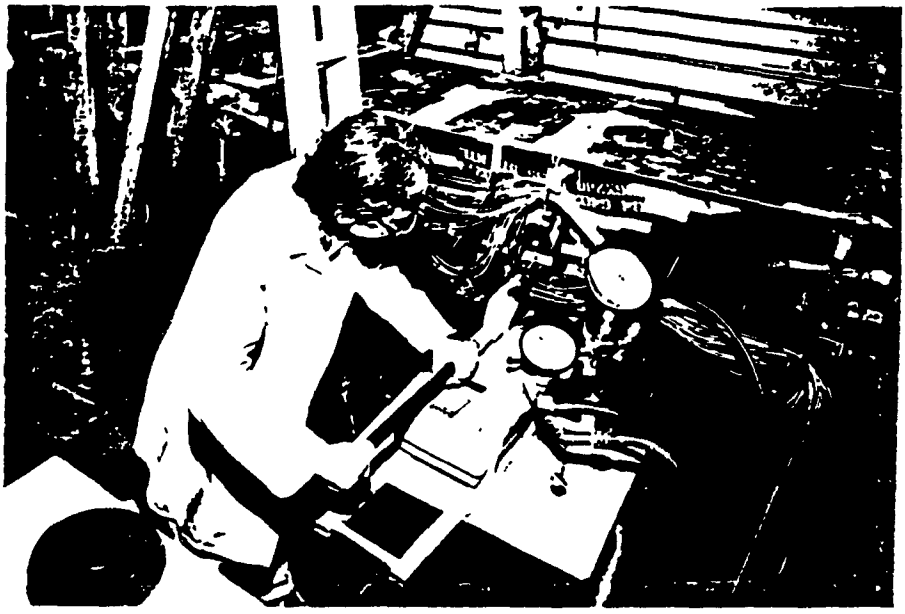

Figure 6.22. The vertical loading are applied by hydraulic jacks.

Figure 6.23. The load cell is placed under the jack to measure the apllied vertical loadings.

6.6. EXPERIMENTAL SET UPS

To achieve the objective of the experiment - to measure the strains, stresses, applied loads and prestressing force, the prestressing force increment, etc. - several sets of tests were performed. The test procedures differ from one to the other in accordance to the application of prestressing force, vertical load and the priorities of the loadings.

a) Test procedure to measure the losses of prestressing:

To measure the losses of prestressing two load cells were installed at the two ends of the draped tendon. The tendon was stretched by prestressing jacks from one side only and the jack was released while the stretched cable was fixed between the two end anchorages. The other side of the tendon was anchored tightly to the end diaphragm. The differences between the measured values (by the load cells) of the induced prestressing forces at the two ends present the total instant prestressing losses due to cable slippage, saddle friction, anchorages slip in, etc.

The readings from the load cells were stored through the data acquisition system into the computer. The readings were done within one hour, giving ample time for the prestressed cables to adjust after the jack was released. The exact value of the prestressing force which is different from the forces induced by the jacks are transferred to the computer through the load cells. The prestressing force was increased at random and the results were stored. The value of the prestressing losses so obtained will be considered in all model computations.

b) Non-prestressed girder:

The girder is tested for the concentrated loads applied to the girder at the critical sections, creating the maximum positive and negative bending moments. The concentrated loads induced by hydraulic jacks are uniformly distributed across the sections. The applied

forces were transformed from the jacks to the top flanges of very deep W sections while the W sections were placed at the desired loading positions across the girder, providing a uniform distribution of the forces across the girder. The vertical applied loads were measured by load cells placed under the jacks. The intensity and the position of the vertical loads are changed to obtain the maximum positive or negative bending moments.

The strains for the self weight of the girder were not considered since they will remain constant throughout the experiment. The readings were recorded at various time intervals, providing enough time for the system to settle down.

The test results and the theoretical computed stresses of similar non- prestressed girder subjected to the application of vertical loads at the same positions and equal intensities were compared and found to be satisfactory. This specifies the accuracy of the strain gauge readings, confirming that: the strain gauges were properly fixed to the model, the wiring and attachments of the load cells to the data acquisition system were perfectly functioning. The computer program to read, transfer and save the signals (storing data) from the data acquisition system to the computer also precisely working.

c) Prestressed girder:

The tests are performed in various stages including: one span loaded, two spans loaded, the two side tendons prestressed and all three tendons prestressed.

1) The side tendons were simultaneously stretched by two prestressing jacks and the concentrated vertical load(s) were induced uniformly across the girder at the desired critical sections (two different positions on one span and both spans) and is increased gradually. The loading process was repeated by increasing the prestressing force and the vertical load(s). The strain readings are recorded for the different loading cases,

prestressed tendon only, prestressed and loaded girder combined.

2) The middle cable was prestressed and fixed by the end anchorages. Then the two side tendons were stretched by one prestressing jack to secure the application of similar stretching forces. Then the vertical load(s) are applied. Similar to the loading case 1, the process was repeated while the prestressing and vertical loads were increased.

In fulfilling the objectives of the experiment the prestressing and vertical loadings have been gradually increased. For each value of loading about 4 scans, within an approximate 15 minutes time intervals, were read and recorded.

6.7. TEST RESULTS

The performed tests can be summarized as follows:

1) To establish the prestressing losses.

2) To measure the incremental prestressing force.

3) To evaluate the increase in the stress carrying capacity of the prestressed box girder due to the vertical loadings on one span only, to obtain the effect of maximum positive moment.

4) To increase the load carrying capacity of the prestressed girder at the middle support representing the location of the maximum negative bending moment.

7) To measure the effect of prestressing only.

6.7.1. PRESTRESSING LOSSES

See section 3.7 for the theoretical equations of the prestressing losses due to:

a) Saddle friction which occurs at the points of contact of the tendons and the saddles where the slopes of the tendons are changing. The friction losses were substantially

reduced by the application of grease on the saddles.

b) Cable relaxation has a long time effect but it gains about 70% of its total value within the first few minutes after the cables are stretched [84].

c) Release of the prestressing jacks and anchorage slippage. The release of the prestressing jacks will cause an immediate reduction in the induced force in the tendons and also the cable will slip in prior to the tightening of the tendons by the active end anchorage.

In this experiment the total value of the prestressing losses has been established which will be accordingly considered in the future calculations. Table 6.1 provides the data readings of the two load cells at the two ends of the middle cable under variable prestressing loads. The tendon was stretched from one side only (the active end) and was fixed at the other end (passive end). Since the properties, the configurations, the guides and the end anchorages of the tendons are similar for all three tendons (two side cables and one middle cable), therefore the prestressing losses of the side tendons are assumed to be equal to the values measured for the middle tendon.

	Instantly	10 minutes	15 minutes	20 minutes	35 minutes	45 minutes
Active end	56.86	56.65	56.56	56.5	56.44	56.42
Passive end	50.45	50.50	50.49	50.49	50.48	50.49

Table 6.1. Test results to determine the prestress losses, prestressing forces in kN

A total value of 10.5% will be considered in the calculation of the stresses due to the prestressing force. This value is assumed to be equally divided at the points of slope change along the tendons.

6.7.2. PRESTRESSING FORCE INCREMENT

For the purpose of obtaining the analogous value of the prestressing force increment (ΔP) of the prototype based on the test results a correction factor of 29.7 is established - the calculated magnitude of ΔP = 27.6 kN for the prototype subjected to V= 438 kN divided by ΔP = .93 kN from the test result of the model due to V = 72.11 kN.

	Two spans loaded	one span loaded
Test Results	1.41x29.7 = 41.9 kN	.77x29.7 =22.9 kN
Calculations	436x.10166 = 44.3 kN	438x.06313 = 27.6 kN

The computed ΔP for the prototype differs from the test results by about 5% when both spans are loaded and 17% when one span is loaded. This variation is acceptable since the 10.5% losses should be considered, since the measuring devices (the load cells) are installed at the left end but the vertical load is applied at the right span. Although the prestressing force increment is irrespective of the prestressing force but it is directly in proportion to the cross sectional area of the tendons. Note that the prestressing losses should be considered for the design purposes.

6.7.3. PROTOTYPE BENDING MOMENTS

The bending moment diagrams of the prototype girder under the effect of prestressing only, P_i = 5000 kN, are compared to the bending moment of the non-prestressed girder, see Figure 6.24 and the corresponding data are given in Table 6.2. The girder is subjected to the standard highway lane loadings including impact and lane distribution factor.

DL = 20 kN/m, SD = 5 kN/m and live loads V = 136.1 kN q = 15 kN/m

DL and SD are the dead and superimposed dead loads, respectively. V and q are the

concentrated and uniformly distributed loads corresponding to the standard lane loadings which include the impact and wheel distribution factors.

Length,	non-prestressed		only prestressed
m	one span loaded	two spans loaded	
0.0	0	0	-5000
5.5	2909	5703	"
22.0	7100	15552	"
37.0	5003	15055	"
46.5	766	10085	"
58.0	-7383	-2327	"
65.0	-13961	-12471	-731
70.0	-19410	-20917	2243
80.0	-32183	-40809	5850
81.8	-28552	-36934	4949
90.0	-13650	-20917	2128
102.0	3310	-2327	-4500
106.0	7683	2590	"
113.5	14159	10085	"
123.0	19130	15055	"
130.0	20483	16406	"
138.0	18541	15552	"
154.5	6450	5703	"
160.0	0	0	"

Table 6.2. Non-prestressed and only prestressed prototype bending moments (kNm), due to: DL=20 kN/m, SD=5 kN/m, V=136.1 kN, q=15 kN/m and P_i =5000 kN

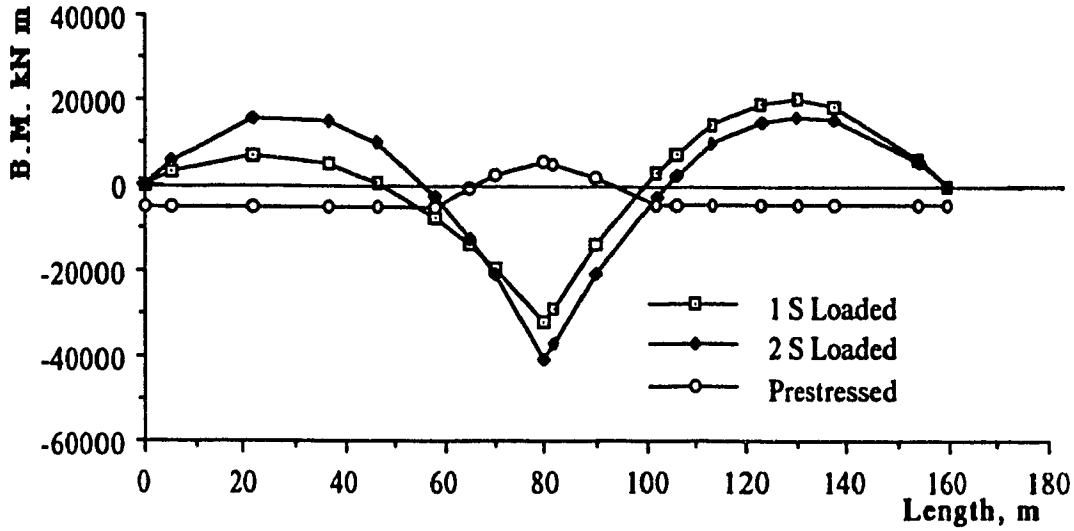

Figure 6.24. Bending moments of the prototype box girder, due to vertical service loads and prestressing force.

The combined bending moments of the prestressed girder loaded on one span and both spans and subjected to similar loadings are illustrated in Figures 6.25 and 6.26 based on the given data in Table 6.3.

	1 Span Loaded		2 Spans Loaded	
Length, m	Non-Prest'd	Prest'd	Non-Prest'd	Prest'd
0.0	0	-5064	0	-5240
5.5	2909	-2142	5703	483
22.0	7100	2085	15552	10391
37.0	5003	22	15055	9947
46.5	766	-4195	10085	5012
58.0	-7383	-12318	-2327	-7359
65.0	-13961	-14557	-12471	-13004
70.0	-19410	-16983	-20917	-18316
80.0	-32183	-26079	-40809	-34392
81.8	-28552	-23366	-36934	-31456
90.0	-13650	-11339	-20917	-18432
102.0	3310	-1119	-2327	-6835
106.0	7683	3246	2590	-1932
113.5	14159	9704	10085	5536
123.0	19130	14655	15055	10471
130.0	20483	15992	16406	11798
138.0	18541	14033	15552	10915
154.5	6450	1905	5703	1007
160.0	0	-4558	0	-4716

Table 6.3. Prototype bending moments (kNm) are compared for two cases.

a)Non-prestressed, due to: DL=20 kN/m, SD=5 kN/m, V=136.1 kN, q=15 kN/m

b)Prestressed, due to: DL=20 kN/m, SD=5 kN/m, V=136.1 kN, q=15 kN/m and P_i =500[illegible] kN

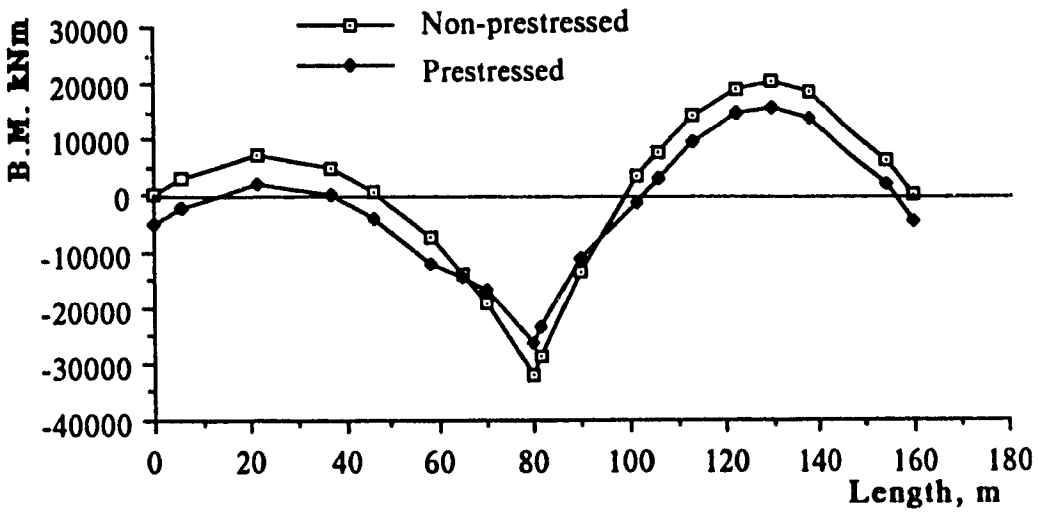

Figure 6.25. Bending moment diagrams for the prestressed and non-prestressed box girder while live loads on one span only.

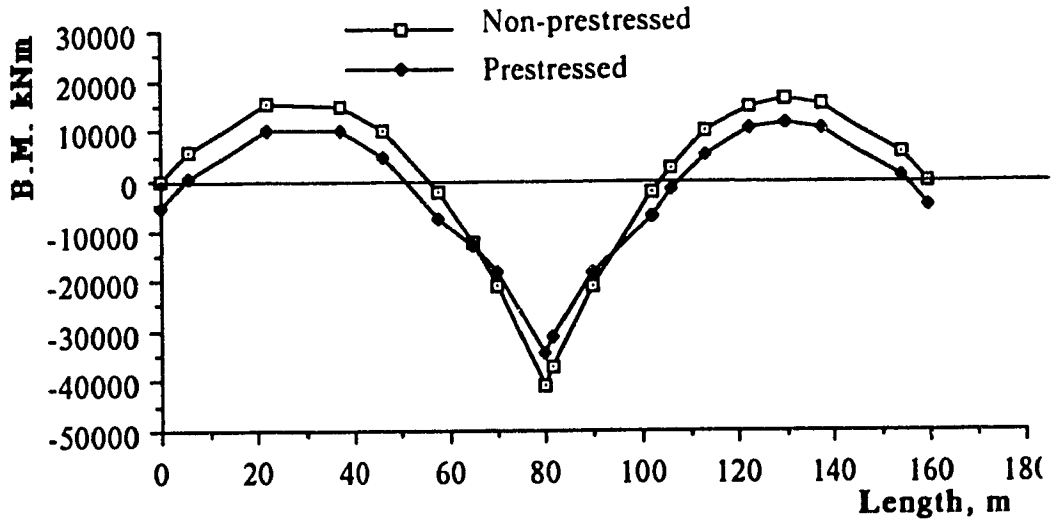

Figure 6.26. Bending moments for the prestressed and the non-prestressed box girder due to the application of live loads on both spans.

6.7.4. MODEL BENDING MOMENTS

The bending moment diagrams of the model when subjected to the following loadings are shown in Figures 6.27 and 6.28 with regard to the given data in Table 6.4. Also, the

bending moments for the non-prestressed girder due to similar vertical loadings are given.

One span loaded	DL = 1.4 kN/m	V = 72.11 kN	P_i = 142.61 kN
Two spans loaded	"	V = 71.85 kN	P_i = 144.86 kN

	1 Span Loaded		2 Spans Loaded	
Length, m	Non-Prest'd	Prest'd	Non-Prest'd	Prest'd
0.00	0.00	-28.52	0.00	-28.97
0.20	-1.10	-29.60	3.05	-25.87
0.79	-4.7	-33.13	11.74	-17.07
1.32	-8.34	-36.72	19.12	-9.57
1.66	-10.88	-39.22	23.65	-4.97
2.07	-14.16	-42.46	-.24	-28.77
2.33	-16.36	-20.28	-15.51	-19.25
2.50	-17.85	-5.06	-25.50	-12.29
2.86	-21.14	12.54	-46.92	-12.40
2.92	-18.97	10.37	-43.35	-13.24
3.22	-8.17	4.01	-25.50	-12.29
3.65	7.09	-18.31	-.24	-25.91
3.78	10.60	-14.81	5.61	-20.08
4.06	21.40	-4.34	23.65	-2.11
4.40	33.08	7.66	19.12	-6.71
4.65	41.56	16.14	15.68	-10.20
4.93	30.85	5.35	11.74	-14.21
5.52	7.89	-17.75	3.05	-23.01
5.72	0.00	-25.69	0.00	-26.11

Table 6.4. Bending moments, kN.m, when one or both spans are loaded.

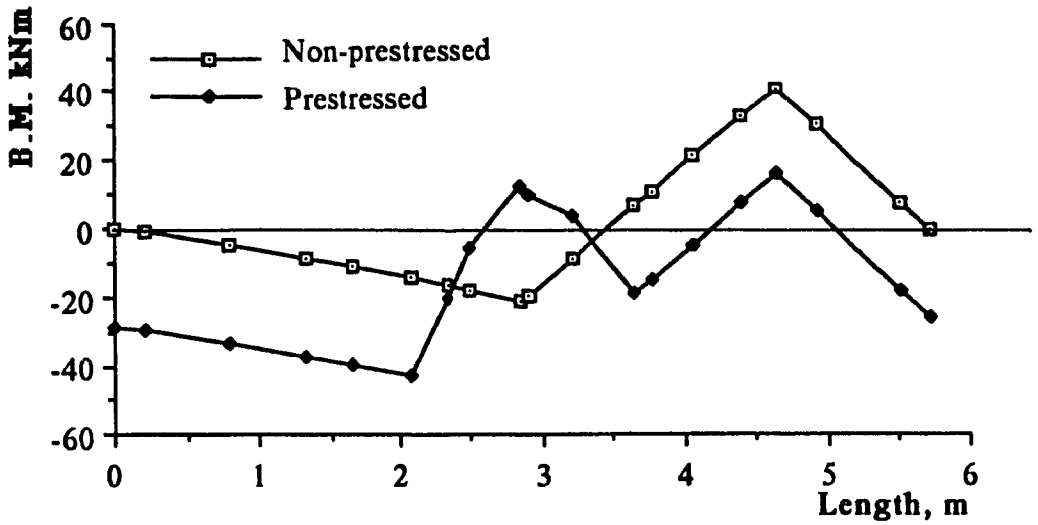

Figure 6.27. Bending moment diagrams when one span loaded

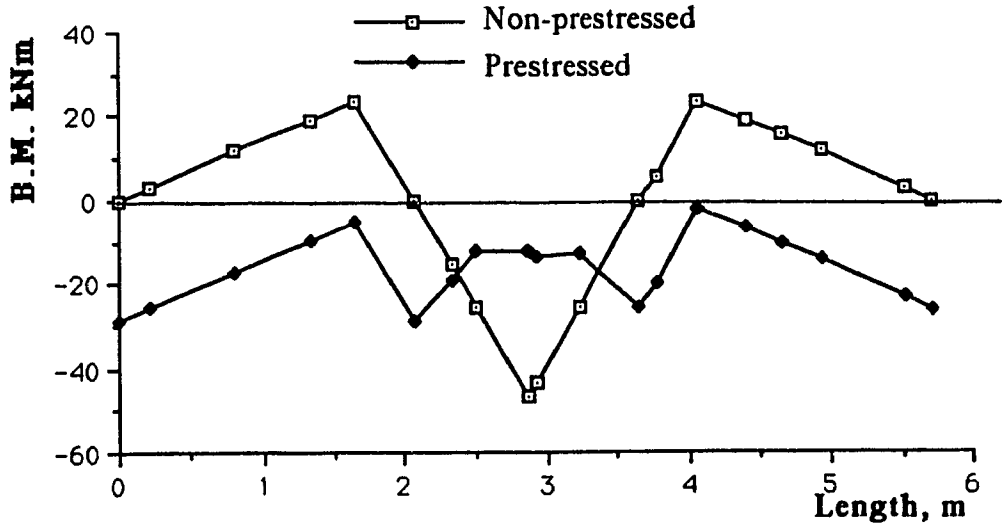

Figure 6.28. Bending moment diagrams corresponding to live load on both spans.

6.7.5. MODEL STRESSES

A comparison between the test results and the theoretical calculated stresses of the model when subjected to similar loadings are provided. It should be noted that the stress due to dead load has been computed and added to the stresses obtained from the experiments. Tables 6.5 and 6.6 provide a satisfactory deviation between the test results

and the calculated stresses. In Figures 6.29 through 6.32 the stresses at the top and bottom fibers of the girder are shown due to the applied vertical live loads on one span or two spans. The applied loadings are similar to those given in Section 6.7.4.

	Top			Bottom		
Length, m	Non-Prest'd	Prest'd	Test	Non-Prest'd	Prest'd	Test
0.00	0.00	1.80		0.00	-22.83	
0.20	0.38	2.17	.91	-0.58	-23.39	-25.86
0.79	1.60	3.38	3.76	-2.46	-25.24	-25.64
1.32	2.84	4.60	4.77	-4.36	-27.11	-27.65
1.66	3.71	5.45		-5.69	-28.42	
2.07	4.83	6.56		-7.4	-30.11	
2.33	4.93	-1.02	-.86	-5.68	-14.17	-14.17
2.50	4.82	-5.76		-4.64	-7.77	
2.86	5.71	-9.84		-5.50	-3.19	
2.92	5.13	-9.25	-8.59	-4.94	-3.75	-4.39
3.22	2.21	-7.53		-2.13	-5.41	
3.65	-2.42	-.90		3.71	-16.71	
3.78	-3.61	-2.09	-2.03	5.54	-14.88	-14.95
4.06	-7.30	-5.66		11.19	-9.41	
4.40	-11.28	-9.75	-9.23	17.30	-3.14	-3.65
4.65	-14.17	-12.64		21.73	1.30	
4.93	-10.52	-8.96	-9.24	16.13	-4.34	-4.64
5.52	-2.69	-1.09	-1.91	4.12	-16.42	-17.86
5.72	0.00	1.62		0.00	-20.57	

Table 6.5. Stresses due to live loads on one span, MPa.

Note that the stresses due to the self weight of the model are added to the test results. The calculated stresses (MPa) at the strain gauges are presented in the following table.

Length, m	.20	.79	1.32	2.33	2.92	3.78	4.40	4.93	5.52
Top Flange	-.09	-.24	-.23	.14	.41	-.03	-.23	-.24	-.09
Bottom Flange	.14	.36	.35	-.17	-.39	.05	.35	.36	.14

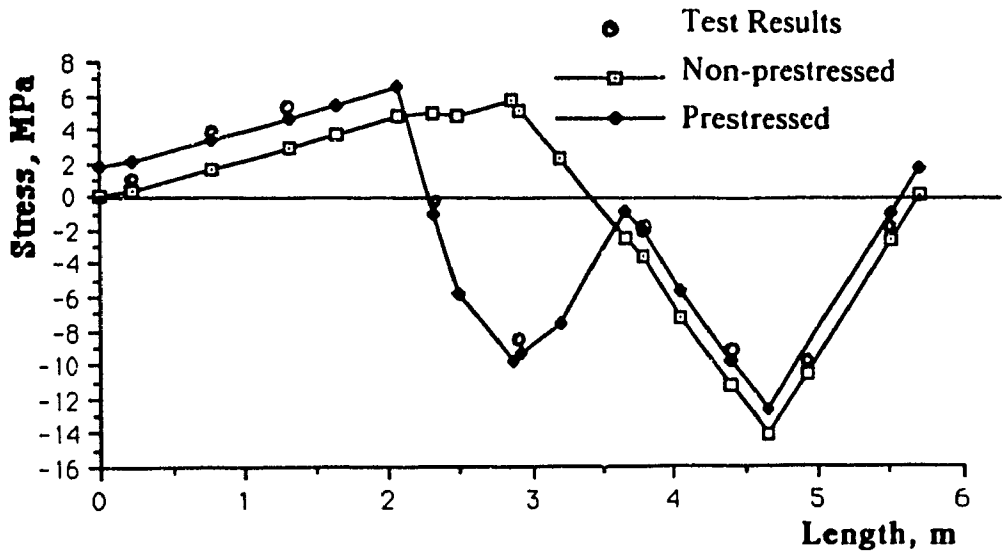

Figure 6.29. Top fiber stresses when one span is loaded

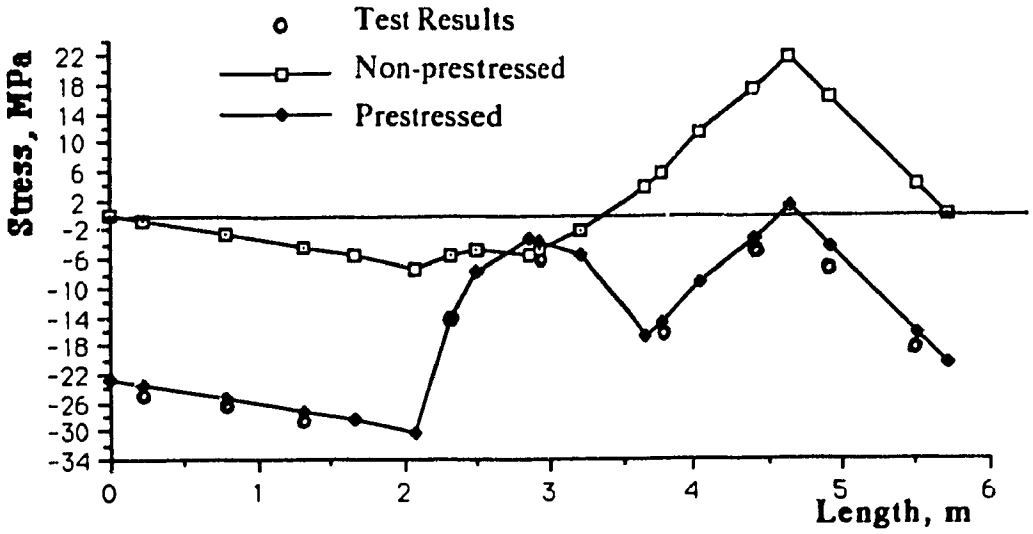

Figure 6.30. Bottom stresses due to vertical live load on one span.

	Top			Bottom		
Length,m	Non-Prest'd	Prest'd	Test	Non-Prest'd	Prest'd	Test
0.00	0.00	1.83		0.00	-23.19	
0.20	-1.04	.77	-.09	1.59	-21.57	-23.86
0.79	-4.00	-2.23	-2.24	6.14	-16.97	-17.64
1.32	-6.52	-4.79	-5.23	10.00	-13.05	-12.65
1.66	-8.06	-6.36		12.36	-10.65	
2.07	.08	1.74		-.13	-23.09	
2.33	4.67	-1.45	.14	-5.39	-13.93	-14.17
2.50	6.89	-3.24		-6.64	-9.76	
2.86	12.68	-3.21		-12.21	-9.79	
2.92	11.72	-2.98	-2.59	-11.28	-10.00	-10.39
3.22	6.89	-3.07		-6.64	-9.92	
3.65	.08	1.58		-.13	-20.79	
3.78	-1.91	-.40	-.03	2.93	-17.75	-17.95
4.06	-8.06	-6.53		12.36	-8.35	
4.40	-6.52	-4.96	-5.23	10.00	-10.76	-10.65
4.65	-5.35	-3.77		8.20	-12.58	
4.93	-4.00	-2.41	-2.24	6.14	-14.68	-14.64
5.52	-1.04	.60	-.09	1.59	-19.28	-21.86
5.72	0.00	1.65		0.00	-20.90	

Table 6.6. Stresses due to live loading on both spans, MPa.

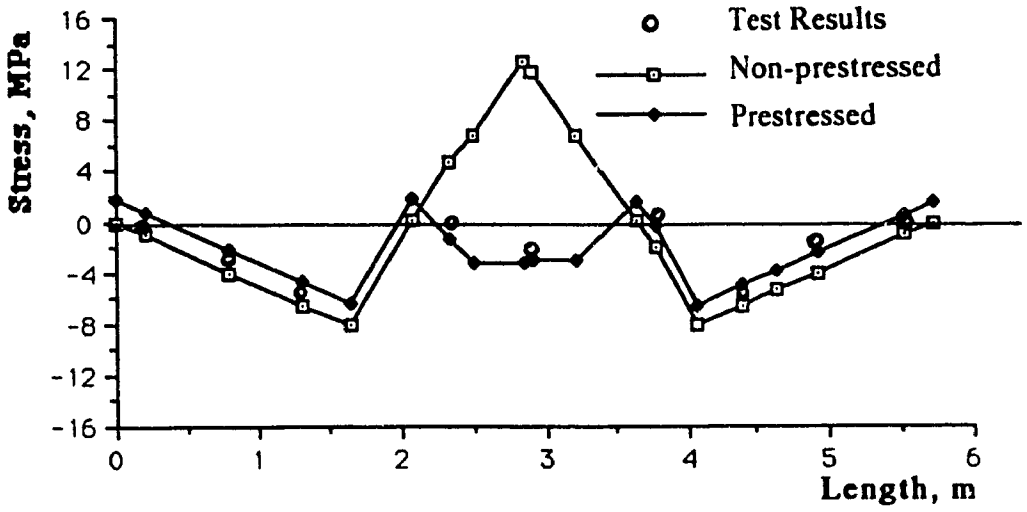

Figure 6.31. Top stresses when both spans are loaded.

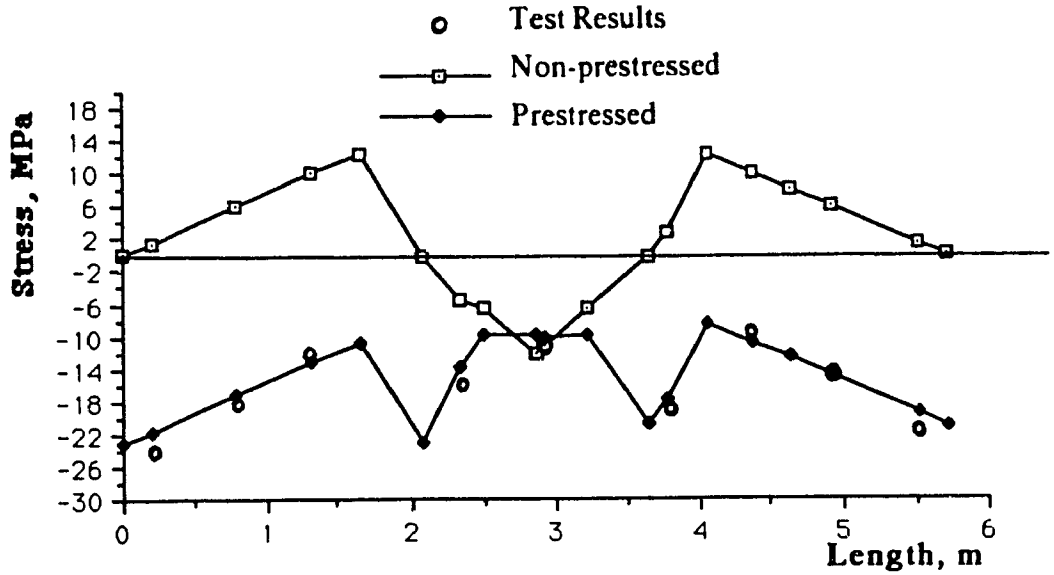

Figure 6.32. Bottom fiber stresses when live load is applied on both spans.

6.7.6. PROTOTYPE STRESSES

To evaluate the prestressing effect in increasing the load carrying capacity of the prototype steel box girder, the top and bottom fiber stresses at selected points along the prestressed girder are compared with the non-prestressed. The data are presented in Tables 6.7 and 6.8 and accordingly the stresses are drawn in Figures 6.33 through 6.36. The

applied loads are: DL = 20 kN/m, SD = 5 kN/m, live loads of V = 136.1 kN, q = 15 kN/m and P_i=5000 + ΔP. A total prestressing loss of 10% has been considered which has been equally distributed at the tendons' slope changes.

	Top		Bottom	
Length, m	Non-Prest'd	Prest'd	Non-Prest'd	Prest'd
0	0	2.3	0	-57.0
5.5	-13.5	-11.2	20.6	-36.3
22.0	-32.9	-30.8	50.4	-6.3
37.0	-23.2	-21.2	35.5	-20.9
46.5	-3.6	-1.7	5.4	-50.9
58.0	34.2	35.9	-52.4	-108.5
65.0	62.9	45.8	-75.1	-98.1
70.0	71.4	44.8	-68.8	-77.8
80.0	118.3	78.3	-114.1	-110.1
81.8	105.0	69.2	-101.3	-99.6
90.0	50.2	25.0	-48.4	-56.9
102.0	-15.3	-13.8	23.5	-26.9
106.0	-35.6	-34.0	54.5	4.0
113.5	-65.6	-63.9	100.4	49.8
123.0	-88.6	-86.9	135.7	84.9
130.0	-94.8	-93.0	145.3	94.4
138.0	-85.8	-84.0	131.5	80.5
154.5	-29.9	-27.8	45.7	-5.5
160.0	0	2.1	0	-51.3

Table 6.7. Stresses corresponding to live loads on one span, MPa.

	Top		Bottom	
Length, m	Non-Prest'd	Prest'd	Non-Prest'd	Prest'd
0	0	2.5	0	-59.0
5.5	-26.4	-24.0	40.4	-15.0
22.0	-72.0	-69.9	110.3	51.9
37.0	-69.7	-67.9	106.8	48.8
46.5	-46.7	-45.0	71.5	13.8
58.0	10.8	12.3	-16.5	-74.0
65.0	56.2	38.2	-67.1	-90.3
70.0	76.9	49.1	-74.2	-83.2
80.0	150.0	108.2	-144.7	-140.2
81.8	135.8	98.3	-131.0	-128.9
90.0	76.9	50.5	-74.2	-82.7
102.0	10.8	11.9	-16.5	-68.2
106.0	-12.0	-10.8	18.4	-33.4
113.5	-46.7	-45.3	71.5	19.6
123.0	-69.7	-68.2	106.8	54.6
130.0	-76.0	-74.3	116.4	64.0
138.0	-72.0	-70.2	110.3	57.7
154.5	-26.4	-24.4	40.4	-12.6
160.0	0	2.1	0	-53.2

Table 6.8. Stresses due to live loads on two spans, MPa.

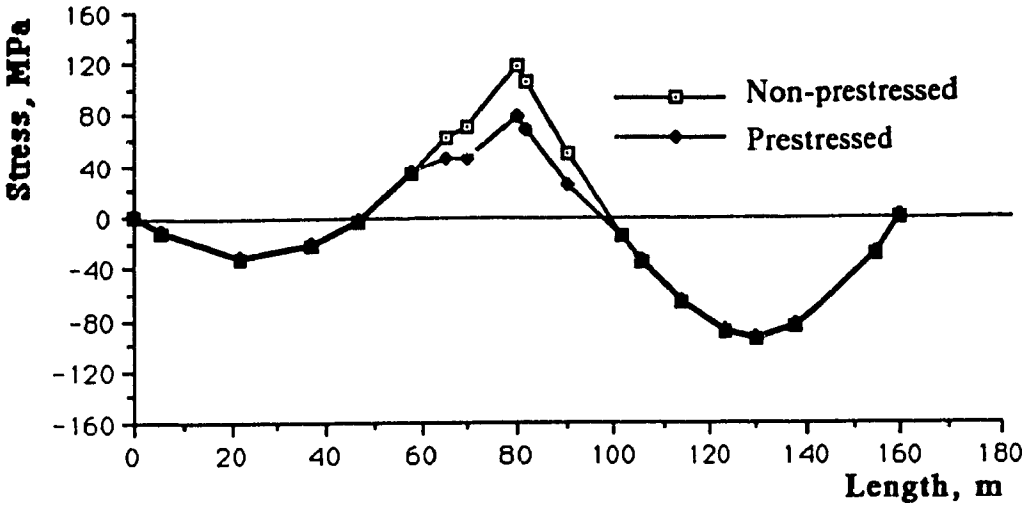

Figure 6.33. Top fiber stresses due to live loads on one span.

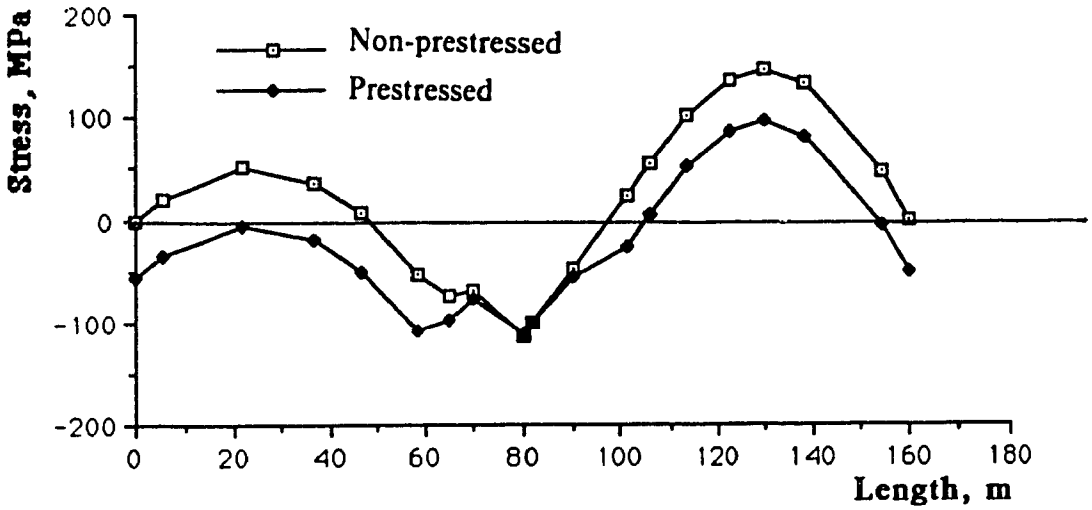

Figure 6.34. Bottom stresses when live loads are applied on one span

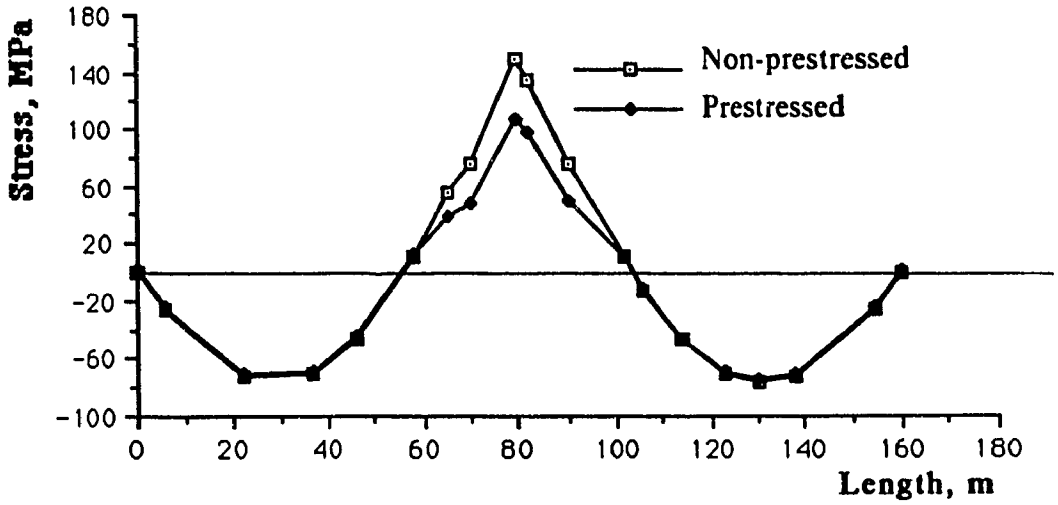

Figure 6.35. Top fiber stresses due to live loadings on both spans.

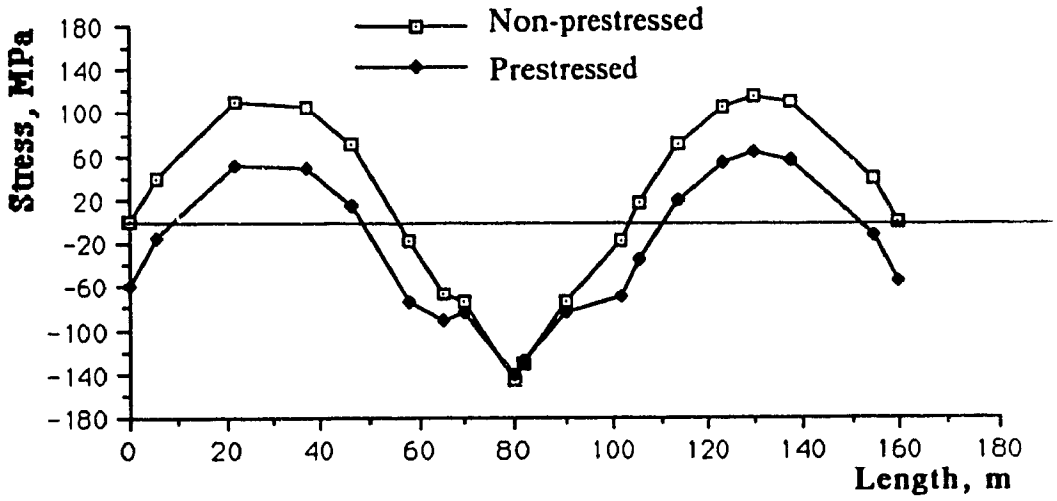

Figure 6.36. Bottom fiber stresses due to live loads on two spans.

The stresses corresponding to the induced prestressing force are provided in Table 6.9 in which no vertical load is applied. The stresses obtained from the test results (recorded values from the strain gauges) when the model is subjected to the prescribed reduced prestressing and vertical loads, are transferred into equivalent values for the prototype in accordance with the procedure given in Section 6.3.4. For example the stress at the point

x = 106 m on the prototype under the application of the prestressing force P_i = 4846 kN is the analogous values of stress at x = 3.78 m on the model when subjected to P_i = 141.62 kN. The strain gauges at x = 3.78 m on the model has recorded the equivalent stress values of 2 at the top and -20 at the bottom. The resolved stresses into axial and bending stresses are:

f_b = -2 - 20 = -22.0

$-f_{bt}$ = -22 × 150/380 = -8.7

$-f_{bb}$ = -22 × 230/380 = -13.3

f_a = 2 × 230/380 + (-20) × 150/380 = -6.68

Finally the analogous stresses on the prototype will be equal to:

At the top fiber 8.7 × 2.31 - 6.68 × 2.55 = 3.1 MPa

At the bottom -13.3 × 2.31 - 6.68 × 2.55 = -47.8 MPa

Figures 6.37 and 6.38 illustrate the stresses of the prototype versus the transferred test results. In both cases the prestressing loss of 10% has been considered at the cable guides. The test result at the strain gauges as recorded for the model are given below. Note that the strain readings are transfered to stresses, $\sigma = E.\varepsilon$. All stress units are in MPa.

Length, m	.20	.79	1.32	2.33	2.92	3.78	4.40	4.93	5.52
Top Flange	1	2	2	-5	-14	2	2	1	2
Bottom Flange	-23	-21	-21	-8	1	-20	-20	-20	-20

Length, m	Top fiber		Bottom fiber	
	Calculation	Test	Calculation	Test
0	2.2		-54.5	
5.5	"	.3	"	-55.2
22.0	"	2.9	"	-50.2
37.0	"	2.9	"	-50.2
46.5	"		"	
58.0	"		"	
65.0	-15.7	-18.5	-22.7	-20.0
70.0	-24.9		-9.2	
80.0	-37.7		3.2	
81.8	-33.6	-34.3	1.0	.4
90.0	-23.6		-8.7	
102.0	2.0		-49.1	
106.0	"	3.1	"	-47.8
113.5	"		"	
123.0	"	3.1	"	-47.8
130.0	"		"	
138.0	"	3.1	"	-47.8
154.5	"	.6	"	-48.0
160.0	"		"	

Table 6.9. Stresses due to prestressing force only, MPa.

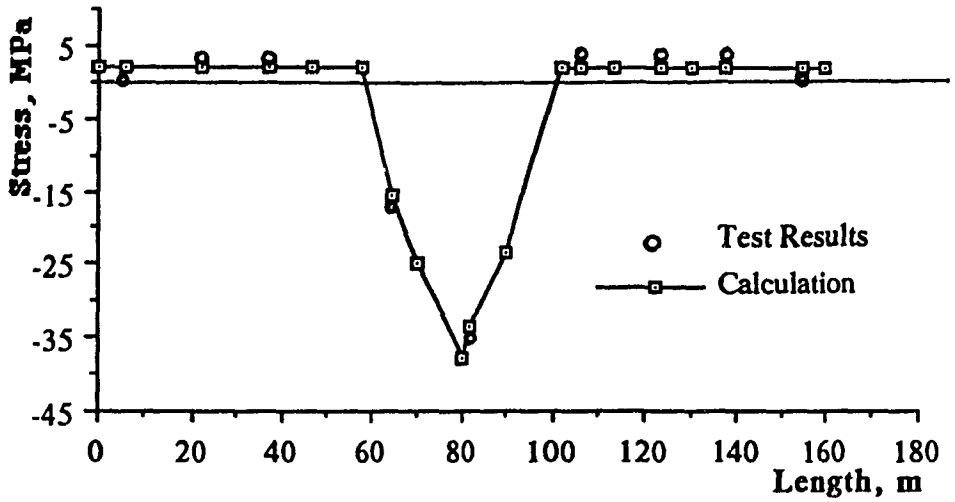

Figure 6.37. Top fiber stresses due to prestressing only.

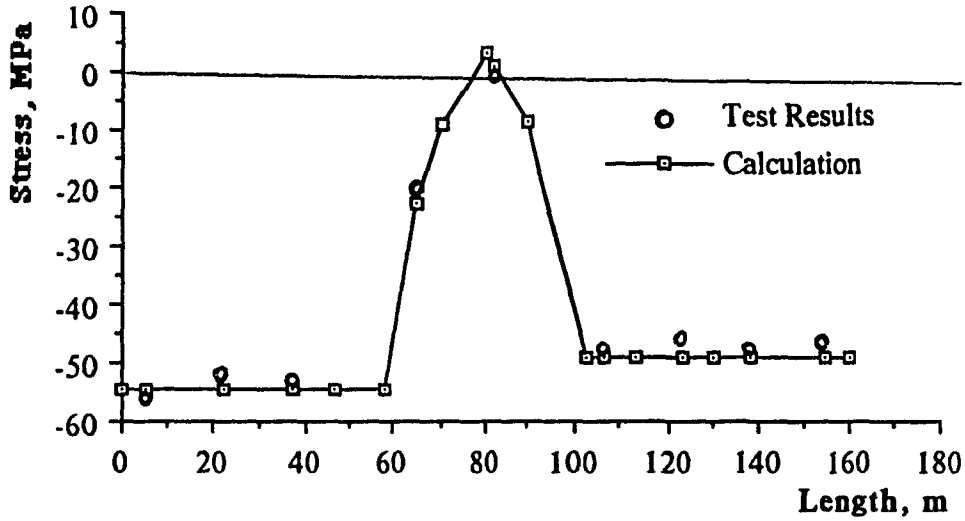

Figure 6.38. Bottom fiber stresses due to prestressing only.

Stresses of the prototype when subjected to a vertical concentrated load applied to the girder on one span or both spans, after prestressing is achieved, are provided in Tables 6.10 and 6.11. The equivalent stresses transferred from the analogous loaded model are also presented. Furthermore as a matter of comparison similar values for the non-prestressed prototype girder are also calculated, Tables 6.10 and 6.11. Figures 6.39

through 6.42 illustrate the stress graphics at the top and bottom fibers of the prototype steel box girder when loaded on one span and two spans. The corresponding loadings are:

- Only one span loaded (critical loadings for the maximum positive moment)

Prototype	V = 438 kN	(P+ΔP) = 4846 + 28 = 4874 kN
Model	V = 72.11 kN	(P+ΔP) = 141.68 + .93 = 142.61 kN

- Two spans loaded (critical loadings for the maximum negative moment)

Prototype	V = 436 kN	(P+ΔP) = 4924 + 44 = 4968 kN
Model	V = 71.85 kN	(P+ΔP) = 143.36 + 1.50 =144.86 kN

The analogous stresses for the prototype can be predicted from the test results using the procedure explained in Section 6.3.4. For example, at strain gauge x = 1.32 m, the total combined stress at the top fibre f_{tt} = 5 MPa and similar stress at the bottom f_{tb} = -28 MPa.

$$f_b = -5 - 28 = -33.0$$

$$-f_{bt} = -33 \times (150/380) = -13.0$$

$$f_{bb} = -33 \times (230/380) = -20.0$$

$$f_a = 5 \times (230/380) + (-28) \cdot (150/380) = -8.0$$

The top and bottom stresses at x = 37.0 m on the prototype will be equal to:

Top fiber stress	13 x 2.31 - 8.0 x 2.55 = 9.6 MPa
Bottom fiber	-20 x 2.31 - 8.0 x 2.55 = -66.6 MPa

The test results, stresses in MPa, when one span loaded are given in the table below.

Length, m	.20	.79	1.32	2.33	2.92	3.78	4.40	4.93	5.52
Top Flange	1	4	5	-1	-9	-2	-9	-9	-2
Bottom Flange	-26	-26	-28	-14	-4	-15	-4	-5	-18

	Top			Bottom		
Length, m	Non-Prest'd	Prest'd	Test	Non-Prest'd	Prest'd	Test
0	0	2.3		0	-54.9	
5.5	1.1	3.4	-.01	-1.8	-56.6	-62.4
22.0	4.6	6.8	7.4	-7.1	-61.8	-61.9
37.0	7.8	9.9	9.6	-11.9	-66.6	-66.6
46.5	9.7	11.8		-15.0	-69.6	
58.0	12.2	14.2		-18.6	-73.2	
65.0	13.3	-1.9	-4.2	-15.8	-39.5	33.8
70.0	11.7	-13.5		-11.2	-20.3	
80.0	13.3	-24.8		-12.9	-9.4	
81.8	11.9	-22.1	-22.5	-11.5	-10.3	-10.9
90.0	5.6	-18.3		-5.4	-14.0	
102.0	-4.6	-2.7		7.0	-42.0	
106.0	-8.4	-6.6	-6.3	12.9	-36.2	-36.4
113.5	-15.7	-13.8		24.1	-25.0	
123.0	-24.9	-23.0	-22.5	38.2	-11.0	-10.9
130.0	-31.7	-29.8		48.6	-0.6	
138.0	-23.2	-21.3	-22.6	35.6	-13.6	-13.3
154.5	-5.8	-3.8	-6.62	8.9	-40.4	-43.6
160.0	0	2.0		0	-49.4	

Table 6.10. Stresses for the case of one span loaded, MPa.

Test results, stresses in MPa at strain gauges, when two spans are loaded are:

Length, m	.20	.79	1.32	2.33	2.92	3.78	4.40	4.93	5.52
Top Flange	0	-2	-5	0	-3	0	-5	-2	0
Bottom Flange	-24	-18	-13	-14	-10	-18	-11	-15	-22

	Top			Bottom		
Length, m	Non-Prest'd	Prest'd	Test	Non-Prest'd	Prest'd	Test
0	0	2.3		0	-55.9	
5.5	-2.0	0.3	-2.3	3.0	-52.8	-57.7
22.0	-9.9	-5.7	-6.7	15.1	-43.6	-43.6
37.0	-13.3	-11.2	-13.5	20.4	-35.2	-32.0
46.5	-16.7	-14.7		25.6	-29.9	
58.0	2.4	4.3		-3.6	-59.0	
65.0	13.6	-2.9	-1.3	-16.2	-39.1	-33.7
70.0	17.7	-8.1		-17.1	-26.2	
80.0	30.9	-8.2		-29.8	-26.1	
81.8	28.5	-6.4	-8.3	-27.5	-26.1	-24.5
90.0	17.7	-6.8		-17.1	-25.7	
102.0	2.4	4.1		-3.6	-53.4	
106.0	-4.3	-2.5	-1.7	6.5	-43.3	-43.3
113.5	-16.7	-14.9		25.6	-24.3	
123.0	-13.3	-11.4	-13.3	20.4	-29.6	-27.2
130.0	-10.8	-8.9		16.5	-33.6	
138.0	-9.9	-6.0	-6.3	15.1	-38.0	-36.4
154.5	-2.0	0	-2.1	3.0	-47.3	-52.9
160.0	0	2.1		0	-50.3	

Table 6.11. Stresses for the case of two spans loaded, MPa.

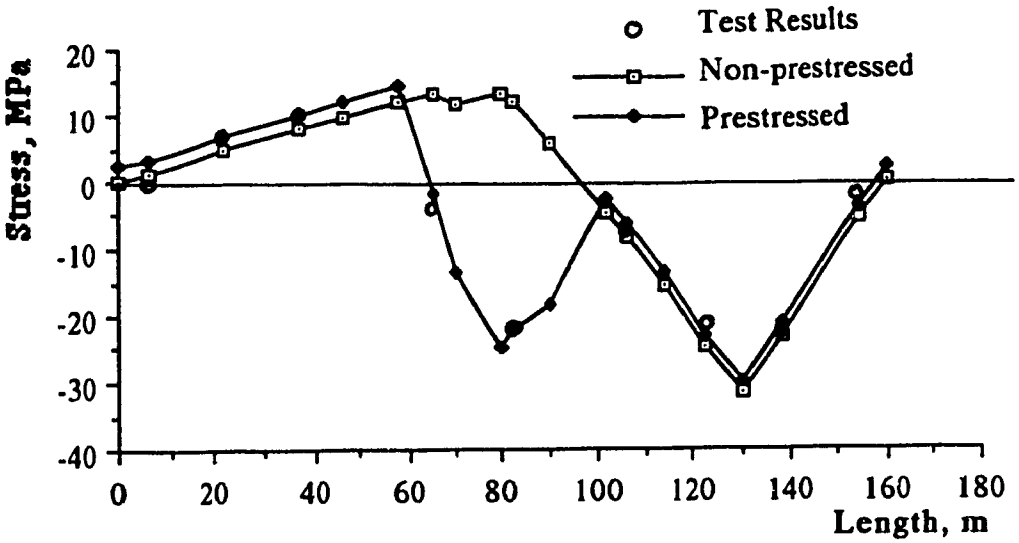

Figure 6.39. Top stresses corresponding to live load on one span.

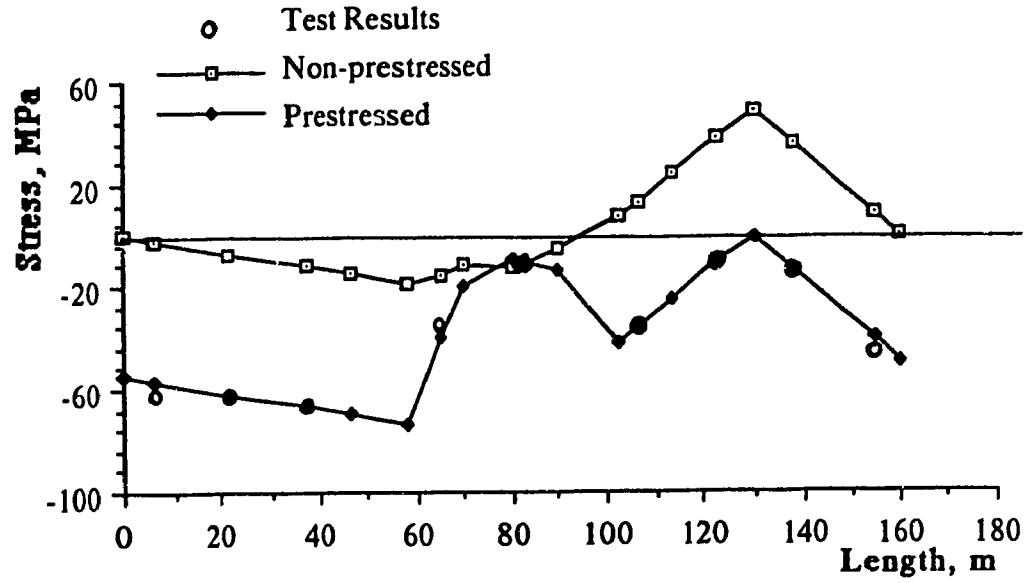

Figure 6.40. Bottom stresses due to live load on one span.

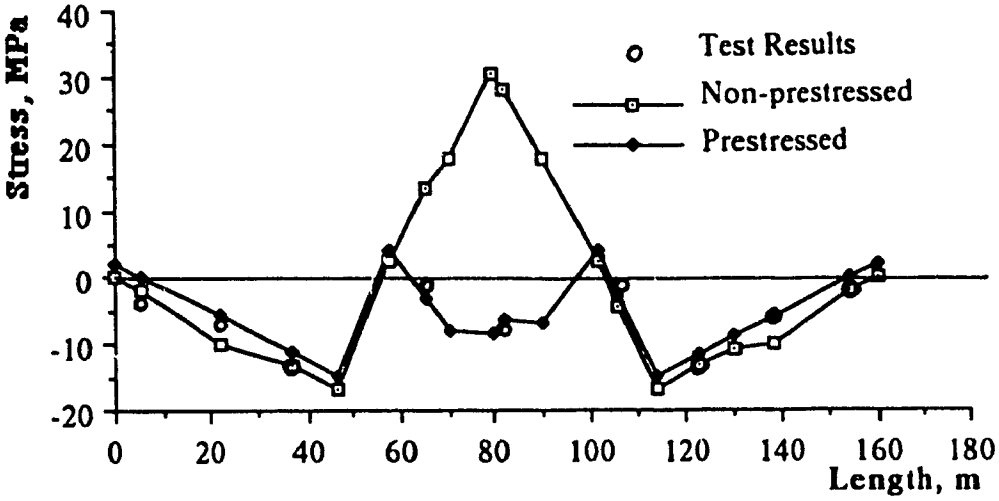

Figure 6.41. Top stresses when both spans are loaded.

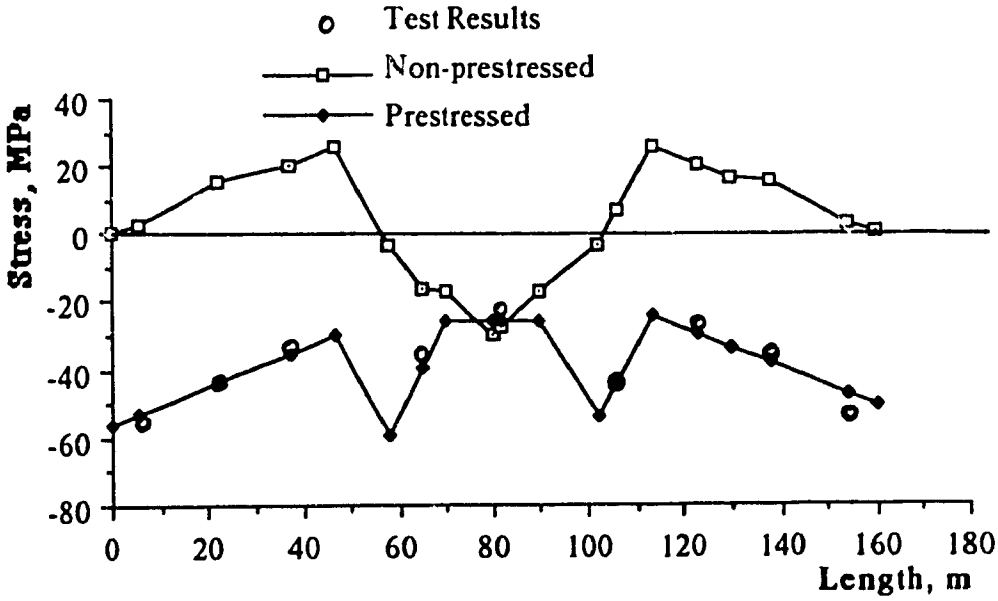

Figure 6.42. Bottom stresses when both spans are loaded.

VII. CONCLUSION AND FUTURE WORK

Two functional considerations for economy in bridge design are:

a) Efficient utilization of the material by optimization of the dead weight of the structure

b) Minimizing the fabrication and erection expense.

A steel box girder prestressed by cables of high strength steel with an orthotropic top deck satisfactorily fulfills the above conditions for medium and long span girder bridges. The collective advantages of steel box girders when prestressed by tendons provide efficiency in the use of material which directly contribute to economy and increase in the load carrying capacity of the girder bridges.

Box girders are built of relatively thin plates to the desired shape and when prestressed with tendons at the tension region the economy gain is considerable in comparison to the conventional bridge design, the weight of the conventional steel girder bridges can be reduced about 25-45% by using prestressed steel box girders instead. Prestressed steel girders are among the new structural technologies developed recently. The technique provides a variety of advantages including: use of less heavier girders and comparatively shallower depth, increasing the load bearing capacity, reducing the deflection and the effect of fatigue. The use of a less heavier steel box section contributes not only to the gain in the superstructure but also the gain includes the substructures as well.

The basic concepts for selecting the tendon configuration and cross-sectional geometry of the steel box girder bridges are recommended. In general tendons have to be placed as far as possible from the neutral axis in the tension side which contributes to the increase in the induced counterbalance prestressing moment. The ideal tendon configuration is considered in accordance with the bending moment diagram of the girder. Asymmetrical

sections in which the neutral axis is closer to the extreme compressive fibers are among the favorite sections to be used in the prestressed / post-tensioned steel box girders.

The developed theory for the design of prestressed steel continuous box girders show a reduction in the negative bending moment and an increase in the value of initial prestressing force (prestressing force increment) due to the applied service loads after prestressing process is accomplished. The proposed analysis is based on the flexibility method. The deformations are calculated by virtual work method. The analysis is limited to elastic range which is improved significantly by the effect of prestressing force induced in opposite direction to the applied service loads. The equations for calculating the prestressing force increment and the negative bending moments at the middle supports of prestressed steel continuous box girders are presented. Numerical examples are provided and the results are compared with similar non-prestressed box girders. Based on the given results it can be concluded that:

1) The value of prestressing force increment is increasing with the span length and is in proportion to the cross-sectional area of the tendons, cross-sectional properties of the box girder and tendon configurations. This value is independent of the induced prestressing force.
2) The negative bending moment at the middle support shows about 17% decrease in comparison to a non-prestressed girder having the same cross-sectional and longitudinal geometry and subjected to similar service loads. This is in addition to the effect of counterbalance moments induced to the girder by tendons.

In particular, the general formulas for the influence lines of the negative bending moment and the prestressing force increment of a typical two-equal-spans continuous girder is provided. From the derived equations it can be concluded that the influence lines

depend on many various parameters including which can not be generalized for all types of equal span continuous girders.

The design concepts of prestressed steel continuous box girders are proposed. The combined stress due to service loads and the counterbalance effective prestressing force (considering Losses of prestressing and the incremental prestressing force) is elaborated. Limits of prestressing are defined and the gains of prestressing in increasing the load carryimg capacity and reducing the dead weight of the girder are demonstrated. At the tension region the stress compensation by prestressing is directly in proportion to the value of prestressing force and eccentricity of the tendons from the neutral axis of the girder. For this reason asymmetrical sections are more favorable to be used in prestressing design. The decrease of the stresses due to service loads when combined with the effect of prestressing at the compression zone is limited to certain values of the eccentricity of the tendons and the radius of gyration of the cross-section of the girder, see Section 4.4 for more details. In general the effect of prestressing at the compression zone ranges from small values to negligible.

Prestressing can be used in major structural areas such as :

- design of new structures (mostly in bridge industry),
- a potential recommended technique for rehabilitation of bridges and parking structures,
- strengthening and improving the serviceability of the bridges and buildings.

The design concepts of steel box girders have been already given ample considerations, although not to the full extent, but the prestressing techniques are recently introduced and there are relevant topics to be studied in the future. The following subjects are suggested for further study and experimental work.

a) The behavior and strengthening of end sections where the prestressing force is induced to the box section. Also, a detailed investigation seems necessary of the sections along the girder where cable guides are installed (for sloped tendon configurations)

b) The response of cables and the prestressed girder under the application of moving loads should be should be provided through future experiments.

c) The fixing elements such as end anchorages and saddles have to be modified for use in prestressed steel members.

d) For more efficient and regular use of the prestressing techniques in the Canadian construction industry and in the structural design consultant offices it is desirable that the Canadian Building Code and the Canadian Bridge Code provide certain provisions and standards such as the provisions already exist for prestressed concrete.

REFERENCES

1. N.Taly and H.V.S.Gangarao, "Prefabricated Press-Formed T-Box Girder Bridge System", Engineering Journal of AISC, third quarter 1979, pp.75-83.
2. G.B.Godfrey, "The Evaluation and International Devlopment of Box Girder Bridges", Canadian Structural Engg. Conference 1974, pp.
3. O.A.Kerensky, "A Brief Historical Survey of Development in Steel Bridge Building", presented at the International Conference on Steel Bridge Design and Construction, Johannesberg, Soyth Africa, 1974, pp.1-13
4. C.O'Connor, Design of Bridge Superstructures , published by John Wiley and Sons Inc., 1971, p.230.
5. M.S.Troitsky, Orthotropic Bridges Theory and Design , published by the James F.LincolnArc Welding Foundation, Cleveland, Ohio, 1968
6. R.J.Gill and S.Dozzi, "Concordia Orthotropic Bridge: Fabrication and Erection", Engg. Journal, AISC, May 1966, pp.10-18.
7. J.G.Demers and O.F.Simonsen, "Montréal Boats Cable Stayed Bridge", Civil Engineer, ASCE, Aug.1971, pp.59-63.
8. C.P.Heins, "Box Girder Bridge Design - State of the Art", Engg. Journal, AISC, fourth quarter 1978, pp.126-142.
9. F.W.Klaiber, K.F.Dunker and W.W.Sanders, "Strengthening of Single Span Steel Beam Bridges", J.of Structural Div., ASCE, Dec.1982, pp.2766-2780.
10. Y.Tachibana, K.Kando and K.Ito, "Experimental Study on Composite Beams Prestressed With Wire Cables", Preliminary Report IABSE 7th Congress, Brazil, 1964, pp.678-683.
11. H.K.Preston, "Design of Prestressed Hollow Box girder bridges", Engineering News-Record, Dec.27, 1956, pp.34-35.
12. "Prestressed Steel Makes a Bridge", Engg. News -Record, Nov. 5, 1964, pp.24-27.

13.H.M.Hadley, "Steel bridge Girders with Prestressed Composite Tension Flanges", J.of Civil Engg., ASCE, May 1966, pp.70-72.

14.P.F.Barnard, "Prestressed Steel Bridges", Proceedings of the ASCE Conference May 12, 1961, pp.75-82.

15.P.S.A.Berridge and D.H.Lee, "Prestressing Restores Weakened Truss Bridge", J.of Civil Engg., Sept. 1956, pp.48-49.

16."Prestressed Steel Bridge a Winner", Engg. News-record, Dec.22, 1983, pp.48-49.

17.E.Belenya, Prestressed Load Bearing Metal Structures , Mir Publishers, Moscow, 1977, p.19.

18.Z.A.Zielinski, Prefabrikowane Betonowe Olzwigary Spzezone , (Precast Prestressed Concrete Girders), 2 nd Edition, Arkady, Warszawa, 1962, Poland, pp.1-309.

19.M.S.Troitsky, Prestressed Steel Bridges Theory and Design , published by Reinhold Co., New York, 1990, pp.255-267

20.H.Saadatmanesh, P.Albrecht and B.M.Ayyub, "Experimental Study of Composite Beams", J.of Structural Engg., AISC, Sept.1989, pp.2348-2381.

21.M.S.Troitsky, Prestressed Welded Steel Structures Theory and Design , The J.F.Lincoln Arc Welding Foundation, Cleveland, Ohio, 1988, pp. 9.1-9.3.

22.O.Vinay, A.Ben-Arroyo and E.Racah, "Prestressed Steel Grid Erected with Bent Forms", Proc. ASCE, March1982, pp.579-590.

23.J.S.Ellis, "Prestressed Latticed Beam-Columns with Offset Diagonals", Published by National Research Counsil of Canada, No.4, Dec.1980, pp.573-580.

24.B.O.Aalami and D.T.Swanson, "Innovative Rehabilitation of a Parking Structure", Concrete International:Design and Construction, published by ACI, Feb.1988, pp.1-6.

25.R.Wolchuk, "The first Cost Syndrom in Bridge Rehabilitation", Civil Engg., ASCE, Oct.1988, p.6.

26.C.Eckberg, "Development and Use of Prestressed Steel Flexural Members", Proc. Str.Div., ASCE, Sept. 1988, pp.2033-2059.

27.S.I.Al-Noury, M.A.Choudhry, S.A.Ali and S.Huq, "Behavior of Prestressed Steel Continuous Beams of Variable Sections", J. of Engg. and Applied Sciences, vol 3, 1986, pp.151-160.

28.L.Baes and A.Lipski, "The Preflex Beam", Joint session of the ACI and The Structural Division of the ASCE, Centennial of Engineering, Chicago, 1952.

29.E. Belenya, same as 17, p.9

30.C.Seim, "Steel Beats Concrete for Idaho Bridge", Civil Engineering, ASCE, Aug.1983, pp.28-32.

31.S.R.Abdel-Samad, R.N.Wright and A.R.Rabinson, "Analysis of Box Girders with Diaphragms", proc. J. of the str. div., ASCE, Oct.1968, pp.2231-2256.

32.R.Halasz, "Bauingenieur - Praxis", published by Verlag von Wilhelm Ernst & Sohn, Berlin, 1975, pp.80-87, (in Germany).

33.Post-Tensioning Manual , published by Post-Tensioned Institute, 1976, p.38.

34.Design of Highway Bridges , published by National Standard of Canada, Can3-S6-M78.

35.M.S.Troitsky, Cable Stayed Bridges Theory and Design , published by Crosby Lock Wood Staples, London, pp.136-141.

36.M.C.Tang, "Design of Cable Stayed Girder bridges", proc., str.div., ASCE, Aug.1972, pp.1789-1801.

37."Blue Strand Steel Wire Rope", published by Wire Rope Industeries of Canada Ltd., pp.103-107.

38.Prestressed Steel Cables , published by Prestressing Cocrete Institute, p.282.

39.M.S.Troitsky, same as 19, pp.50-55.

40.Z.A.Zielinski, same as 18, pp.

41. R.Halasz, same as 32, p.301.

42.K.Wobner, W.Andra, R.Kahmann and D.Hammel, "Neckar Valley Bridge", Stahlbau, 3, 1983, pp.65-125.

43. R.Halasz, same as 32, p.338.

44. R.Halasz, same as 32, p.289.

45.J.R.Libby, Modern Prestressed Concrete , published by Van Nostrand Reinhold, 1977, p.19.

46.Z.A. Zielinski, same as 18, pp.

47.J.R. Libby, same as 45, p21.

48.E. Belenya, same as 17, p.125.

49.M.S.Troitsky, same as 19, pp.55-63.

50.J.R. Libby, same as 45, p.515.

51.R.Szilard, "Design of Prestressed Composite Steel Structures", proc., str.div., ASCE, Nov.1959, pp.97-123.

52. R.Szilard, "Strengthening Steel Structures by means of Prestressing", The Engg. J., Oct.1955, pp.1377-1381.

53.J. Brodka, K. Jerka-Kulawinska and M. Kwasniewski, Vorgespannte Stahltrager Statische Berechnung, in Germany, published by Verlagsgesellschaft Rudolf Muller, Koln, 1957, pp.32-57, (Prestressed Steel Construction).

54.M.S.Troitsky, Z.A.Zielinski and N.F.Rabbani, "Prestressed Steel Continuous Span Girders", J. of str.Engg., June 1989, pp1357-1370.

55.N.F.Rabbani, "Prestressing Steel Structures", presented at the seminar of Montréal Structural Engineers, Mc Gill University, Nov. 17, 1988.

56.M.S. Troitsky, Z.A. Zielinski and N.F. Rabbani, "Strengthening of Girders by Post-Tensioned Cables", proc. str., CSCE Annual Conference 1989, pp.445-453.

57. Z.A. Zielinski, same as 18, p.309.

58.P. Pamar, "Prestressed Steel Continuous Girders", M.Sc. Thesis in the Department of Civil Engineering, Concordia University, 1987.

59.A. Nouraeyan, "Prestressed / Post-Tensioned Composite Steel Girders", M.Sc. Thesis in the Department of Civil Engineering, Concordia University, 1987.

60.M. Yadlosky, R.J.Brungraber and J.B.Kim, "Bridge Rehabilitation: an Alternate Approach", Proc., Str.Div., ASCE, Jan. 1982, pp.163-176.

61.J.B.Kim, R.J.Brungraber and M.Yadlosky, "Truss Bridge Rehabilitation Using Steel Arches", J. of Str. Engg., ASCE, July 1984, pp.1589-1597.

62.K.F. Dunkar, F.W. Klaiber and W.W. Sanders Jr., "Design Manual for Strengthening Single-Span Composite bridges by Post-Tensioning", Final Report part III, Issued by Department of Civil Engineering, Engineering Research Institute, Iowa State University, March, 1985.

63.K.F. Dunkar, F.W. Klaiber W.E. Wiley and W.W. Sanders Jr., "Strengthening of existing Continuous Composite Bridges", same as 62, July 1989.

64.F.W. Klaiber , T.J. Wipf, K.F.Dunkar, R.B. Abu-Kishk and S.M.Planck, "Alternate Methods of Bridge Strengthening", Same as 62, Feb.1989.

65.P.S.A. Berridge and D.H. Lee, "Prestressing Restores Weakened Truss Bridge", J.of Civil Engg., Sept.1956, pp.48-49.

66.A.C. Scordelis, "Analysis of Continuous Box Girder Bridges", a report to The Division of Highways Department of Public Works, State of California, published by College of Engineering, Office of Research Services, University of california

67.C.P. Heins, "Box Girder Bridge Design - State of the Art", Engg.J., AISC, Fourth Quarter 1978, pp.126-142.

68. C.P. Heins, "Steel box girder Bridges - Design Guides and Methods", In Memoriam of, Engg. J., fourth quarter 1983, pp.121-142.

69. C.P. Heins, "Proportioning of Box Girder Bridges", proc. Str. Div., ASCE, Nov. 1980, pp.2345-2349.

70.F. Leonhardt and D. Hommel, "The Necessity of Quantifying Imperfections of Structural members for Stability of box Girders", proc. of the International conference Feb.1973, published by The Institute of Civil Engineers, pp.11-19.

71.F.De Miranda and M.Mele, "Some Basic Design Principles for Steel Girder bridges", proc. of the International conference, Feb.1973, published by The Institute of Civil Engineers, pp.21-31.

72.M.S.Troitsky, same as 5.

73.Proposed Design Specification for Steel Box Girder Bridges , Final Report, prepared for Federal highway Administration, Washingto D.C., Jan.1980.

74.M.R.Horne and R.Narayanan, "An Approximate method for the Design of Stiffened Steel Compression panels", proc. Institute of Civil Engineers, Sept.1975, pp.501-515.

75.Precast Segmental Box Girder Bridge Manual , published by Prestressed Concrete Institute, 1978, pp.52-53.

76.ibid, pp.53-59.

77.E. Belenya, same as 17, pp.193-195.

78.M.S. Troitsky, Z.A. Zielinski and N.F. Rabbani, "Moving Loads on Prestressed Steel Girders", proc. Annual Conference CSCE, May 1988, pp.

79. M.S.Troitsky and N.F. Rabbani, "Tendon Configurations of Prestressed Steel Girder Bridges", proc. Centennial Conference CSCE, May 1987, pp.

80.G. Murphy, Similitude in Engineering , published by the Ronald Press Co, New York, 1950, pp.57-59.

81.J.S. Kinney, Indeterminate Structural Analysis , published by Addison-Wesley Co., 1957, pp.584-637.

82."Strain Gage Selection", Technical notes, Published by M.G.Inc., 1983.

83."Surface Preparation for Strain Gage Bonding", prepared by Measurements Group Inc., 1976, USA.

84.A.V.Koretsky and R.W.Pritchard, "Assessment of Relaxation Loss Estimates for Strands", proc., Str.Div., ASCE, Dec.1982, pp.2819-2836.

85.M.S.Troitski, Z.A.Zielinski and N.F.Rabbani, "Prestressing Force Increment of Two Span Steel Bridges", to be published in Canadian Journal of Civil Engineeing, April 1991.

86.M.R.Horne and R.Narayanan, "An Approximate Method for the Design of Stiffened Steel Compression Panels", proc. Instn. of Civ. Engrs., Sept. 1975, pp.501-514.

87."Proposed Design Specifications for Steel Box Girder Bridges", final report No.FHWA-TS-80-205, Jan. 1980, prepared for Federal Highway Administration, Washington D.C., USA.

88.Steel Box Girder Bri'ges , Proceedings of the International Conference organized by the Institution of Civil Engineers, London, Feb.1973.

89.Merrit, Structural Steel Design Manual , pp. 4.42-4.53, 10.54-10.63 and 11.96-11.118.

90.M.S.Troitsky, same as 19, pp.102-104.

91. Z.A.Zielinski and H.Mobasher, results of the tests performed in the Structural Laboratory, Department of Civil Engineering, Concordia University, Montréal.

92. H.Nakai and C.H.Yoo, Analysis and Design of Curved Steel Bridges, published by McGraw Hill, New York, 1980, pp.25-130.

93. B.G.Johnston, "SSRC, Guide to Stability Design Criteria for Metal Structures", John Wiley & Sons, New York, 1976.

94. S.P.Timoshenko and T.M.Gere, Theory of Elastic Stability, published by McGraw Hill, New York, 1961.

95. W.Weaver Jr. and T.M.Gere, Matrix Analysis of Framed Structures, published by D.Van Nostrand, 1980, pp.30-35.

APPENDIX A. NUMERICAL EXAMPLES

A parametric study on the computed bending moments of prestressed continuous span girders shows a decrease in the value of the negative bending moments at the middle supports in comparison to a similar non-prestressed girder having similar longitudinal and cross-sectional properties and subjected to the same service loadings. The decrease corresponds to the deformations of the girder caused by the action of the prestressing force increment.

To elaborate on the effect of prestressing, several two spans prestressed girders are considered. The designed continuous girders have asymmetrical trapezoidal box sections, which remains constant along the girder. The total cross-sectional areas of the tendons are also assumed to be constant. A comparison is made among three various types of tendon configurations, Figure 5.6, depending on whether the girder is prestressed or non-prestressed. Table A.1, provides the designed length and the cross-sectional properties of the girders and of the tendons.

Based on Equations (5.37) through (5.47) a computer program is written, in which the input data includes the type of tendon placement, loading case, the cross-sectional properties, the length and lengths of the draped tendons and the output is the negative bending moment at the middle support and the incremental prestressing force. The output results of the two spans continuous girders for the input data given in Table A.1 and subjected to a unit concentrated load at .6 L, to produce the maximum negative bending moment and at .4 L to create the maximum incremental prestressing force, are computed, Table A.2.

The variations of the moment versus the span length, for tendon configurations type I and type III are presented in Figures A.1 and A.2. The results for type I and type II are

very similar and are not shown. In FigureA.2 a comparison is made between the prestressed girder and similar non-prestressed girder. The decrease of up to 17% in the negative bending moment due to the effect of prestressing is illustrated in Figure A.3. The incremental prestressing force and the corresponding comparison for the proposed types of tendon configurations are presented in Figures A.4 to A.7 [85].

Data	L m	L_1 m	L_2 m	L_3 m	m m	e m	e_1 m	A m^2	I m^4	A_t m^2
1	60.	5.	40.	50.	36.	1.	.4	.15	.13	.010
2	80.	10.	60.	65.	48.	1.4	.6	.20	.16	.012
3	100.	10.	70.	80.	60.	1.8	.8	.25	.20	.015
4	120.	20.	90.	100.	72.	2.1	.9	.31	.24	.017
5	150.	20.	100.	110.	90.	2.5	1.0	.40	.30	.020
6	200.	20.	150.	165.	120.	2.8	1.2	.50	.38	.030

A.1. Cross-Sectional Properties of the two equal span prestressed girders.

Span,	Bending Moment, kNm			Decrease,	Prestg.Force Increment, kN	
m	Non-Prest'd	Conf.Type I	Conf.Type III	%	Conf.Type I	Conf.Type III
60	5.65	5.76	5.76	1.9	1.1	0.2
80	7.33	7.61	7.68	4.6	1.9	0.4
100	9.04	9.58	9.60	5.8	3.1	0.6
120	10.55	11.39	11.52	8.4	3.7	0.7
150	12.63	14.24	14.40	12.3	4.7	1.0
200	16.24	18.81	19.20	15.4	8.5	2.6

Table A.2. Computed data for the two equal span girders due to a unit concentrated load.

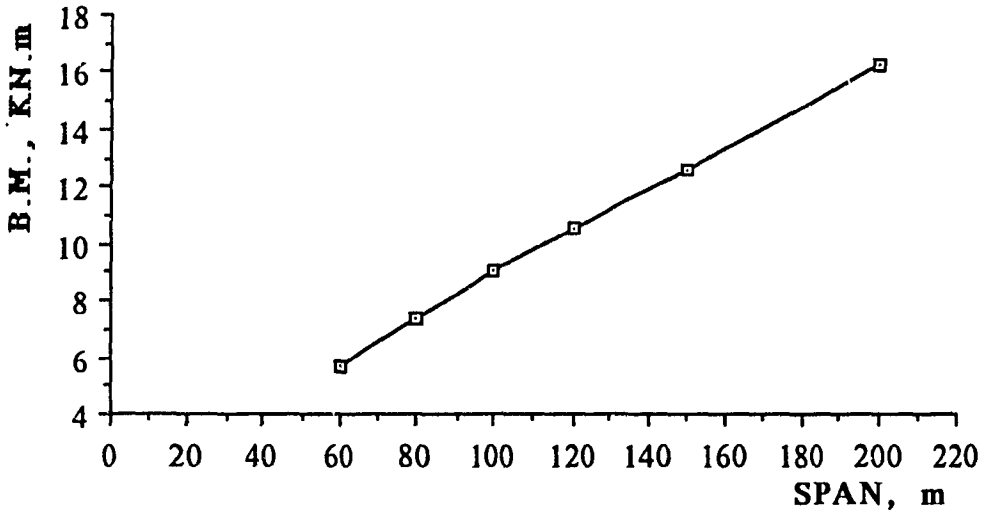

Figure A.1. Maximum negative bending moments at the middle support due to a unit concentrated load, tendon configuration Type I.

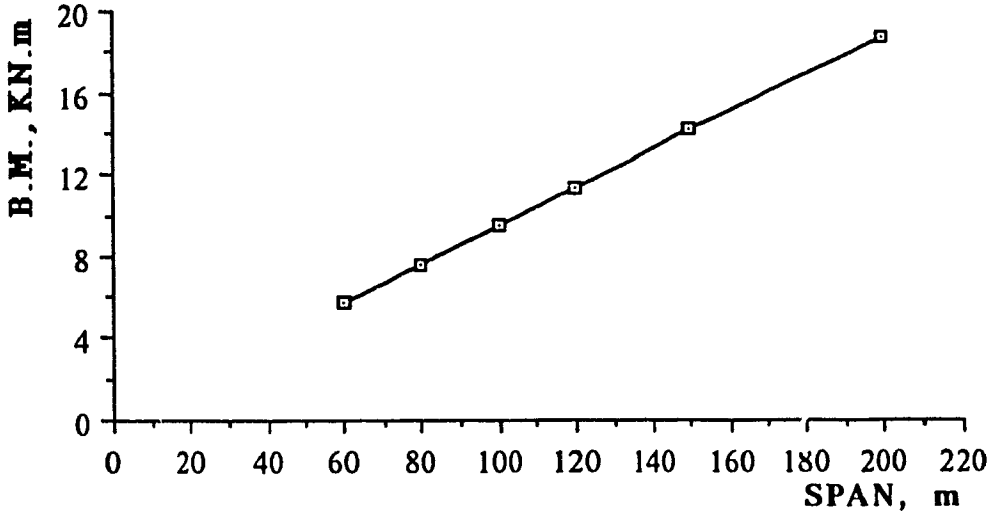

Figure A.2.Maximum bending moment at the middle support due to a unit vertical load, tendon configuration Type III.

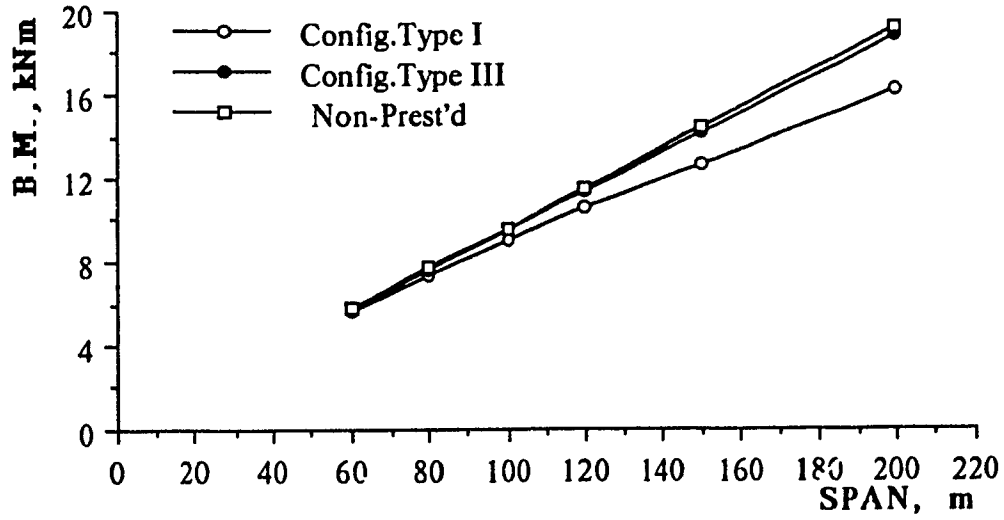

Figure A.3. The bending moments are compared with similar non-prestressed girders.

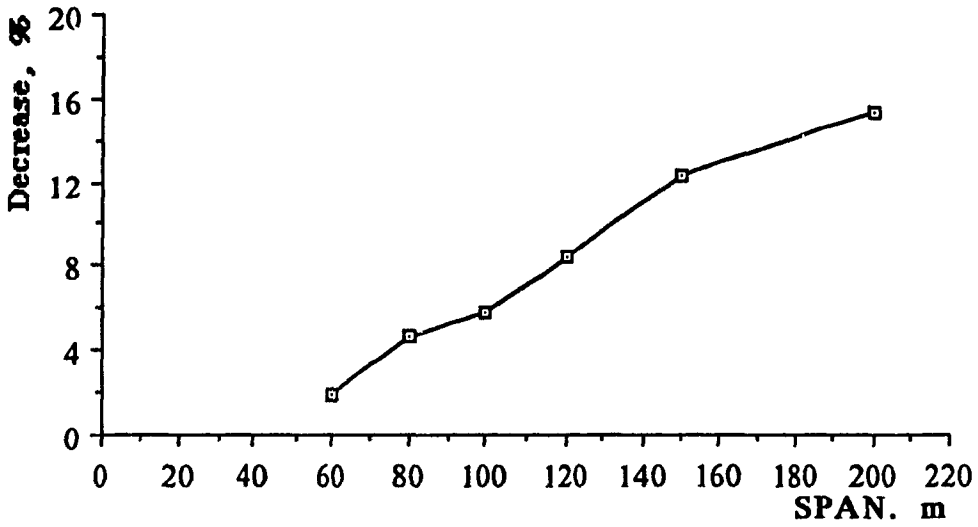

Figure A.4. Decrease of the bending moment of the prestressed versus the non-prestressed girders.

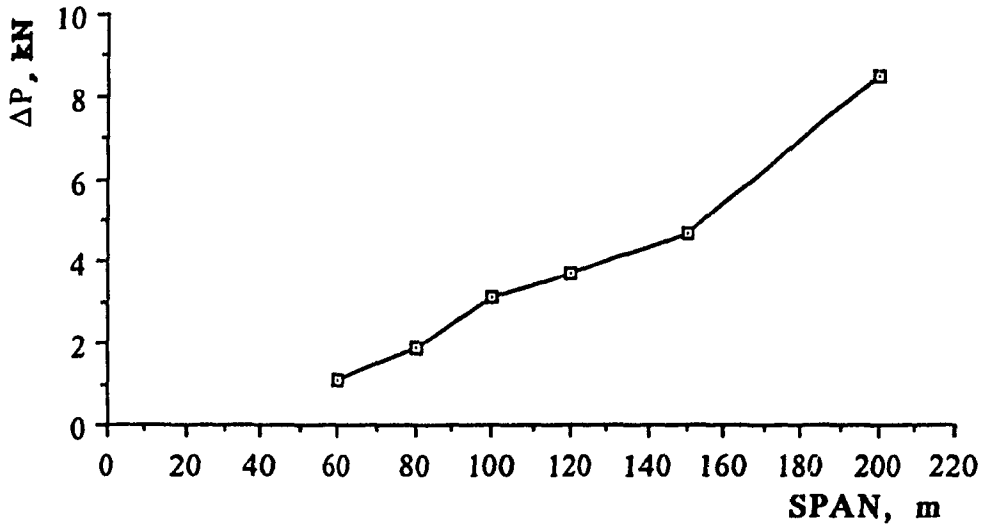

Figure A.5. Maximum incremental prestressing force, tendon configuration Type I.

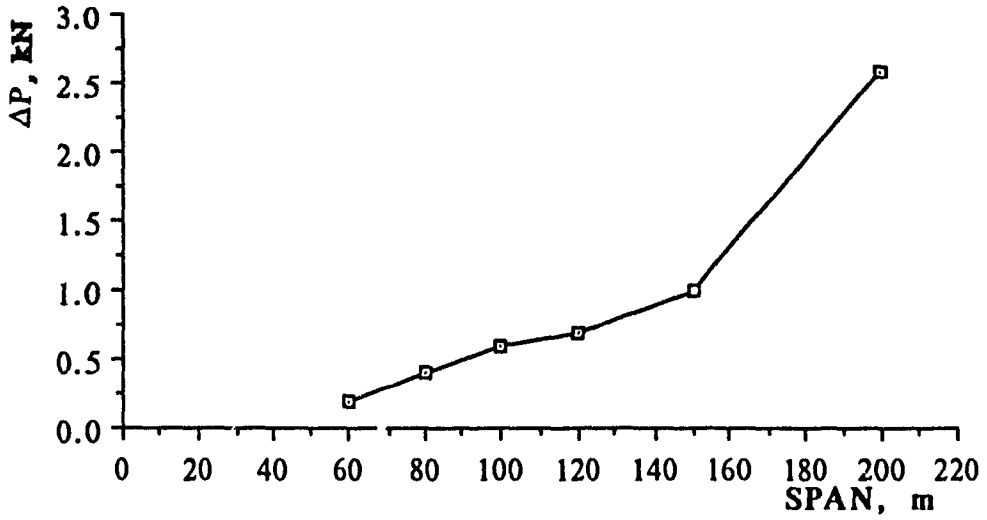

Figure A.6. Maximum incremental prestressing force, tendon configuration Type III.

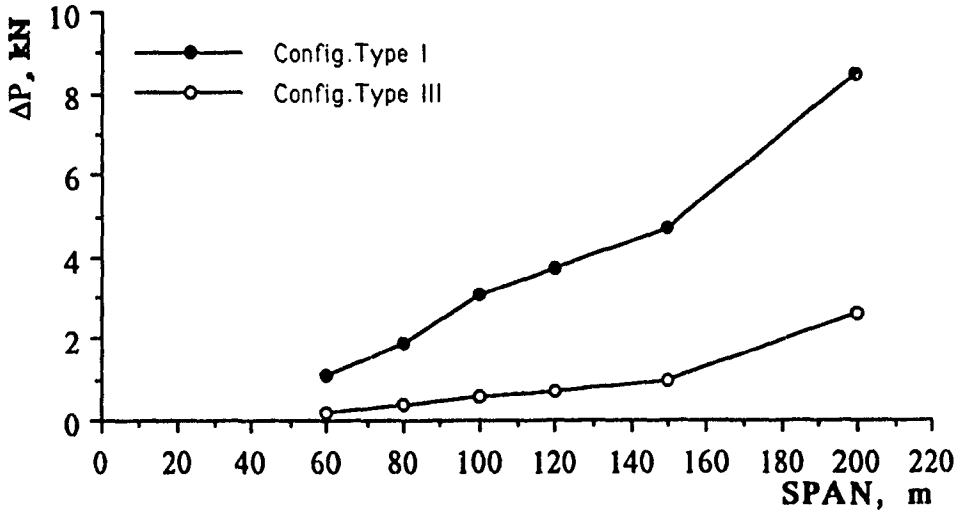

Figure A.7. The maximum incremental prestressing forces corresponding to the configurations Type I and Type III are compared

The computed negative bending moments at the middle supports of several three spans continuous girders prestressed by tendons, Figure 3.4.a, are compared with the moments of similar non-prestressed girders [54]. The values of the incremental prestressing force (ΔP) are also calculated. The cross-sectional properties, span length and the applied loadings are the same in both cases. Only two adjacent spans are loaded for the calculation of maximum negative bending moments, while all three spans are loaded for the computation of maximum prestressing force increment. Comparing the maximum negative bending moments for the two cases (non-prestressed m_1 and prestressed m_2) show a reduction of about to 20 % in the case of prestressed girder. The output results for m_1, m_2 and ΔP, for five girders of unequal spans are given in Table A.3. Figures A.8 and A.9 illustrates the corresponding values of the bending moments and the prestressing force increment. Figures A.10 and A.11 show the comparison of the negative bending moments and ΔP for six continuous girders having three equal spans. The respective data are provided in Table A.4 [54].

	Span, m	m_1, kNm	m_2, kNm	ΔP, kN
1	60 - 90 - 60	9221	8975	384
2	80 - 120 - 80	16059	15437	644
3	100 - 150 - 100	24857	22921	1087
4	150 - 225 - 150	54505	48206	3008
5	200 - 300 - 200	95174	78509	5149

Table A.3. Computed data of the bending moments and the prestressing force increment for unequal span girders.

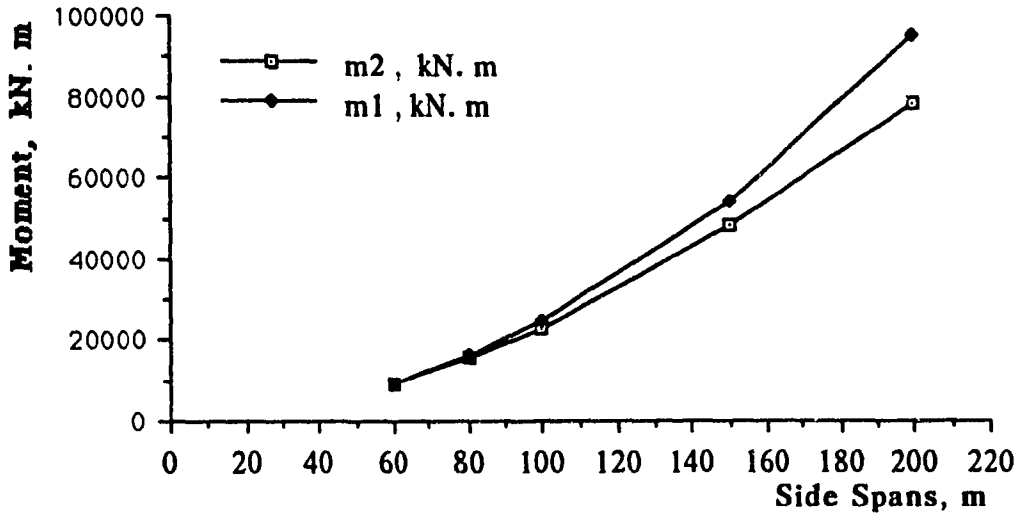

Figure A.8. The maximum negative bending moments of unequal three span girders are compared in two cases of non-prestressed m_1 versus prestressed m_2.

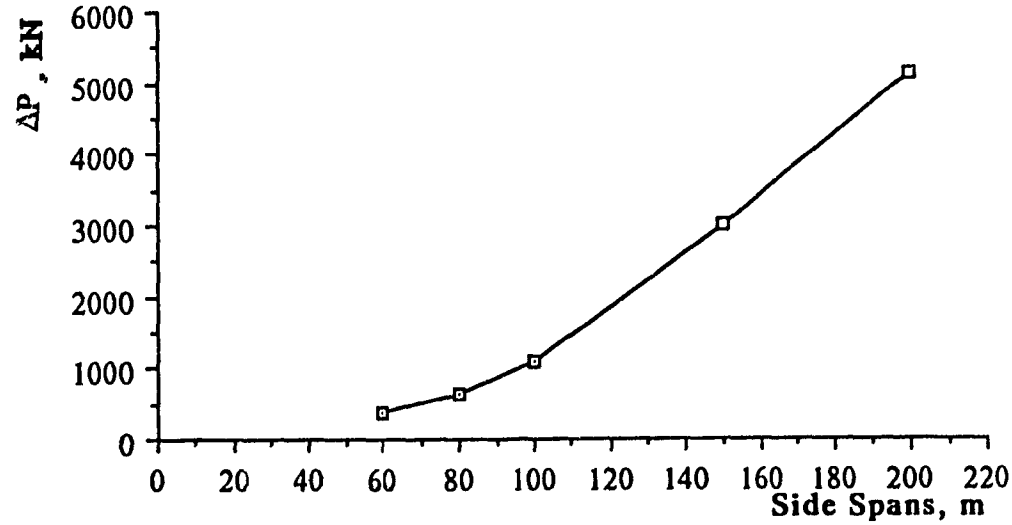

Figure A.9. Maximum prestressing force increment for unequal three span girders.

	Span, m	m_1, kNm	m_1, kNm	ΔP, kN
1	60 - 60 - 60	6481	6364	172
2	80 - 80 - 80	10975	10603	421
3	100 - 100 - 100	16635	16007	639
4	150 - 150 - 150	35890	33398	1680
5	200 - 200 - 200	62437	54811	3787
6	250 - 250 - 250	96276	81560	6598

Table A.4. Computed data of the bending moments and the prestressing force increment for equal span girders.

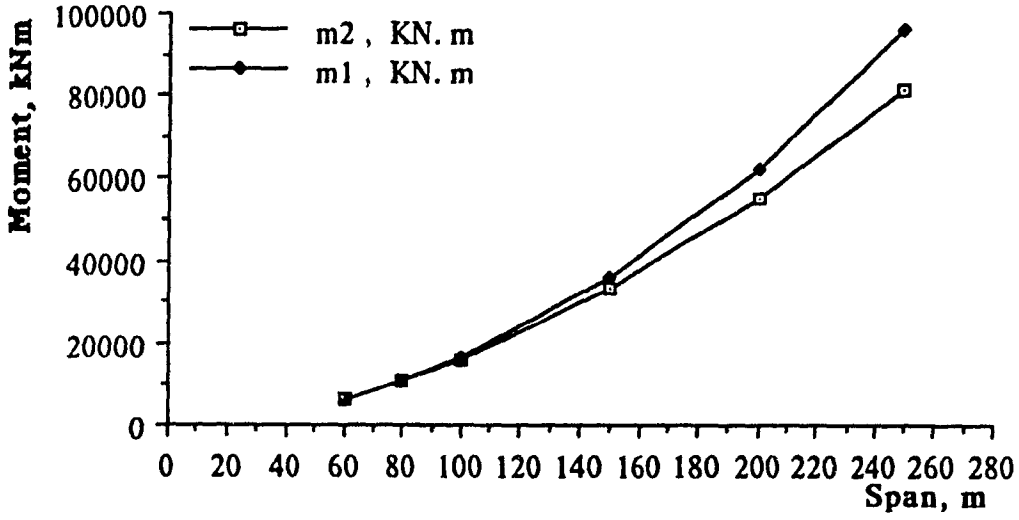

Figure A.10. The maximum negative bending moments of equal three span girders are compared in two cases of non-prestressed m_1 versus prestressed m_2.

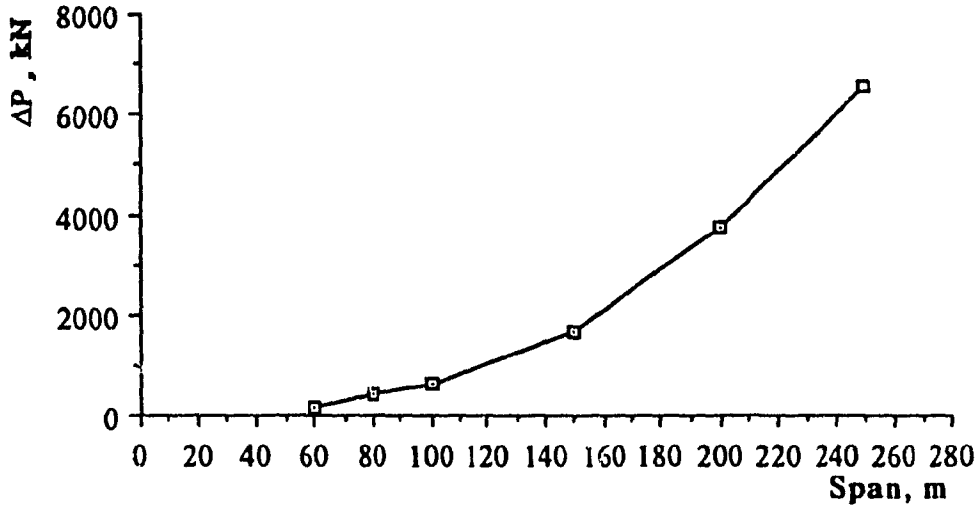

Figure A.11. Maximum prestressing force increment for equal three span girders.

APPENDIX B. DESIGN OF THE PROTOTYPE STEEL BOX GIRDER

To evaluate the behavior of the prestressed steel box girders a two-span girder bridge is designed as the prototype, Figure 6.1.a. The span lengths are 80 m each and width of the roadway is 9.6 m. The two steel box girders have a variable trapezoidal shape along the girder, Figure 6.1.b. The height is increasing at the vicinity of the middle support. The tendon configuration is shown in Figure 6.1.b. An orthotropic deck is deigned for the top flange (for details of the design of orthotropic deck see reference 87).

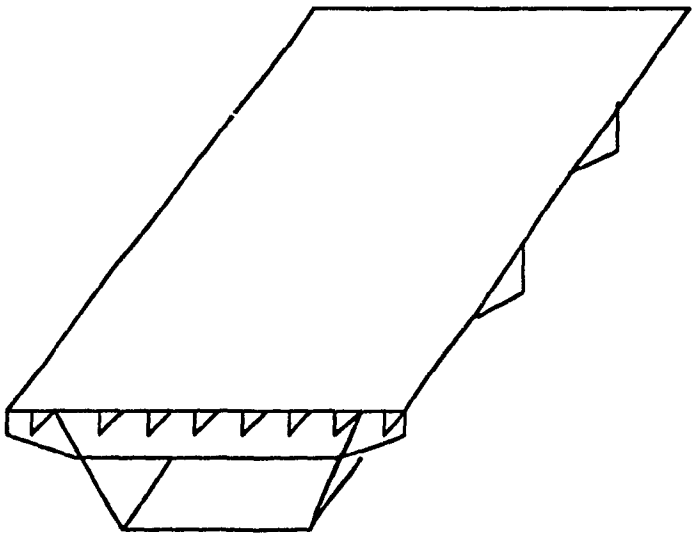

Figure B.1. Steel box girder with orthotropic deck.

1. Loadings:

- Dead Load, DL = .26x77 = 20.0 kN/m
- Superimposed Dead Load, SD = .05x4.8x19 = 4.6 5.0 kN/m
- Live Loads, MS 250 in accordance with the Canadian Highway Bridge Design
- Load distribution factor for box girders, $W_L = .1 + 1.7\,R + .85/N_w$,

  where, $N_w = W_c/3.7$, but reduced to the nearest digit

$R = N_w$ / No. of box girders, but $.5 \le R \le 1.5$

W_c is the width of the roadway between curbs.

$W_c = 8.7$ m, $N_w = 8.7 / 3.7 = 2.35 \approx 2$, $R = 2/2 = 1$.

$W_L = .1 + 1.7\ 1 + .85/2 = 2.2$

- Impact: $I = 15/(38 + 80) = .1$
- Concentrated Live Load $V_L = .5 \times 2.2 \times 1.1 = 136.1$ kN
- Uniformly Distributed Live Load $w_L = .5 \times 12.5 \times 2.2 \times 1.1 = 15.0$ kN/m
- Prestressing:

The initial prestressing force, $P_i = 5000$ kN

Tendon cross-sectional area, $A_t = .005$ m^2

Total Losses of prestressing are assumed as 10 % of the prestressing force and to be equally divided between the cable guides.

2. Computed bending moments at the middle support M, and the prestressing force increment, ΔP, due to a unit concentrated load V = 1 kN and a uniformly distributed load of unit intensity w = 1, are given in Table B.1.

	Non-prest'd		Prest'd			
	1 Span Loaded	2 Spans Loaded	1 Span Loaded		2 Spans Loaded	
	M, kNm	M, kNm	M, kNm	ΔP, kN	M, kNm	ΔP, kN
V=1 kN	8.28	19.26	8.14	6.31×10^{-2}	19.02	10.16×10^{-2}
w=1 kN/m	493.4	986.8	486.6	2.98	973.2	5.96

Table B.1. The computed values of M and ΔP when the prototype box girder is subjected to vertical loadings with unit intensity.

3. Maximum negative bending moments at the middle support, when both spans are loaded and the concentrated live load is applied at x = 46.5 m from the side supports.

- Due to DL	- 986.8 × 20 = - 19736
- Due to SD	- 973.2 × 5 = - 4866
- Due to LL	- 19.02 × 136.1 = - 2589
	- 973.2 × 15 = - 14598

Maximum negative bending moment due to service loadings, M_{d+s+L} = - 41789 kNm

- Due to prestressing

$\Delta P = 136.1 \times 10.16 \times 10^{-2} + (15 + 5) \times 5.96 = 133$ kN

$P_{ei} = P_i + \Delta P = 5000 + 133 = 5133$, consider prestressing losses equal to .025 × 5133 = 130 kN at the middle support (after the first saddle), the effective prestressing force is equal to $P_e = 5133 - 130 = 5003$ and the respective bending moment due to prestressing is $P_e \ e_1 = 5003 \times 1.2 = 6004$ kNm

4. Maximum positive bending moment at x = 30. m from the right support (.375 L), when the live loads are applied on one span only and the concentrated load at x = 30. m.

- Moments at the middle support

DL	- 986.8 × 20 = -19736 kNm
SD	- 973.2 × 5 = - 4866 kNm
LL	- 8.14 × 136.1 = -1108 kNm
	- 486.6 × 15 = -7299 kNm
	Total = - 33009 kNm

- Maximum positive bending moment at x = 30. m, due to service loads M_{d+s+L}

$$M_{d+s+L} = [-33009/80 + (40\times 80)/2 + (136.1\times 50)/80]\times 30 - (40\times 30^2)/2$$

$$M_{d+s+L} = 18299 \text{ kNm}$$

- Moment due to prestressing

$$\Delta P = 20\times 2.98 + 136.1\times 6.3\times 10^{-2} = 68 \text{ kN}$$

$$P_e = P_i + \Delta P - .1\,(P_i + \Delta P) = 5068 - 507 = 4561 \text{ kN}$$

$$P_e \cdot e = -4561\times 1 = -4561 \text{ kNm}$$

5. Cross-sectional geometry of the prototype.

- A trial geometry for the steel box girder is selected considering the design of steel box girders, the theory and design of orthotropic deck plates and the proposals recommended in this thesis [86, 87, 88, 89 and 90].
- To achieve a shallower section the roadway is supported on two similar box girders, Figure 6.1.
- The cross-sectional area of the trapezoidal steel box section varies along the girder. A deeper section provides more strength at the vicinity of the middle support and also the eccentricity of the tendon is increased (the neutral axis moves closer to the compression fiber of the section), Figures 6.1 and 6.2.
- The plate thicknesses and the longitudinal geometry of the girder are shown in Figures 6.1 and 6.2. The cross-sectional properties of the girder are accordingly calculated, see Section 6.2.
- The configuration of the tendon is shown in Figure 6.1.b.

6. Stresses due to bending moments.

- Stresses at various stages of loadings should be checked as provided in Section 4.3, equations (4.5) through (4.11). The control of the final combined stresses due to the applied service loads and the induced prestressing force, for the maximum values of the positive and negative bending moments (at x= 30.m and x = 80. m) are calculated based on equations (4.10) and (4.11).

a. At x = 30. m

$$f^{comp}_{d+s+L} = -\frac{18299\times10^6}{.216\times10^9} + \frac{4561\times10^6}{.216\times10^9} - \frac{4561\times10^3}{.240\times10^6}$$

$$= -84.7 + 21.1 - 19.0 = -86.8 \le 152 \text{ MPa, OK}$$

$$f^{tens}_{d+s+L} = \frac{18299\times10^6}{.141\times10^9} - \frac{4561\times10^6}{.141\times10^9} - \frac{4561\times10^3}{.240\times10^6}$$

$$= 129.8 - 32.3 - 19.0 = 78.5 \le 110 \text{ MPa, OK}$$

b. Middle support, x = 80. m

$$f^{tens}_{d+s+L} = \frac{41789\times10^6}{.272\times10^9} - \frac{6004\times10^6}{.272\times10^9} - \frac{5003\times10^3}{.280\times10^6}$$

$$= 153.6 - 22.1 - 17.9 = 113.6 \ge 110 \text{ MPa, Acceptable}$$

$$f^{comp}_{d+s+L} = -\frac{41789\times10^6}{.282\times10^9} + \frac{6004\times10^6}{.282\times10^9} - \frac{5003\times10^3}{.280\times10^6}$$

$$= -148.2 - 21.3 - 17.9 = 144.8 \le 152 \text{ MPa, OK}$$

7. Check shear stress

- The girder is loaded to calculate the maximum shear force

$$V = -31901/80 + (40\times80)/2 + 136.1\times78/80 - 40\times2 = 1253.7 \text{ kN}$$

Shear stress is equal to: $v = VQ/It$,

where, $Q = 4.8\times.016\times.742 + 13\times.042\times(.750 - .178) + 2\times.750\times.01\times.750/2 = .094$

$I = .162\times10^{12}$ mm^4, and $t = 2\times10$ mm.

$v = 36.4 < 44$ MPa, allowable shear stress, OK.

8. Check deflections

- The deflection due to live load is calculated at the middle span based on P-Frame computer program, since the girder has a variable cross-section.

$$\delta_L = 235 \text{ mm}$$

- The reverse effect of prestressing force (camber in the opposite direction to the applied service loads) is given as the following expression [92].

$$\delta_{pre} = -\frac{(P_e + \Delta P)\ e\ L^2}{8\ E\ I}$$

$$\delta_{pre} = 126.7 \text{ mm}$$

- The total deflection δ due to the combined effect of applied live loads and the induced prestressing force is: $\delta = 235 - 126.7 = 109.3$ mm, $L/740$, OK.

```
      PROGRAM PRST2S (INPUT,OUTPUT,TAPE5=INPUT,TAPE6=OUTPUT)

C     THIS PROGRAM CALCULATES THE BENDING MOMENT (BM)
C     AT THE MIDDLE SUPPORT AND PRESTRESSING FORCE
C     INCREMENT (DX) OF TWO SPAN GIRDERS.

      REAL I, M, N, L1, L2, L3, L
      INTEGER CASE
C
C     L IS THE SPAN LENGTH
C     L1, L2, L3, M REPRESENT THE POSITIONS OF
C     THE TENDONS (SLOPE CHANGES)
C     AND LOADINGS (SEE FIGURE 5.6).
C
C     EB AND ET ARE THE BOTTOM AND THE TOP TENDONS
C     ECCENTRICITIES, RESPECTIVELY.
C
C     CASE REPRESENTS THE TYPE OF TENDON CONFIGURATION.
C
C     I, AG AND AT ARE THE MOMENT OF INERTIA AND THE AREA
C     OF THE GIRDER AND THE CROSS-SECTIONAL AREA OF
C     THE TENDON.
C
C     P AND Q ARE THE CONCENTRATED AND UNIFORMLY
C     DISTRIBUTED LOADS, RESPECTIVELY.
C
C     CA AND CB ARE THE COS(A) AND COS(B), WHERE A AND B
C     ARE THE ANGLES OF THE SLOPED TENDONS, SEE FIGURE 5.6.

10    READ (5, *)  CASE
      READ (5, *)  EB, ET
      READ (5, *)  L, L1, L2, L3
      READ (5, *)  M, N
      READ (5, *)  I, AG, AT
      READ (5, *)  P, Q

      IF (CASE.NE.1) GO TO 50

      CA=L1/SQRT(L1**2+(ET+EB)**2)

      GO TO 60

50    CA=1.

      L1=0.
```

```
60  IF (CASE.EQ.3)  GO TO 70

    CB=(L3-L2)/SQRT((L3-L2)**2+(ET+EB)**2)

    GO TO 80

70  CB=1.

    L2=L3
    EB=0.
C
C   A, B, C AND ARE THE COORDINATES OF THE B.M.
C   DIAGRAM OF THE RELEASED GIRDER DUE TO A
C   UNIT PRESTRESSING FORCE, FIGURE 5.10.
C
80  A=ET
    B=EB+ET*L1/L
    C=EB+ET*L2/L
    D=ET*(1.-(L3/L))

    C1=L2**2+L1*L2
    C2=-L1**2+L3**2-L1*L2+L2*L3
    C3=L2**2-L**2+L2*L3-L*L3
    C4=(A+C)*(A-B-C)+(3.*I/AT)*((1./CA**3)-1.)
    C5=(B+D)*(B+C-D)+(3.*I/AT)*(1.-(1./CB**3))
    C6=C*(C-D)+(3.*I/AT)*((1./CB**3)-1.)
    C7=D*D+(3.*I/AG)*(1.+(AG/AT))
    C8=A*L1**2/6.-B*L1**2/3.
    C9=((B-C)/(L2-L1))*(M**3/3.+L1**3/6.-L1*M*M/2.)
    C10=(B/2.)*(M*M-L1*L1)
    C11=(B-C)*(L2-M)/(L2-L1)
    C12=(L2+M)*(L/2.+L1/2 -L2/3.)-L*L1-M*M/3.
    C13=(L2-M)*(-B*L+B*L2/2.+B*M/2.)
    C14=C+D
    C15=(L3+L2)*(L/2.+L2/6.)-L*L2-L3**2/3.
    C16=(L3-L2)*(-L+L3/2.+L2/2.)
    C17=(D/3.)*((L-L3)**2)
    C18=L1*L1*(L/6.-L1/12.)
    C19=(L1+L2)*(-L*L2/6.)
    C20=(L2/12.)*(L2**2+L1*L2+L1**2)
    C21=(L*L1/6.)*(L1+L2)-(L1/12.)*(L1**2+L1*L2+L2**2)
    C22=(-L+L3/6.)*(L3+L2)+(L3/12.)*(L3**2+L2*L3+L2**2)
    C23=(-L*L2/6.)*(L2+L3)+(L2/12.)*(L3**2+L2*L3+L2**2)
    C24=(L/12.)*(-L3**2+L**2+L*L3)
    C25=-2.*L2*((I/AG)+(I/AT))
```

```
      IF (CASE.NE.3.) C25=0.
C
C     D(IJ) DEFINES THE DEFORMATION AT POINT (I)
C     DUE TO A UNIT FORCE AT POINT (J)
C
      D11=2.*L/3.
      D12=(1./(3.*L))*(-A*L1**2+B*C1+C*C2+D*C3)
      D22=(2./3.)*(L1*C4+L2*C5+L3*C6+L*C7)
C
C     D1CL AND D1UL ARE THE DEFORMATIONS OF THE
C     RELEASED GIRDER DUE TO CONCENTRATED
C     LOAD (P) AND UNIFORMLY DISTRIBUTED LOAD (Q).
C
      D1CL=(-P/(L*L))*((N*M**3/3.)+(M*M*N*N/2.)+
     1          (M*N**3/6.))

      D1UL=-Q*L**3/24.

      D1L=D1CL+D1UL

      D2CL=(P/L)*(N*(C8+C9-C10)+M*(C11+C12+
     1             C13+C14+C15+C16+C17))

      D2UL=(Q/2.)*(A*C18+B*(C19+C20)+C*(C21+
     1                    C22)+D*(C23+C24))

      D2L=D2CL+D2UL

      BM=(D1L*D22-D2L*D12)/(D12**2-D11*D22)

      DX=(D2L*D11-D1L*D12)/(D12**2-D11*D22)

      WRITE (6,100) BM, DX

  100 FORMAT ('          ', ////, 'THE BENDING MOMENT',
     1          T60, '  BM=', F9.2, ///, ' THE PRESTRESSING
     1          FORCE INCREMENT', T60, '  DX=' ,F7.2)

      WRITE (6,200)  L, L1, L2, L3, M

      WRITE (6,250)  EB, ET

      WRITE (6,300)  I, AG, AT
```

```
200 FORMAT ('          ',////,'SPAN LENGTH', T60,'   L=',
   1          F6.2,///,' TENDON POSITIONS FROM THE LEFT
   1           SUPPORT',//, T60,' L1=', F6.2,//, T60,' L2=',
   1           F6.2,//, T60,' L3=', F6.2,///,'POSITION OF
   1           CONCENTRATED LOAD FROM THE LEFT SUPPORT',
   1           T60,'   M=', F6.2)

250 FORMAT (//,'TENDON ECCENTRICITIES FROM THE N.A.',
   1          T60,' EB=', F6.2,//, T60,' ET=', F6.2)

300 FORMAT (////,' CROSS SECTIONAL PROPERTIES',//,
   1          'MOMENT OF INERTIA', T60,'  I=', F10.8,//,
   1          'CROSS-SECTIONAL AREA OF THE GIRDER',
   1          T60,' AG=', F10.8,//,'CROSS-SECTIONAL
   1          AREA OF THE TENDONS', T60,' AT=', F10.8)

    GO TO  10

    STOP
    END
```

```
      PROGRAM PRST3S(INPUT,OUTPUT,TAPE5=INPUT,TAPE6=OUTPUT)

C     THIS PROGRAM CALCULATES THE BENDING MOMENTS (BM)
C     AT INTERMEDIATE SUPPORTS AND PRESTRESSING
C     FORCE INCREMENT (DX) OF THREE AND MORE SPANS GIRDERS.

      DIMENSION  D(3,3), DB(3,3),  DL(3)
      REAL  L, L1, L2, LM,  M, N,
C
C     L AND LM ARE THE SIDE SPANS AND MIDDLE SPAN LENGTHS
C     L1, L2, M AND N  PROVIDE THE POSITION OF THE TENDON
C     AND THE LOADINGS (SEE FIGURE 3.4).
C
C     E AND E1 ARE THE BOTTOM AND THE TOP TENDONS'
C     ECCENTRICITIES, RESPECTIVELY.
C
C     SI1, AS1, SI2 AND AS2  ARE THE MOMENT OF INERTIA AND
C     THE AREA OF THE GIRDER ALONG THE SIDE SPANS AND
C     THE MIDDLE SPAN, RESPECTIVELY.  AT IS THE CROSS-SECTIONAL
C     AREA OF THE TENDONS.
C
C     CA IS THE COS(A) , WHERE A IS THE ANGLE OF THE SLOPED
C     TENDON, SEE FIGURE (  )
C
C     NS  REFERS TO THE NUMBER OF SPANS

      READ (5,*)  NS
      READ (5,*)  L, LM, M, N
      READ (5,*)  L1, L2, E, E1
      READ (5,*)  SI1, AS1, SI2, AS2, AT
C
C     A, B AND C  ARE THE COORDINATES OF THE BENDING
C     MOMENT DIAGRAM OF THE RELEASED GIRDER DUE TO
C     A UNIT PRESTRESSING FORCE, ONLY, FIGURE 3.5.

      A=E
      B=E+E1*L1/L
      C=E1*(1.-L2/L)

      CA=(L2-L1)/SQRT((L2-L1)**2+(E1+E)**2)
C
C     D(I,J) IS THE DEFORMATION AT POINT (I) DUE TO A UNIT
C     FORCE AT POINT (J).
```

```
      D(1,1)=(1./(3.*SI1))*(L/SI1+LM/SI2)
      D(2,2)=D(1,1)
      D(1,2)=LM/(6.*SI2)
      D(2,1)=D(1,2)

      C1 =A*L1**2+B*L2*(L1+L2)
      C2 =C*(L1-L)*(L1+L+L2)
      C3 =B*(L2+L1+LM-2.*L)+C*(L1-L)

      D(1,3)=(1./(6.*SI1*L))*(C1+C2)+(1./(2.*SI2))*C3
      D(3,1)=D(1,3)
      D(2,3)=D(1,3)
      D(3,2)=D(1,3)

      C4 =(A**2+B**2+A*B)*L1+C**2*(L-L2)
      C5 =(B**2+C**2-B*C)*(L2-L1)
      C6 =(1.5*B**2)*(LM-2.*(L-L1))+C**2(L-L2)
      C61=2.*L/AS1+LM/AS2+2.*L/AT+LM/AT
      C62=(4.*(L2-L1)/AT)*(1/CA**3-1)

      D(3,3)=(2./(3.*SI1))*(C4+C5)+(2./(3.*SI2))*(C5+C6)+C61+C62

      C7 =-(L**3/(24.*SI1))
      C8 =-(LM**3/(24.*SI2))
C
C     D1LU AND D1LC ARE THE DEFORMATIONS OF THE FIRST
C     SPAN DUE TO UNIFORMLY DISTRIBUTED AND
C     CONCENTRATED LOADS OF UNITY, RESPECTIVELY.
C     SIMILARLY, D2LU, D2LC; D3LU AND D3LC REPRESENT THE
C     RESPECTIVE DEFORMATIONS AT SPANS 2 AND 3.
C
      D1LU=C7+C8

      C9 =-(M*(L**2-M**2))/(6.*SI1*L)
      C10=-(N*(LM-N)*(2.*LM-N))/(6.*SI2*LM)

      D1LC=C9+C10

      DL(1)=D1LU+D1LC

      D2LU=D1LU

      C11=-(N*(LM**2-N**2))/(6.*SI2*LM)

      D2LC=C9+C11
```

```
      DL(2)=D2LU+D2LC

      C12=(L*L1**2/6.)*(A+2.*B)-(L1**3/12.)*(3.*B+A)
      C13=B*(L*L2+(L2**2+L1**2)/2.)
      C14=C*(L*L1+(L2**2+L1**2)/2.)
      C15=(L2**2+L1**2+L1*L2)/3.
      C16=-(B*(L+L2)+C*(L+L1))
      C17=(2.*L/3.)*(L**2+L2**2+L*L2)
      C18=((L+L2)/4.)*(3.*L**2+L2**2)
      C19=-M/2.+M*M/(6.*L1)+L1/2.-L1**2/(6.*L)
      C20=-M*M/(6.*L1)+L2/2.-L2**2/(6.*L)-L1*L2/(6.*L)
      C21=L2/6.+L1/2.-L1*L2/(6.*L)-L1**2/(6.*L)-L/3.
      C22=L1**2+L1*L2+L2**2
      C23=L**2/3.-L*L2/6.+L1*L2/6.-L*L1/2.+L1**2/6.
      C24=C22/6.+(L/2.)*(L-L1-L2)-LM**2/12.
      C25=(L1/12.)*C22+(L**2/4.)*(-L+L2+2.*L1)
      C26=-L*L2**2/12.-(L*L1/3.)*(L1+L2)
      C27=(L1/12.)*C22-L**3/3.+(L**2/2.)*(L1+L2)
      C28=-(L/3.)*C22+L2**3/12.
      C29=(L/6.)*(2.*L-L2)+(L1/6.)*(L1-3.*L+L2)
      C30=C22/6.+(L/2.)*(L-L1-L2)
      C31=N*LM/2.-N**2/2.
      C32=((L1+L2)/2.)*(C13+C14)

      D3LU1=-(.5/SI1)*(C12+C15*C16+C*(C17+C18)+C32)
      D3LU2=(1./SI2)*(C*(LM*C23+C25+C26)+B*(LM*C24
     1          +C27+C28))
      D3LU=2.*D3LU1+D3LU2

      D3LC1=-(M/SI1)*(A*C19+B*C20+C*C21)
      D3LC2=(1./SI2)*(C*C29+B*C30-B*C31)

      D3LC=2.*D3LC1+D3LC2

      DL(3)=D3LU+D3LC

      DO 10   I=1, NS

   10 WRITE (6, *)  (D(I,J), J=1, NS)

      DO 20   K=1, NS
      DO 15   J=1, NS

   15 DB(K, J)=0.
```

```
      DO 30   J=1, NS
30    DB(I, J)=D(1,J)
      DO 45   I=2, NS
      DO 40   J=1, NS
      IF ((J+I-1).GT.NS)   GO TO 45
40    DB(I, J)=D(I, I+J-1)
45    CONTINUE
20    CONTINUE
      DO 11   I=1, NS
11    WRITE (6, *)   (DB(I, J),  J=1,NS)
      WRITE (6, *)   'DL = ',  DL
      CALL SBANEQ (NS, NS, DB, DL)
      WRITE (6, *)  'XXX = ', DL
      STOP
      END
C
C
      SUBROUTINE SBANEQ (NP, NBAND, A, P)
      DIMENSION  A(3,3), B(3,3), P(3)
C
C     NP IS THE NUMBER OF EQUATIONS
C     NBAND IS THE BANDWITH
C
      DO 210  NELIM=1, NP-1
      IF (A(NELIM, 1).EQ.0.)   GO TO 300
      DO 215   NROW=NELIM+1, NELIM+NBAND-1
      IF (NROW.GT.NP)   GO TO 215
```

```
      DO 220  NCOL=1,NELIM+NBAND-NROW

220 A(NROW,NCOL)=A(NROW,NCOL)-A(NELIM,NROW
     1 -NELIM+1)*A(NELIM,NROW-NELIM+NCOL)/A(NELIM,1)

      P(NROW)=P(NROW)-P(NELIM)*A(NELIM,NROW
     1              -NELIM+1)/A(NELIM, 1)

215 CONTINUE

210 CONTINUE

      P(NP)=P(NP)/A(NP,1)

      DO 245    NBSUB=1, NP-1

      NX=NP-NBSUB

      DO 252   K=1, NBAND-1

      IF ((NX+K).GT.NP)  GO TO 252

      P(NX)=P(NX) - A(NX, K+1)*P(NX+K)

252 CONTINUE

245 P(NX)= P(NX)/A(NX, 1)

      RETURN

300 STOP
      END
```

```
      PROGRAM PROTOTYPE
C     THIS PROGRAM CALCULATES THE BENDING MOMENT (MN)
C     AT THE MIDDLE SUPPORT AND THE PRESTRESSING FORCE
C     INCREMENT (DP) OF THE TWO SPAN STEEL BOX GIRDER,
C     SHOWN IN FIGURES  6.1 AND 6.3.  THE CROSS-SECTIONAL
C     PROPERTIES OF THE TENDO  S AND THE GIRDER AND THE
C     INTENSITY OF THE LOADINGS ARE THE INPUT DATA.

      IMPLICIT REAL (A-Z)

C     P AND Q ARE THE APPLIED CONCENTRATED AND THE
C     UNIFORMLY DISTRIBUTED  LOADS

      P=?
      Q=?

C     L'S  AND M ARE THE DISTANCES FROM THE LEFT SUPPORT
C     OF THE TENDONS AND THE CONCENTRATED LOAD.

      L1=?
      L2=?
      L3=?
      L=?
      M=?
      N=?

C     I'S  AND  A'S  ARE THE PROPERTIES OF THE RESPECTIVE
C     GIRDER (THE PROTOTYPE OR THE MODEL)

      I1=?
      I2=?
      I3=?
      I4=?
      A1=?
      A2=?
      A3=?
      A4=?
      AT=?
      I=?

C     E AND E1 ARE THE TOP AND BOTTOM TENDON
C     ECCENTRICITIES

      E=?
      E1=?
      A5=(L2**4-L1**4)/(4.*L*I2)
```

```
      A=(L2**3-L1**3)/(3.*I2*L**2)
      B1=(L3**4-L2**4)/(4.*L*I3)
      B=(L3**3-L2**3)/(3.*I3*L**2)
      C1=(L**4-L3**4)/(4.*L*I4)
      C=(L**3-L3**3)/(3.*I4*L**2)
      D=(E*L+E1*L1)/(L-L1)
      G=(L2**2-L1**2)/(2.*I2*L)
      H=(L3**2-L2**2)/(2.*I3*L)
      J=(L**2-L3**2)/(2.*I4*L)
      K=(L2-L1)/I2
      R=(L3-L2)/I3
      S=(L-L3)/I4
      T1=(L1**4)/(4.*L*I1)
      T=(L1**3)/(3.*I1*L**2)
      U=(L1**2)/(2.*I1*L)
      V=L1/I1
      X=(L1**3-M**3)/(3.*I1*L**2)
      Y=(L1**2-M**2)/(2.*I1*L)
      Y1=(L1-M)/I1
      Z=(M**3)/(3.*I1*L**2)
      Z1=(M**2)/(2.*I1*L)
      D11=2.*(T+A+B+C)
      D12=2.*(E*U+E1*T+D*(-A+G-B+H-C+J))
      D22=2.*(V*E**2+T*E1**2+2.*E*E1*U+(D**2)*
     /     (A-2.*G+K+B-2.*H+R+C-2.*J+S)+
     /        (L1/A1)+(L2-L1)/(A2)+(L3-L2)/(A3)+
     /        (L-L3)/(A4)+(L1/AT)+I*(L-L1)/(AT))
          D1P=P*(-N*Z+M*(-Y+X-G+A-H+B-J+C))
       D2P=P*(-E*N*Z1-E1*N*Z-M*E*Y1+M*Y*(E-E1)+
     /       M*E1*X+D*M*(2.*G-K-A+2.*H-R-
     /        B+2.*J-S-C))
      D1Q=.5*Q*(T1+A5+B1+C1-(L**2)*(T+A+B+C))
      D2Q=.5*Q*(E1*T1+(E-E1)*T*L**2-E*U*L**2+D*(2.*A*L**2-
     /    G*L**2-A5+2.*B*L**2-H*L**2-B1+2.*C*L**2-J*L**2-C1))
      D1T=D1P+D1Q
      D2T=D2P+D2Q
     MN=(D1T*D22-D2T*D12)/(D12**2-D11*D22)
      DP=(D2T*D11-D1T*D12)/(D12**2-D11*D22)
      PRINT *, 'THE NEGATIVE BENDING MOMENT, MN= ', MN
      PRINT *, 'THE PRESTRESSING FORCE INCREMENT, DP= ', DP
      STOP
      END
```